Kurt Aasly

Properties and behavior of quartz for the silicon process

Thesis for the degree of philosophiae doctor

Trondheim, August 2008

Norwegian University of Science and Technology
Faculty of Engineering Science and Technology
Department of Geology and Mineral Resources Engineering

NTNU
Norwegian University of
Science and Technology

NTNU
Norwegian University of Science and Technology

Thesis for the degree of philosophiae doctor

Faculty of Engineering Science and Technology
Department of Geology and Mineral Resources Engineering

ISBN 978-82-471-1163-5 (printed ver.)
ISBN 978-82-471-1164-2 (electronic ver.)
ISSN 1503-8181

Doctoral theses at NTNU, 2008:236

Printed by NTNU-trykk

Preface

The work presented in this PhD-thesis was carried out at the Department of Geology and Mineral Resources Engineering at NTNU from June 2003 until May 2008.

The project was mainly funded as a four-year PhD position by the Department of Geology and Mineral Resources Engineering. However, Elkem AS funded the analytical and experimental work and made traveling to conferences etc. possible. Elkem AS also co-sponsored the purchase of necessary analytical equipment.

The PhD-project was carried out in close cooperation with other researchers in the Strategic University Program "The value chain from mineral deposit to beneficiated product with emphasis on Quartz". However, this particular PhD-project was not funded by this SUP, but the cooperation with several PhD-candidates through the SUP gave additional motivation and contribution to the results of this PhD.

First of all, I want to thank my supervisors Professor Terje Malvik at the Department of Geology and Mineral Resources Engineering and Dr. ing. Edin Myrhaug at Elkem AS for their encouragement and support, and for their contributions with ideas for the analytical work and investigations.

Paper IV is the result of cooperation with Prof. Jens Götze at the department of Mineralogy at TU-Bergakademie Freiberg. He helped with carrying out the cathodoluminescence microscopy and spectroscopy investigations as well as discussing the results. I want to thank him for welcoming me to Freiberg and sitting down with me for the week it took to carry out the CL investigations.

All the discussions with my fellow PhD-candidates, both technical discussions and social discussions have been of great importance. Special thanks to Kari Moen and Bjørn E. Sørensen for many important discussions around quartz and technical questions.

Thanks to Trond Brenden-Veisal and Halvard Tveit at Elkem AS for many good discussions and contributions to the thesis work through the reference group.

Arild Monsøy and Kjetil Eriksen at the IGB preparation lab are thanked for their important help with preparing the polished thin sections and thick sections as well as preparing samples for the shock-heating experiments.

Kjell Kvam and Torill Sørløkk were important for carrying out the XRD- and DTA analysis.

Thanks to Steinar Prytz at SINTEF Materials and Chemistry for help with shock heating of quartz in the ASEA induction furnace.

Thanks to Elkem AS for giving me the chance to spend my first few months to finish my thesis before I started working fully on my new challenges.

Finally and most importantly, I would like to thank my wife Kari and two little daughters Sofie and Guro for being there in the everyday life and being patient and supportive through my PhD work. I love you!

Trondheim, May 2008

Kurt Aasly

Abstract

This PhD-thesis is a result of the study on important properties of quartz as a raw material for the metallurgical production of ferrosilicon and silicon metal. This includes defining mechanical properties important for the size reduction experienced during transport and storage and thermo-mechanical properties of quartz that is important for how the quartz reacts to the high temperatures experienced as it is charged on the furnace. Additionally, softening properties of quartz have been briefly discussed in some of the papers. Another important goal has been to test analytical and experimental methods for investigating the various properties.

The investigations of important factors for the mechanical properties of ores and industrial minerals have been carried out as a literature study. The mining operation and transport from mine to smelter has been discussed and several factors that are significant for achieving best possible mechanical properties of the quartz have been identified. The most important factors are related to production in the mine and processing plant, which should be carefully planned to minimize the amount of blast-induced damage in the rock and thus achieve the best possible mechanical strength of the raw material. The amount of fines can be minimized by controlling the handling of the raw materials during the transport and storage. It is especially important to avoid high drops, both high single drops and accumulated height of all the drops in total.

Investigations of the thermo-mechanical properties of quartz have been carried out by using different experimental and characterization methods. The petrographic investigations of the raw materials by polarized light microscopy have been important. Thermo-mechanical investigations have been high-temperature microthermometry and shock heating of quartz samples in an induction furnace with subsequent investigations of the heated material. The subsequent investigation included polarized- and fluorescence light microscopy of polished thin sections, cathodoluminescence microscopy and spectroscopy and x-ray diffraction. Combining high-temperature microthermometry and shock-heating investigations has proved to provide useful knowledge about the effects of high temperatures on quartz.

Results from earlier research have been confirmed showing that mica is the cause of the effects seen in the temperature interval 900 – 1000 °C. This has been shown by the total absence of tridymite in the samples and the fact that mica has been seen in the unheated reference samples.

Cathodoluminescence microscopy and spectroscopy was used to investigate sample from shock-heating experiments and corresponding reference samples. These investigations show that cathodoluminescence is a useful tool for petrographic investigations of quartz. The shock-heated samples showed a significant change in cathodoluminescence characteristics that need to be investigated further to understand the cause of these changes. A spotted red luminescence was seen in two of the samples indicating the formation of cristobalite or the transition phase within these samples.

Cristobalite has been shown in samples after heating to different temperatures in the interval 1250 to 1550 °C, although in different amount in the different types of quartz. However, the transformation rates seem to be more similar after prolonged heating at the highest temperature. Experiments also indicate that the quartz-cristobalite transformation may be a cause of the disintegration of quartz at high temperatures. This is related to the severe volume expansion as the quartz transforms to cristobalite via the amorphous intermediate transition phase.

The last paper presented in the thesis presents investigations of two furnaces that have been producing ferrosilicon and silicon metal respectively. The results from these investigations show that cristobalite is formed relatively rapidly inside the furnace, however, indicating that the cristobalite formation takes place earlier at a distance from the electrode, than closer to the electrode. Another surprising discovery was to find tridymite in the ferrosilicon furnace. The investigations of silica phase transformation by shock-heating experiments did not show any tridymite even in the same type of quartz as used in the ferrosilicon furnace. The cause of the tridymite formation seen in this furnace is probably related to the total impurity content in the furnace as well as the long retention time of the quartz in the rather inactive parts of the furnace where the tridymite was found.

Table of contents

Part two:

Contributions to the papers

Paper I: A Review of Previous Work on Important Properties of Quartz for FeSi and Si Metal Production

Kurt Aasly, Edin Myrhaug and Terje Malvik

Aasly has been the main author of this paper doing all the writing and interpretations. Prof. T. Malvik was contributing with finding much of the unpublished work presented in the paper and with commenting on the parts that were not well documented. Dr. ing. E. Myrhaug contributed with process related information and discussions around this subject. Both co-authors contributed to reading corrections and discussions around organization of the paper.

Paper II: Quartz for carbothermic production of silicon - effect of the process steps, handling and transport from mine to furnace

Kurt Aasly, Edin Myrhaug and Terje Malvik

Aasly has been the main author of this paper. The writing and collection of literature was by Aasly. However, both Malvik and Myrhaug contributed to identifying the problematic areas in the production cycle of the quartz raw materials that were discussed. They also contributed to getting hold of the literature needed for making the paper. They also contributed by adding ideas and reading through drafts and commenting on the organization of the paper.

Paper III: Advanced Methods to Characterize Thermal Properties of Quartz

Kurt Aasly, Edin Myrhaug and Terje Malvik

Aasly has been the main author doing the experimental work and writing of the paper. Malvik and Myrhaug contributed with discussion of the results and gave important feedback to performing the experimental work as well as reading through the drafts.

Paper IV: Application of Cathodoluminescence to evaluate the physical properties of metallurgical quartz

Kurt Aasly, Jens Götze, Edin Myrhaug and Terje Malvik

Aasly has been the main author planning and carrying out the experimental work. Prof. Dr. J. Götze provided the CL equipment and performed CL investigations together with Aasly. Götze also contributed to the interpretations and discussions.

Malvik and Myrhaug contributed to the discussion and organization of the paper.

Paper V: Heating of Quartz and Formation of Cristobalite

Kurt Aasly, Edin Myrhaug and Terje Malvik

Aasly has been the main author of this paper carrying out the experimental work and writing the paper. Malvik and Myrhaug contributed to planning the experiments and acted as supervisors and important discussion partners. Myrhaug also provided some background data for the discussion and interpretation of the results.

Paper VI: Quartz in the Silicon Furnace

Kurt Aasly, Edin Myrhaug and Terje Malvik

Aasly has been the main author carrying out the writing, interpretation and discussion of the results. Malvik and Myrhaug contributed to the interpretation and discussion and reading of the manuscript.

This paper would not have been the same without the work of Myrhaug on the pilot scale furnace and his description of the drill cores from the furnace.

Part One

1. Introduction

Quartz is the main raw material for Si in the production of ferrosilicon and silicon-metal ((Fe)Si). Up to date, most commercial (Fe)Si is produced from lump size quartz raw materials. This is due to the internal processes in the carbothermic furnace that are affected negatively if the quartz raw materials contain too fine particles when charged on the furnace. Thus, processing of milled materials to improve the chemical quality has not been an alternative. The access to lump size quartz that can meet the chemical quality required for producing silicon metal of high purity is getting more and more difficult.

Characterizing quartz with respect to the properties that are important for the carbothermic process for (Fe)Si is challenging. Several small and larger research projects have been carried out during the last fifty years, resulting in numerous interesting temporary results. Previous work on quartz for (Fe)Si production have been reviewed in Paper 1 (Aasly *et al.*, 2007).

As has been described in Paper 2 (Aasly *et al.*, 2006), the most important factor for these properties is the geological history of the raw material. To achieve the optimal raw material, the quartz needs to have undergone the correct deposition cycle, and evolution throughout its existence from deposition through metamorphism and tectonics up to present time when mined. Knowledge about the geological history is best acquired by thorough investigations of the regional geology and detailed investigations of the rock. Petrographical investigations are carried out by using optical microscopic and chemical analysis. The petrographical investigations provide knowledge about the type of deposit, metamorphic grade and tectonic history. This is basic knowledge that should be prioritized during investigations of possible new raw materials. When the petrographic investigation shows that the quartz is suitable for further investigations, then more advanced methods may be applied. However, industrially, the identification of possible new raw materials is based on chemistry. If initial chemical analyses meet the requirements set for raw materials used to produce a silicon or ferrosilicon quality, further investigations are carried out such as detailed mapping and sampling of the deposit. Thermal strength is also measured to test the raw material for performance on the furnace.

1.1 Objectives and Scope

The objectives of this PhD work have been:

1. Investigating important properties for the quartz as a raw material for production of (Fe)Si
    a. Define mechanical properties for the quartz that are important for the size reduction experienced during transport and storage.
    b. Define thermo-mechanical properties for the quartz that are assumed important for the melting behavior on the furnace.
    c. Additionally, the softening properties have been briefly discussed in some of the papers.
2. Testing analytical and experimental methods for investigating these properties.

This work is not in any way meant to include geological mapping or exploration for new quartz raw-materials suitable for (Fe)Si production. The focus has been on quartz deposits in use by the (Fe)Si industry today (or past/future), and the properties of these raw-materials that are important for the metallurgical process.

The knowledge about the incorporation of trace elements into quartz is a field where a lot of work still needs to be carried out. However, this thesis does not focus on the trace elements in the quartz. Nevertheless, where considered important for the behavior of the quartz, chemical impurities are discussed.

1.2 Outline of the thesis

The thesis is based on the results of different types of experimental work. Some of the work is interlaced and are connected to the basis in the pre-treatment of the samples before investigations were started. Other work is more independent from the rest of the work. Nevertheless, the thesis is organized in two main parts:

1.2.1 Part one

Part one contains the introductory chapters and the background for the thesis. A detailed petrographical description of the investigated quartz is provided in the Materials chapter. The Methods chapter describes in detail the different experiments that were carried out in the thesis. A summary of the papers presented

in Part two is also presented before the general discussion and conclusion of the results obtained from the papers. Finally, a suggestion of further work is presented.

1.2.2 Part two

Part two of the thesis presents the main contribution to the thesis in the form of six papers. The six papers present work from the early stages in the project up to the final stages and have been published at international conferences, submitted to international journals or prepared for later submission to international journals. The author of this thesis is the main author on all the papers.

2. Background

2.1 The ferrosilicon and silicon metal production

2.1.1 The Carbothermic Process of silicon

Ferrosilicon and silicon metal is produced industrially by carbothermic reduction of silicon dioxide with carbon in electric submerged arc furnaces. The ideal reaction for silicon production can be written as:

$$SiO_2(quartz) + 2C(coal / coke / woodchips) = Si + 2CO \qquad \textbf{2-1}$$

Additionally for ferrosilicon production, scrap metal, iron pellets or iron oxide ore is used as the source for iron.

The size of a silicon furnace is given in electric load and varies from 1-2 MW up to more than 40 MW. Pot sizes are typically up to 10 m in diameter and 3.5 m in depth (Pers. Com Tveit, 2008). Figure 2-1 shows a typical ferrosilicon or silicon metal plant. Electric energy is supplied through three-phase alternating current by three electrodes submerged deep in the charge.

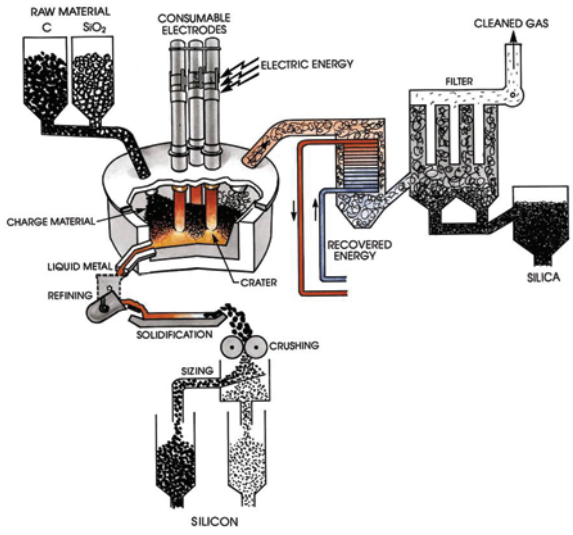

Figure 2-1 Illustration of a typical silicon metal production site (from Schei *et al.*, 1998).

Silicon furnaces are usually operated in cycles with stoking, charging and tapping as the main operations. During stoking, the thin crust on top of the charge is broken and old charge is pushed towards the electrode. The new charge is then laid on top of the old charge. The furnace is tapped through pre-prepared holes in the transition

between the side and bottom lining of the furnace. The specific energy consumption is typically up to 11-13 MWh/ton produced Si-metal (Schei *et al.*, 1998).

Trace element content of the raw materials (including quartz, reduction materials and electrodes) finally defines the purity of the silicon metal produced. The usage of the different quality silicon products are according to Schei *et al.* (1998):

Ferrosilicon (typical qualities 65%, 75% and 90% silicon) is mainly used for alloying of steel and cast iron. However, some high silicon ferrosilicon may also be used in the chemical industry.

Silicon metal (>99% Si) is used for different purposes according to chemical purity:

– Alloying of metals, especially aluminum
– Chemical industry (e.g. silicones)
– Semiconductor industry (electronic devices and solar cells)

Microsilica is filtered from the gas from the furnace and are widely used as a filler to concrete, ceramics, refractory, rubber etc.

2.1.2 Important properties of quartz

Quartz and quartzite are the sources for silicon in the carbothermic process. Quartzite is mainly used for ferrosilicon metal production. This is because the purity of quartzites is usually lower than for other types of quartz deposits and thus is not suitable for silicon production. Nevertheless, relative pure quartzites may be used in the silicon process as well, especially if mixed with other quartzes.

Furnaceability is a common international industrial quality term. A definition is given by Kallfelz (2000b):

> *A quartz is of good "furnaceability" when all its chemical and physical criteria are such to make it an appropriate Silica raw material for the production of first grade Silicon Metal at high rates of process performance.*

The industry has defined a list of absolute requirements to the quartz raw material that are necessary to achieve for the process to be optimized (Schei *et al.*, 1998):

– Chemistry (e.g. Al, Ti, B, P, Fe and Ca)
– Lump size (typically 10 – 150 mm)
– Mechanical strength
– Thermal strength
– Softening properties

Chemistry and size are the most common specifications used by all ferrosilicon and silicon metal producers. The requirements to chemistry are related to the content of impurity elements especially elements such as Al, Ti, B, P, Fe and Ca. Generally, elements more noble than Si (e.g. Al and Ca) end up in the product, whereas the volatile components follow the off-gas (e.g. Schei *et al.*, 1998). However, the reactions in the furnace are much more complicated than that, and the distribution of the elements in the raw materials also determines where the elements go. Some elements, especially alkalis (e.g. Na and K) may actually lower the melting point of quartz (Seltveit, 1992).

Generally, the requirements to the raw materials are connected to the requirements to the products of the furnace. Ferrosilicon production usually has requirements that allows for higher contents of the most difficult elements than for silicon metal production.

The sizing requirements may vary for the different plants and 10-150 mm is a general requirement. However, some producers have specifications for narrower sizing.

Some ferrosilicon and silicon metal producers focus on, or measure the mechanical- and thermal strength, although these are not included in the specifications to the supplier. Additionally, some producers focus on the softening properties of the quartz. Further, additional requirements may be defined by the individual producer, according to what is most optimal for the specific operation.

The mechanical properties of quartz affect the size reduction of the raw materials during production in the mine, transport and storage before charging. The generated fine material creates problems for the carbothermic process as it may lower the permeability of the charge and obstruct the gas flow from the lower parts of the furnace to the upper parts where SiO-gas reacts with the unreacted carbon in the charge to form SiC, which is an important reaction in the furnace. Additionally,

some of the SiO-gas condensates to form a sticky mixture of SiO_2 and liquid Si. Loss of SiO-gas through unwanted gas channels and lowered Si-recovery may be the results of the low permeability charge.

Fines may be defined by two different criteria. In this context, fines are defined as material less than 2 mm size, which is the most critical for the process. Fines <2 mm will lower the permeability of the charge. Fines may also be defined as the material of lump size below specifications (e.g. 10 mm). Too much fines in the quartz raw material is also a problem for the quartz producers from an economical view and generate waste disposal problems, as the fine material in many cases is useless for other customers as well.

As for the mechanical properties, the thermo-mechanical properties is mainly related to the generation of fines, however, in this case, the fines generation occur inside the furnace as bad thermo-mechanical properties results in disintegration of the quartz as a result of the extreme heat in the furnace. Ideally, the lumpy quartz should keep its original size as it moves down through the charge, until the quartz starts to soften and melt in the lower parts of the furnace near the cavity wall. Although, most of the quartz is likely to disintegrate to a certain degree, it should not be pulverized and generate too much fines that lowers the permeability of the charge as described above. This size reduction may also, in extreme cases, result in a popping effect where in some cases fragments of quartz may be thrown up into the air. Quartz with low thermal stability that disintegrates within the charge may also contribute to slag formation in the furnace (Senapati *et al.*, 2007).

The softening properties of the quartz are another side of the thermo-mechanical properties. The softening temperature, or softening interval, is the temperature on which the quartz starts to melt. This is lower than the melting point of quartz at 1723 °C. The softening temperature should be as close to the melting temperature of quartz as possible to achieve the ideal process where quartz move down to the cavity walls before it starts to melt and droplets of molten quartz drip from the cavity wall into the cavity, where Si forming reactions take place. Alkali-elements (and to a lesser extent alkali earths) are known to affect the melting temperature of the quartz (Seltveit, 1992). According to e.g. Kallfelz (2000a), quartz that starts to soften or even melt too high up in the furnace, will create a sticky mass, which will agglomerate with other particles and become electrically conductive and alter the electric paths in the furnace and even reduce the power of the arc.

2.1.3 Previous work on important properties of the quartz

Prior to this study, the reduction materials have been regarded the most important raw material in the carbothermic process for silicon. This has lead to an under-prioritization of research on quartz as a raw material for the same process. At least the available material on research on quartz for this purpose is not extensive. Previous research on quartz raw materials are summarized in Paper I (Aasly *et al.*, 2007). Most of the publications reviewed are from Norwegian projects (e.g. FFF and NTNU/ SINTEF) because these have been available from Elkem or NTNU/ SINTEF. This is an image of the confidentiality politics within the industry. Very little knowledge is published but instead kept confidential for competitive advantage. The lack of international publications reviewed is therefore a result of confidentiality, and is not because of a Norwegian focus in this thesis. Most likely, a lot of work has been carried out in other research communities or within companies, but this has not been possible to study for this project as it has not been published.

2.1.4 Quartz behavior in the furnace

In modern ferrosilicon and silicon metal plants, a predefined mixture of raw materials (quartz + reduction materials (+iron ore)) is charged on top of the furnace. The raw material mix is usually adapted to the requirements of the products and the productivity of the furnace. Additionally, environmental effects have become an increasingly important factor. Charging of the raw materials is carried out in cycles where the top of the charge is stoked down into the furnace and closer to the electrodes. The metal is tapped out from the bottom of the furnace through tap holes.

The temperature at the top of the furnace (charge surface) is probably in the range 700 to 1300 °C (Grådahl *et al.*, 2000). If the raw materials are charged in batches, some of the quartz will probably experience higher temperatures and a lower initial temperature gradient than those in the center of the newly charged pile. A more continuous charging makes the piles of newly charge material smaller and the temperature gradient will not be as diversified.

A temperature profile calculated by SiMod software (Foss *et al.*, 2000) have been made for quartz (Papers III, V, VI and Pers. Com. E. Myrhaug (2005)) showing that the average retention time for quartz in the furnace is approximately 5.7 hrs (Figure 2-2 and Table 2-1). However, the minimum retention time is probably somewhere between one and two hours.

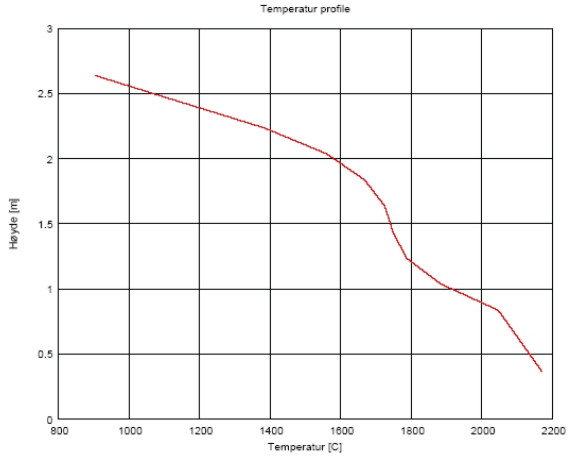

Figure 2-2 Temperature profile for quartz in a 25 MW Si-furnace (Pers. com. E. Myrhaug, 2005)

Table 2-1 Data for calculation of temperature profile in Figure 2-2 (Pers. com. E. Myrhaug, 2005)

Data for 25 MW furnace (Captured from standard model in SiMod)			
Cross-sectional area	20	m^2	
Furnace height (internal)	2.737	m	
Quartz-feeding	5473	kg/h	
Density of quartz	2600	kg/m^3	
Amount of quartz in charge	73	%	
Packing	60	%	i.e. 40% gas
Portion “active” cross sectional area	50	%	
Calculated data			
Retention time for quartz[1]	5.70	h	(average)

[1] I.e. the time from the quartz is charged until it reaches the crater. In the real process, parts of the quartz material will have a much shorter retention time and other parts will have much longer, depending on the initial distance from the electrode. The shortest retention time is probably 1-2 hours.

Schei et al. (1998) proposed an inner structure of the silicon furnace as illustrated in Figure 2-3. The figure shows a silicon- or high silicon ferrosilicon furnace shortly before stoking. The main feature of the furnace is the cavity surrounding the electrode. The cavity walls consist of sintered SiC crystals in the lower parts partly mixed with molten silicon. The upper parts of the cavity walls consist of carbon lumps, molten silica and condensate, where the carbon lumps are partly converted to SiC. Outside the cavity wall, charge material closest to the cavity are reactive, but further outside, the temperature is not high enough to keep the charge reactive. As the roof of the cavity is saturated and no reactions take place in the upper charge, the cavity is stoked down and new charge is filled on top.

The main reactions in the furnace take place in the cavity (inner zone), where the temperature exceeds 2000 °C. Here the silicon forming reactions take place.

The silicon forming reactions creates gasses (CO and SiO) that escape the inner zone. CO and SiO gas flows through the charge and most Si is recovered in the upper zone as SiO_2 and liquid Si as a sticky mass or reacts with carbon to form SiC. This mass will move down through the furnace and finally return to the cavity. However, some SiO-gas will be lost to the off-gas system where it condensates as SiO_2 and are collected by the off-gas filters as micro silica.

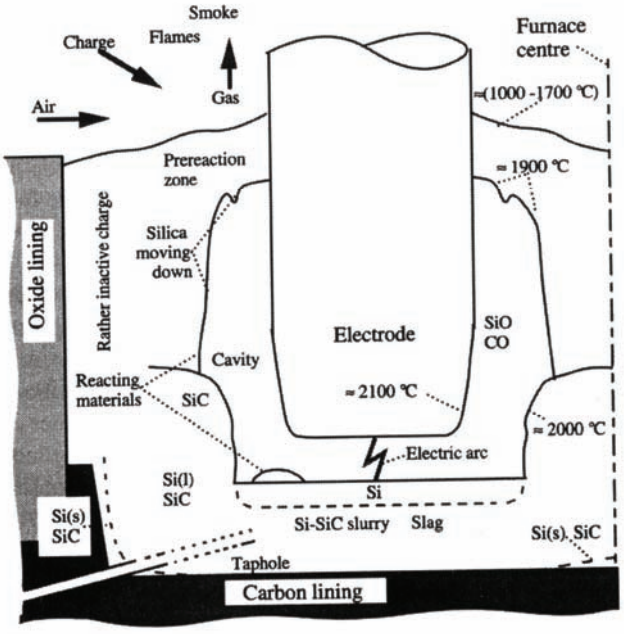

Figure 2-3: The inner structure of a Si furnace as illustrated by Schei *et al.* (1998)

2.2 Quartz and quartz deposits

2.2.1 Quartz

Quartz is the second most abundant mineral in the earth's crust after feldspars (Deer *et al.*, 1992) and is an important constituent in igneous, sedimentary and metamorphic rocks. Quartz is the main constituent in hydrothermal quartz veins and in the core of zoned pegmatite bodies. During sedimentary processes, quartz is concentrated due to its chemical and physical resistance to corrosion. In sediments, quartz may be found as secondary material as authigenic quartz cement.

Resources of high purity quartz are found around the world. Pegmatite bodies and beach sand are the most frequent deposits utilized for this type of materials. Typical industrial use of high purity quartz is mainly for the electronic and semiconductor industry, and as optical fibers and crucibles.

However, metallurgical quartz, in this case quartz for carbothermic production of ferrosilicon and silicon metal need to be charged as lump quartz ranging typically within 10 to 150mm size. This eliminates beach sand that are typically fine-grained. Quartz from small pegmatite bodies with quartz and feldspar intergrown surrounding a small core often needs beneficiation (e.g. flotation) because selective mining is impossible. The beneficiated product comes as very fine-grained material and is not suited for the production of ferrosilicon and silicon metal.

2.2.2 Metallurgical quartz deposits

The raw material for Si in the carbothermic production of ferrosilicon and silicon metal is quartz or quartzite. Nomenclature to distinguish between main types and qualities of quartz may be "rock" and "gravel" quartz, normally used by metallurgists to distinguish quartz mined by drilling and blasting operations and quartz taken mainly from fluvial deposits by simple excavation methods. The quartz goes further through simple processing; for rock quartz, this involves crushing and sieving. For gravel quartz, usually only sieving is necessary, while crushing is only carried out on oversize boulders. Some manual separation may be required to remove none quartz material from the quartz product. Optical separation may be used as alternative where appropriate.

Because of the relatively large variation of impurity content within a gravel deposit, gravel quartz is usually not as pure in trace elements as rock quartz. The same generalization may be used on quartzite compared to vein quartz. With

respect to mechanical and thermo-mechanical strength, gravel quartz may be more resistant to size reduction compared to rock quartz, because the rock quartz has been weakened from blasting operations, whereas gravel quartz has gone through natural selection during fluvial transport and deposition where only the mechanically strongest boulders have survived.

The main types of deposits for lump metallurgical quartz in geological terms are quartzite, hydrothermal quartz and pegmatite quartz (rock quartz) and fluvial quartz (gravel quartz). Pegmatite quartz has been listed here as a source for lump quartz because of its potential as a very pure raw material. However, it is not frequently used today because of the usually small size and need of manual sorting and quality control because of the presence of impurity minerals such as feldspar and mica. These are the main minerals of the pegmatite body together with quartz, outside the quartz core.

Definitions of the types of lump quartz deposits are given below:

Hydrothermal Quartz

Hydrothermal vein quartz is formed by precipitation of quartz from hot aqueous fluids where such fluids flow through faults, fractures or other openings in the rocks (general definitions by e.g. Monroe and Wicander, 1994; Craig *et al.*, 1996; Evans, 1997). The aqueous fluids originate from magmas or from water belonging to the atmospheric cycle. These veins can be less than a cm wide with lateral extends of only a few meters or the width can be up to tens of meters and extending for several km's depending on the size of the original fracture. Large hydrothermal quartz veins are often associated with regional shear zones. The aqueous fluids often dissolve elements from the country rocks and therefore hydrothermal quartz is a common host to ore deposits. However, if the conditions for dissolution or precipitation are unfavorable, hydrothermal quartz veins may be extremely pure, containing only a few ppm of impurity elements. Such hydrothermal quartz veins of significant size are those that are the most suitable as raw material for silicon metal production.

Quartzite

Quartzite form during medium- to high-grade metamorphism of quartz sandstone by recrystallization (general description by e.g. Monroe and Wicander, 1994). If the recrystallization is complete, the quartzite is of uniform strength. If the rock is struck sufficiently hard, the fracture opens through mineral grains instead of around

them along grain boundaries. However, the metamorphic state varies (often even within a single deposit if large) and less metamorphosed quartzite, or even meta-sandstone, may be used as raw materials. Therefore, the strength of the quartzite varies. Quartzite consists mainly of quartz and only traces of other minerals. Such minerals are mica, clay minerals, feldspars as well as other more durable minerals. Pure quartzites are usually white, but iron and other impurities may give color to the quartzite.

Pegmatitic quartz

A pegmatite is a very coarse-grained igneous rock, commonly associated with plutons and consisting mainly of quartz, feldspar and mica (general definitions by e.g. Monroe and Wicander, 1994; Craig *et al.*, 1996; Evans, 1997). They contain minerals that are >1 cm across, and commonly much larger crystals. Pegmatitic melts are volatile-rich and formed during terminal crystallization of a granitic magma. They are located either in the cupola parts of the pluton or crystallized in fractures in the crust. Pegmatites usually have a large quartz core, which may be very pure quartz. The name reflects texture rather than a specific composition, but most are composed largely of quartz, potassium feldspar and sodium-rich plagioclase hence correspond to the composition of granite. It is not unusual to find rare minerals associated with such pegmatites.

For use as raw material for ferrosilicon and silicon metal, the rare mineral content may lead to elevated content of some unwanted elements. Also, for a pegmatite to be suitable as raw material, the quartz core needs to be large enough for mining. This requires pegmatite bodies of significant size.

Fluvial deposits

Fluvial deposits are a result of the actions of rivers and streams. The bedrock is eroded either as direct result of stream activity, or the stream picks up material eroded by other weathering mechanisms. The eroded material is suspended in the stream at places where the stream is of favorable energy (stream velocity is high enough) and deposited as the energy of the stream (velocity) decrease. The size of the deposited material reflects the stream velocity. Gravel quartz is often found as lenses within more fine-grained fluvial deposits. Source material may be any quartz containing rock eroded up stream from the fluvial deposit.

2.2.3 Silica polymorphism

The importance of the different phase transformations in quartz on the thermo-mechanical properties of the quartz raw materials for (Fe)Si-metal has been investigated by several researchers and are summarized in Paper I (Aasly *et al.*, 2007). The α- to β-quartz transformation and the β-quartz to HP-tridymite transformation have been ruled out as important factors. However, the importance of the β-quartz to β-cristobalite transformation has not yet been concluded. Nevertheless, it is known that this transformation necessitates fracturing of the quartz as a result of both the breakage of Si-O bonds and the severe volume expansion that follows this phase transformation (e.g. Mitra, 1977). According to Salmang and Scholze (1982), this volume expansion is more than 15% at 1000 °C (Figure 2-4a).

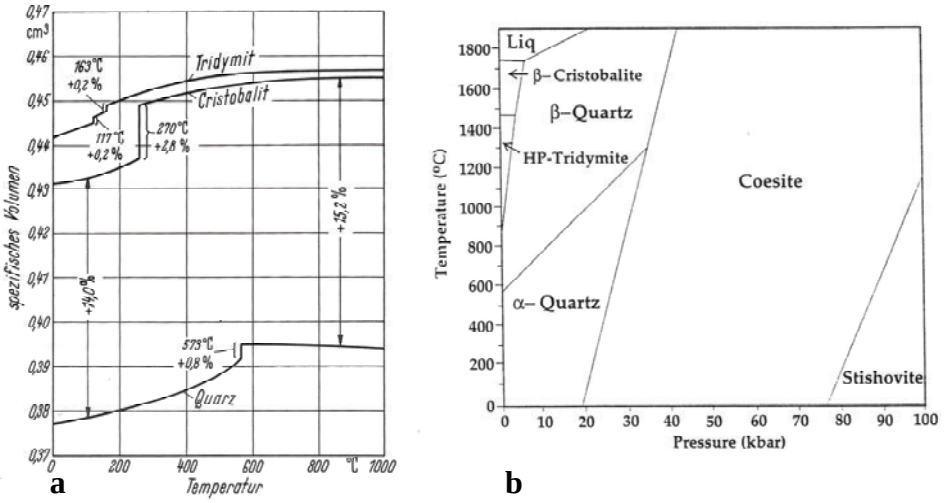

Figure 2-4 a): The temperature dependence of the specific volume for quartz, cristobalite and tridymite (from Salmang and Scholze, 1982); **b):** Phase diagram for the silica system. (from Klein and Hurlbut, 1993)

The stability diagram for the silica system in Figure 2-4b shows that SiO_2 has four main polymorphs that are stable at different temperatures at atmospheric pressure. These are α-quartz, β-quartz, HP-tridymite and β-cristobalite.

The displacive phase transformation from α- quartz to β-quartz takes place at 573 °C and is reversible. The crystal structure changes from trigonal in α-quartz to hexagonal in β-quartz. The α-quartz structure has been interpreted as a distortion of the β-quartz structure. Furthermore, the transformations from β-quartz to HP-

tridymite or β-cristobalite at 870 and 1470 °C respectively are reconstructive and slow. With rapid cooling of HP-tridymite and β-cristobalite, these will undergo displacive phase transformation similar to the α- to β-quartz phase transformation. For tridymite, two transformations occur at 110 and 170 °C. For cristobalite the α- to β-phase transformation occur at 272 °C (some refer to between 180 and 272 °C). Tridymite and cristobalite are meta-stable at ambient temperature and pressure.

Fenner (1913) and Deer *et al.*(1992) for example, places tridymite in the silica system as a true silica polymorph. However, in his establishment of the *Stability Relations of Silica Minerals*, Fenner (1913) used a Na_2WO_4 flux to speed up the reaction rates of the different phase transformations. He also discovered that the flux was crucial for the formation of tridymite from quartz or amorphous silica within the stability field of tridymite. Without the flux, cristobalite was formed and the tridymite structure was totally absent within the tridymite stability field. Several authors (e.g. Floerke, 1957; Holmquist, 1961; Stevens *et al.*, 1997) have discussed whether tridymite is really a member of the silica system as it has been shown that a mineralizing agent, such as Na or K, is needed in order to form tridymite.

The kinetics of the quartz – cristobalite transformation has been studied by several authors and several explanations have been presented. However, Chaklader and Roberts (1961) and Chaklader (1963) showed that the transformation of quartz to cristobalite followed an indirect path with an intermediate non-crystalline transition phase. According to Mitra (1977), the transformation from quartz to cristobalite involves a phase-boundary controlled transition from quartz to transition phase, and further, the transformation from transition phase to cristobalite is concentration-controlled. Thus, the transformation from quartz to cristobalite involves an induction period where total absence of cristobalite is expected until enough transition phase material is produced for the required concentration enabling the formation (nucleation) of cristobalite.

Several researchers have investigated the formation of cristobalite from quartz or microcrystalline silica and found different temperatures for when the transformation is initiated. E.g. Harders and Kienow(1960) summarized the phase transformations in silica and stated that the phase transformation of β-quartz to β-cristobalite is initiated at 1250 °C. Further, Harders and Kienow (1960) also stated that the β-quartz structure is instable already above 870 °C. Stevens (1997) and Stevens *et al.* (1997) stated that cristobalite is not formed at temperatures below

1400 °C in pure quartz (Iota Quartz with max impurities of 35 ppm). They also stated that the amount of cristobalite in samples heated to the same temperature at the same heating rate varies according to the cooling rate. Stevens (1997) and Stevens *et al.* (1997) discovered that samples that were cooled at the natural rate of the furnace were found to contain much less cristobalite than samples cooled at a controlled rate (in the case of Stevens *et al.* (1997) the controlled rate was 3 °C min^{-1}). According to Stevens (1997) and Stevens *et al.* (1997), the natural rate of the furnace was more than 3°C/min at more than 500 °C. Below 500°C it was less than 3°C/min. In another paper, Shoval *et al.* (1997) reported minor cristobalite formation in heated natural chert composed of crypto- and microcrystalline quartz after heating to 1000 °C for one hour. They also reported that the transformation was almost complete after heating to 1300 °C for 24 hours. The same experiments on well-crystallized pure quartz did not show any cristobalite formation.

2.3 Industrial test methods

Today, the Si-industry uses an uncomplicated, but well approved method to test the thermo-mechanical and mechanical properties of quartz. However, the test seems to be carried out after slightly different principles in the different labs - even within each company.

Other methods for testing e.g. softening properties of quartz are not so frequently used, however, they are briefly described in Paper I (Aasly *et al.*, 2007).

2.3.1 Elkem Method (Fiskaa Method)

Heat index (HI) and thermal strength index (TSI)

This test-method is described by Alnæs (1986), Johannesen (1998) and Birkeland (2004): A representative quartz sample is crushed by sledgehammer to a sample size of approximately 400 - 500 g (corresponding to 20 - 30 pieces of 20 – 25 mm samples). The sample is transferred to a crucible and heated in a muffle furnace at 1300 °C for one hour. After cooling at room temperature, the sample is carefully laid on a set of sieves (20mm, 10mm, 4mm, and 2mm) with no mechanical treatment. The percentage of weight +20mm after heating is reported as the heat index (HI or resistance to disintegration). Subsequently, the +20 mm fraction of the sample is treated in a Hannover drum at 100 rotations over 2.5 min. (40 rpm). After treatment in the drum, the sample is screened once more. A thermal strength index (TSI) is then calculated using the equation:

$$TSI = \frac{\%(+20mm) + \%(-20mm + 10mm) + \%(-20mm + 4mm) + \%(-20mm + 2mm)}{4} \quad \textbf{2-2}$$

This method may be carried out slightly differently in various laboratories and production plants. The differences are related to the amount and size of the material tested, the heating cycle etc. (Pers. com. P. Kallfelz, 2004). Often the HI shows that the tested quartz is not of good furnaceability and the tumbling is not necessary (Pers. com. P. Kallfelz, 2004).

From the calculated indexes, and the values for resistance to disintegration, the samples may be divided into classes of quality. This method makes it easy to distinguish between "good" and "bad" quartz, but not between "very good"/"good"/"fairly good" (Birkeland, 1975).

Friability index and dust index

The friability index (FI) is used as a measure of the mechanical strength of the unheated quartz and is meant to give a measure of how much the quartz is disintegrating during transport (e.g. Birkeland, 2004).

This test-method is, basically, the same as the test for TSI, only without the heating. The same Hannover drum is used for tumbling the samples. However, tumbling is carried out for 1 hour at 40 rpm. The same set of sieves and the same formula for calculating the friability index are used as for the TSI. This test also gives an indication of how much dust (dust index, DI) the quartz produce during transportation and crushing and is reported as the weight % -2 mm.

The method for friability- and dust indexes shows similarities with e.g. the Los Angeles- and the Ball Mill methods used for mechanical strength tests for aggregates. However, the steel balls in the mill is not used for FI and DI and only the Los Angeles method uses the ribs similar to those used for FI and DI.

2.3.2 "Spigerverket" method

This method was developed at the Bremanger plant, but is not so much used today and access to detailed method description has turned out to be difficult.

In this test, the samples are heated to 450-1000 °C at a rate of 200 °C/hour. During the heating, the samples are "checked" every half hour. When 1000 °C is reached,

the temperature level is kept half an hour before the sample is cooled and twisted by hand and screened.

2.3.3 Brazilian test for thermal stability

The Brazilian test method is another test method used for testing thermal stability. According to Myrhaug (Pers. Com. 2008) this method is used on a 1Kg sample material 3"/4 to 1" that is heated half and hour to 500°C and sieved on a 3"/4 sieve. Oversize material is heated again on 600°C and the procedure is repeated at 700, 800 and 950°C. The percentage cumulative undersize material (-3"/4) from sieving after each temperature interval is reported as the result. The lower the number the more thermally stable material.

2.3.4 General remarks to established test methods

The thermal test methods already established in the industry, and have been used during the last three to four decades, give good indications of the thermal stability of the tested quartz. However, the methods described in this section are only indicative and give no final answer. Although tested quartz comes out relatively poor in the Elkem method (TSI), the quartz may operate well when used on a furnace in small or large amounts in a raw material mix. It has also been shown examples that poor quartz by the Elkem method may come out with excellent results using the Brazilian test.

The differences of quality in the Elkem method and the Brazilian test may be because the Elkem method includes a mechanical test whereas the Brazilian test does not.

3. Sample Materials

Seven types of quartz have been studied in this PhD-thesis. Six quartz types are included in the main part of the thesis, additionally, one quartz type is included as part of the investigations in Paper VI. All seven samples (Table 3-1) are frequently used for the production of ferrosilicon and silicon metal and includes a selection of rock quartz and gravel quartz. The rock quartz has a known source such as hydrothermal deposit or quartzite. However, the sources of the different gravels are unknown and the classifications used in this thesis are mostly based on the petrographical investigations in the microscope. In the macroscopic descriptions presented below, "fragment" and "boulder" is used to describe the material. "Fragment" is used for rock quartz and "boulder" for gravel quartz.

Because of confidentiality, the names and locations of the investigated quartz deposits are made anonymous. Thus, samples are given names from A to F preceded by quartz type as listed in Table 3-1. Additionally, the quartz used for the Pilot scale furnace in Paper VI is named "Pilot".

Table 3-1 List of samples for the investigations presented in this thesis. Samples A to F are the basis of the research presented in the thesis. Sample Hydrothermal "Pilot" is only described in Paper VI.

Quartz type	**Sample**
Gravel	A
Gravel	B
Hydrothermal	C
Pegmatite	D
Meta-sandstone (quartzite)	E
Gravel	F
Hydrothermal	"Pilot"

Geological samples are used to describe the petrography and geochemistry of a sample from a known location (e.g. defined by UTM coordinates). Such samples are often only descriptive for a small area, as the microscopic textures may vary over small distances and thus several samples from the area is needed to get a full overview of the geology of e.g. an ore deposit. In the case of a (rock) quartz deposit, the geological conditions may vary from one part of the deposit to the

other, especially with respect to structural texture and trace mineral content. For a gravel deposit, the source material for the interesting gravels may vary and more concern of sampling a representative mass is crucial. For a typical geological survey, a sample without an exact sample location is worthless. However, for the work presented in this thesis, the focus is on properties and behavior of quartz connected to use in production of (ferro)silicon in smelter plants, and the positions of the samples are not important. The experiments and investigations carried out are meant for investigation of methods and comparing different types of quartz that are suitable for use in the (ferro)silicon furnace. For that, only a sample that is representative of the raw material delivered to the smelter plant is necessary. It is assumed that through the sampling method described below, and further random selection of a hand specimen from the sampled material, provides sufficient representability of the samples. The samples were collected randomly from shipments being discharged at different smelter plants. The sampling was carried out by staff from Elkem AS, for an internal project as described by Birkeland (2004) and the material was later made available for this PhD work.

The samples were preliminary described by Moen and Malvik (2002) who performed a brief petrographic investigation of the samples based on one polished thin section (PTS) from each of the quartz types. These samples were from the same selection as the samples presented in this thesis.

The petrographic investigations presented in the thesis are based on three polished thin sections (PTS) from each specimen. The samples were cut from three perpendicular orientations. Additionally, the reference samples made for the investigations in Papers III and IV were studied as well as the PTS investigated by Moen and Malvik (2002). In total, the petrographic studies include six PTS from three different boulders/fragments for each quartz type. Additionally, three of the PTS of each quartz type were impregnated with fluorescent epoxy for investigation of grain boundaries, micro cracks and fractures.

Gravels B and F appears heterogeneous, containing quartz boulders from two different sources. Thus, two descriptions are given of these gravels. However, Gravel A appears homogenous and thus, described as one.

3.1 Gravel A

3.1.1 Macroscopic description

The sample material consists of boulders (ca 75 to 95 mm) of typical gravel quartz. The specimen appears massive, white to clear with frequent staining probably from iron-hydroxides on the surface. Quartz is the dominating mineral and no additional minerals can be seen in the hand specimen. Most of the frequent cracking seems sealed on the surface. However, some are filled with rusty material, probably iron-hydroxides. The sample is coarse-grained and the surface appears more dark grayish when cut.

3.1.2 Microscopic description

Mineral content: Quartz: >99%; Mica: <0.5%; trace ore minerals.

Quartz: Figure 3-1a and b shows optical micrographs of Gravel A. PTS are dominated by equigranular very coarse-grained quartz (>15mm). Some grain boundaries and fractures are filled with fine-grained new (recrystallized) quartz. Fractures occur as both inter- and intragranular. The large grain size in the sample makes it difficult to determine crystal growth and grain boundaries. However, anhedral crystal growth and polygonal to lobate grain boundaries are suggested. Real grain boundaries and subgrain boundaries are commonly difficult to distinguish. Characteristic undulating extinction is oriented and shows formation of elongated subgrains. Fluid inclusions are common, giving the quartz a dusty appearance.

Mica: Minor amounts of mica minerals occur as small, elongated grains associated with micro cracks and grain boundaries.

Ore minerals: Ore minerals occur in trace amounts as disseminated iron oxide, probably hematite.

3.1.3 Fluorescent light

Fluorescent light (Figure 3-1c) investigations show that there are minor micro cracks within and across grains and that, the growth of new quartz within fractures is not complete, as fluorescent epoxy has penetrated the voids in these areas.

3.1.4 Cathodoluminescence microscopy and spectroscopy

Cathodoluminescence microscopy and spectroscopy (Paper IV) indicate that the source materials for Gravel A are from igneous rocks as seen from the stable deep blue-violet CL-color and the corresponding emission spectra. Additionally, the CL investigations show that the quartz is overprinted locally by hydrothermal activity seen as transient blue CL around thick bands of fluid inclusions.

3.1.5 Conclusion

From the petrographic investigations, this is a typical metamorphosed hydrothermal or pegmatite quartz. However, the quartz material was deposited as fluvial material and no information about the source material has been provided. When cathodoluminescence microscopy and spectroscopy (Paper IV) indicate that the origin is from igneous rocks, it is difficult to give an interpretation although hydrothermal overprint is shown by the transient blue CL coinciding with large fluid inclusion bands.

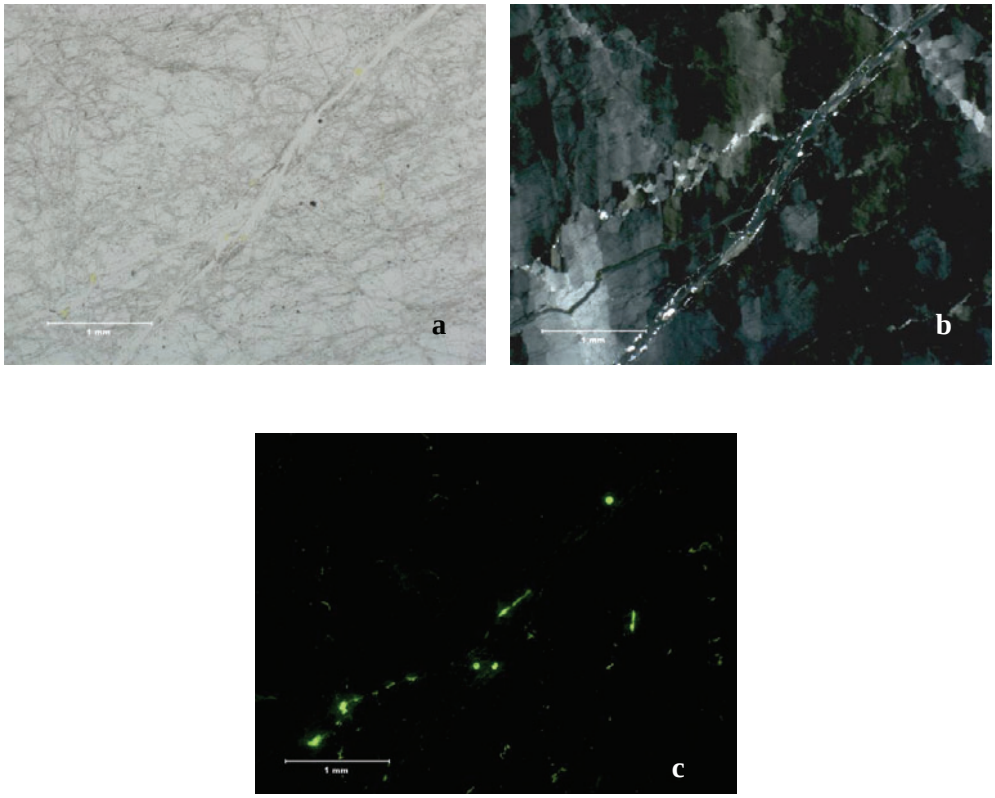

Figure 3-1 The coarse-grained quartz of Gravel A shows oriented undulate extinction and sub-grain formation. The main quartz grain is intersected by a band of recrystallized quartz. The sample is typically homogeneous and therefore representative. Micrographs **a** and **b** are under plane polarized light (ppl) and crossed polarized light (xpl) respectively. Micrograph **c** shows a fluorescent light micrograph of the same area. Note that there are some fluorescent areas along the trace of new grains within the main fracture intersecting the quartz from upper right to lower left. The fracture is typical for this quartz type containing fine-grained recrystallized quartz and occur both commonly intra- and intergranular.

3.2 Gravel B

3.2.1 Macroscopic description

The sample material contains gravel quartz boulders (ca 90 to 120 mm). The quartz appears medium- to coarse-grained, massive, dark grey, spotted with more whitish areas. Fractures are frequent and crosscutting the sample in several directions but no preferred orientation can be described. Some rusty material is seen within some of the fractures as well as minor greenish claylike material. Some cavities are also seen.

3.2.2 Microscopic description

Mineral content: Quartz: >99%; Mica: <1% (muscovite and minor biotite).

Quartz: Sample Gravel B resembles Gravel A and is dominated by equigranular very coarse-grained quartz (>15 mm) see Figure 3-2a and b. The sample shows anhedral crystal growth with mostly polygonal to lobate grain boundaries although, as for Gravel A, distinguishing real grain boundaries and subgrain boundaries may be difficult. Frequent fracturing and micro cracks is seen, both inter- and intragranular. Several micro cracks, fractures and grain boundaries are filled with fine-grained new (recrystallized) quartz. A few fractures contain minor iron-hydroxides. Elongated subgrain formation is seen as undulate extinction in preferred orientation. The sample is loaded with fluid inclusions giving the quartz a dusty appearance. The fluid inclusions seems oriented in traces at right angles to the subgrain orientation.

Mica: Mica occurs as microscopic grains located in grain boundaries as single grains or small bands. However, a band containing large aggregates of small muscovite and biotite grains is seen in one sample.

3.2.3 Fluorescent light

Fluorescent light microscopy (Figure 3-2c) shows a few micro cracks/fractures (intragranular and intergranular) and some cavities within the sample. Grain boundaries seem relatively dense.

3.2.4 Cathodoluminescence microscopy and spectroscopy

No CL available on this sample.

3.2.5 Conclusion

Gravel B is typical metamorphosed vein quartz although distinguishing hydrothermal vein- or pegmatite quartz is difficult to interpret from the sample boulder and PTS only. The quartz boulders were deposited as fluvial material and no information about the source material has been provided.

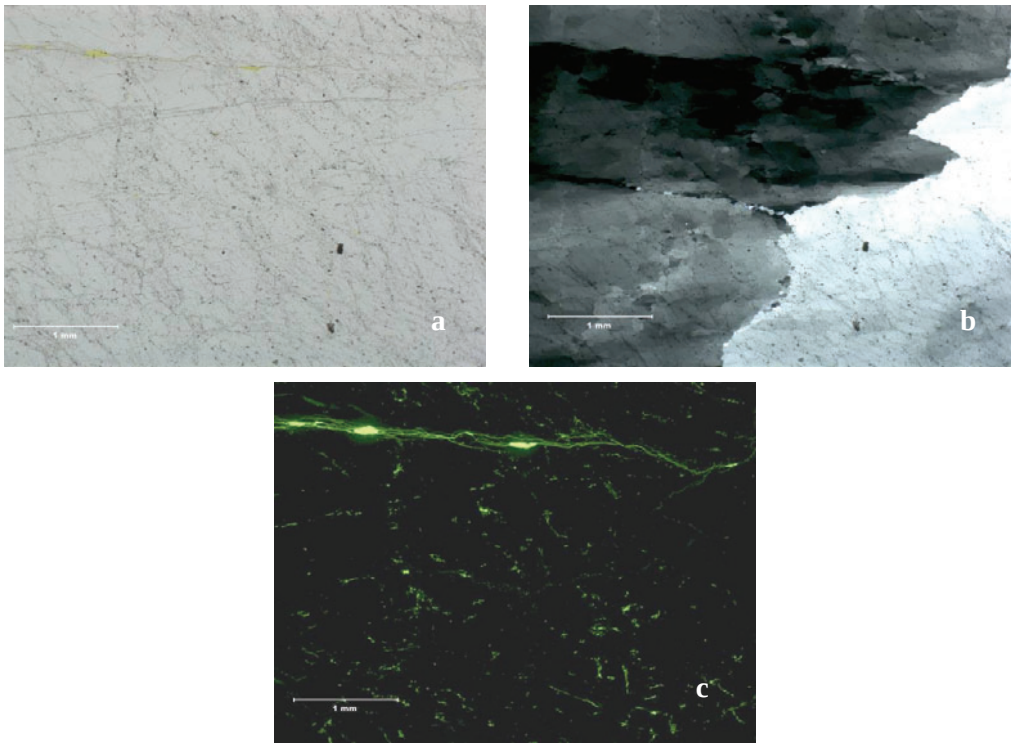

Figure 3-2 An example of a typical grain boundary in Gravel B, between two large quartz grains. The grain boundary is filled with minor amounts of new (recrystallized) fine-grained quartz. The left side grain shows oriented sub-grain formation. The dusty appearance of the sample in Micrograph **c** is caused by trails of fluid inclusions and minor micro cracks and fractures. Micrograph **a** and **b** shows the same area in ppl and xpl respectively. **c** shows the same area under fluorescent light. Note that the main fluorescent trace does not coincide with the main grain boundary but with a possible subgrain boundary. The main grain boundary is only weakly indicted at the (upper) right just below the main fluorescent trace.

3.3 Gravel B-2

3.3.1 Macroscopic investigation

Macroscopically this sample is not so different from Sample B-1. However, it appears less rounded and more light grey.

3.3.2 Microscopic investigation

Mineral content: Quartz: >99%; Mica (muscovite): <1%

Quartz: Sample Gravel B-2 contains inequigranular quartz showing typical elongate subgrain formation in the larger (old) grains (Figure 3-3). Crystal growth is anhedral. The grain size is seriate (0.5 to 10 mm) and the grain boundaries are lobate. Small fractures are seen as intragranular however, some larger fractures occur as intergranular. The quartz is loaded with fluid inclusions, which gives the quartz a dusty appearance.

Mica: Minor mica (muscovite) occurs along grain boundaries as small grains in bands.

3.3.3 Fluorescent light

No fluorescent light microscopy was carried out on this sample.

3.3.4 Cathodoluminescence microscopy and spectroscopy

The yellowish-green luminescence seen in cathodoluminescence microscopy and spectroscopy (Paper IV) indicates that Gravel B-2 is a typical hydrothermal vein quartz.

3.3.5 Conclusion

Gravel B-2 probably represents hydrothermal vein quartz, which is confirmed by the yellowish-green luminescence seen in cathodoluminescence microscopy and spectroscopy. This indicates that the source material to this gravel quartz is typical hydrothermal vein quartz.

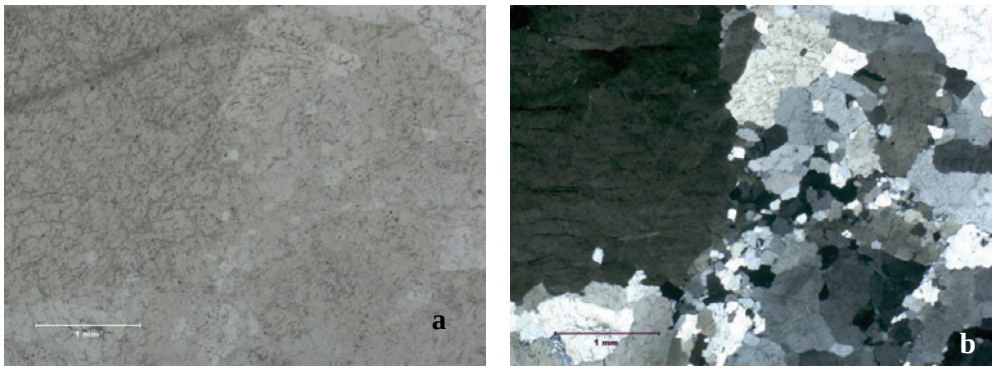

Figure 3-3 Gravel B-2 has seriate grain size and lobate grain boundaries. The largest grains (left) are old and show subgrain formation. The smaller grain (right) are recrystallized from older grains. The dusty appearance in Micrograph a is cause by the high content of fluid inclusions. Micrographs **a** and **b** are the same area under ppl and xpl respectively.

3.4 Hydrothermal C

3.4.1 Macroscopic description

Sample Hydrothermal C contains massive fragments of white, typical milky quartz. The fragments (ca 80 to 150 mm) contain networks of fractures. Quartz is the dominating mineral and no additional minerals are seen. Sample Hydrothermal C represents rock quartz from a hydrothermal vein deposit.

3.4.2 Microscopic description

Mineral content: Quartz: ~99.9%; trace of mica

Quartz: Sample Hydrothermal C shows a very coarse-grained (>15 mm) quartz with characteristic undulating extinction showing elongated subgrains (Figure 3-4a and b). Deformation lamellae are also common. Grain shape and grain boundaries are difficult to determine because of the coarse-grained texture. However, indications of polygonal grain boundaries are seen. Fractures are filled with fine-grained new (recrystallized) quartz. Fluid inclusions are numerous and give the quartz a dusty appearance. Fluid inclusion trails seem to be oriented in planes with varying orientations. Some fluid inclusions contain double rings around the gas-phase (see Figure 3-4d). This is probably caused by the appearance of two liquid phases within the fluid inclusions. There are some fractures of significant distances, both inter- and intragranular. These are filled with epoxy resin.

Mica: A few microscopic mica grains were seen in one sample.

3.4.3 Fluorescent light

Fluorescent light microscopy (Figure 3-4c) shows that this quartz contains minor micro cracks/fractures. The grain boundaries seem relatively dense.

3.4.4 Cathodoluminescence microscopy and spectroscopy

The luminescence characteristics seen from cathodoluminescence microscopy and spectroscopy (Paper IV) indicate that Sample Hydrothermal C is a regional metamorphic rock or that the hydrothermal vein quartz has been exposed to regional metamorphoses.

3.4.5 Conclusion

Optical microscopic investigations indicate that this is a hydrothermal vein quartz which has been exposed to serious stress as seen from the undulating extinction and subgrain formation. Initial recrystallization is seen in the fractures and grain boundaries, indicating metamorphoses, which is supported by cathodoluminescence microscopy and spectroscopy investigations indicating regional metamorphic rock. Accordingly, the quartz vein has been subject to low-grade regional metamorphoses.

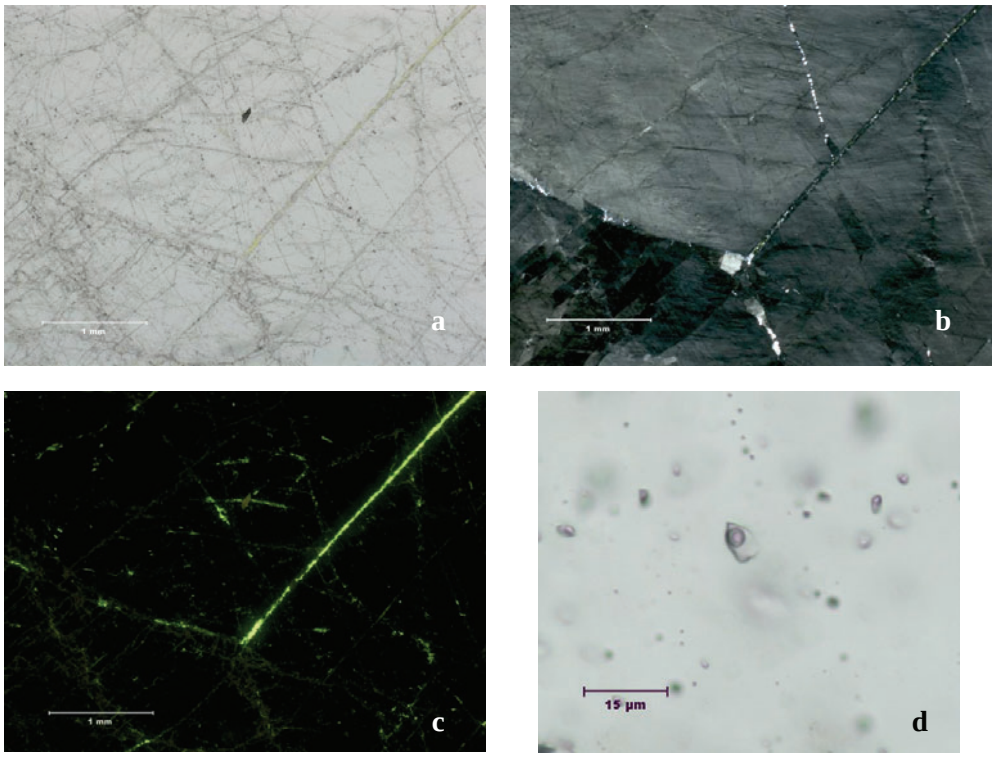

Figure 3-4 Micrographs **a** and **b** shows typical undulate extinction in the Hydrothermal C. Subgrain formation is frequent and grain boundaries are often filled with fine-grained recrystallized quartz. The dusty appearance of the quartz in a is caused by the high content of fluid inclusions. Micrographs **a** and **b** are under ppl and xpl respectively. **c** shows fluorescent light micrograph of the area shown in **a** and **b.** The grain boundaries are pronounced by the luminescent epoxy and appear relatively open. **d** shows large fluid inclusion with double ring for the gas phase which indicates two liquid phases within the fluid inclusion.

3.5 Pegmatite D

3.5.1 Macroscopic description

The sample material represents rock quartz and contains coarse-grained, massive, white typical milky quartz fragments (ca 60 to 100 mm). Some cavities can be seen in the sample material. Quartz is the dominating mineral and no additional mineral can be seen.

3.5.2 Microscopic description

Mineral content: Quartz: >99%; Mica: <1%

Quartz: Sample Pegmatite D is inequigranular to seriate and contains a mixture of grain sizes ranging from fine- to coarse-grained quartz (0.2 – 15 mm) with weak signs of layering with respect to grain size (Figure 3-5a and b). Crystal growth is subhedral in coarse-grained material to anhedral in more fine-grained areas. Grain boundaries are polygonal in the coarse-grained to weak lobate in more fine-grained areas. The largest grains seem to be unaltered original grains, showing subgrain formation as elongated extinction patterns. Some of the larger grains contain fractures or possibly subgrains that have recrystallized to very fine-grained quartz in narrow bands within the original grain. The sample is loaded with fluid inclusions in all generations of quartz.

Mica: mica occurs mainly as small, disseminated grains within large quartz grains.

3.5.3 Fluorescent light

Each grain of quartz is relatively well defined by fluorescent epoxy that has penetrated the grain boundaries (Figure 3-5c) and shows that this rock has relatively open grain boundaries. Minor intra- and intergranular micro cracks/fractures are also seen.

3.5.4 Cathodoluminescence microscopy and spectroscopy

Typical luminescence characteristics obtained from cathodoluminescence microscopy and spectroscopy (Paper IV) indicates that Pegmatite D is a pegmatite quartz.

3.5.5 Conclusion

The inequigranular texture and the somewhat subhedral crystal growth, especially of the larger quartz grains indicate that this may be a pegmatite quartz. The interpretation is supported by the cathodoluminescence investigations that according to the CL spectra show that the quartz may be categorized as pegmatite quartz. However, no geological information has been obtained about the deposit, and it cannot be verified that the deposit actually is a pegmatite vein.

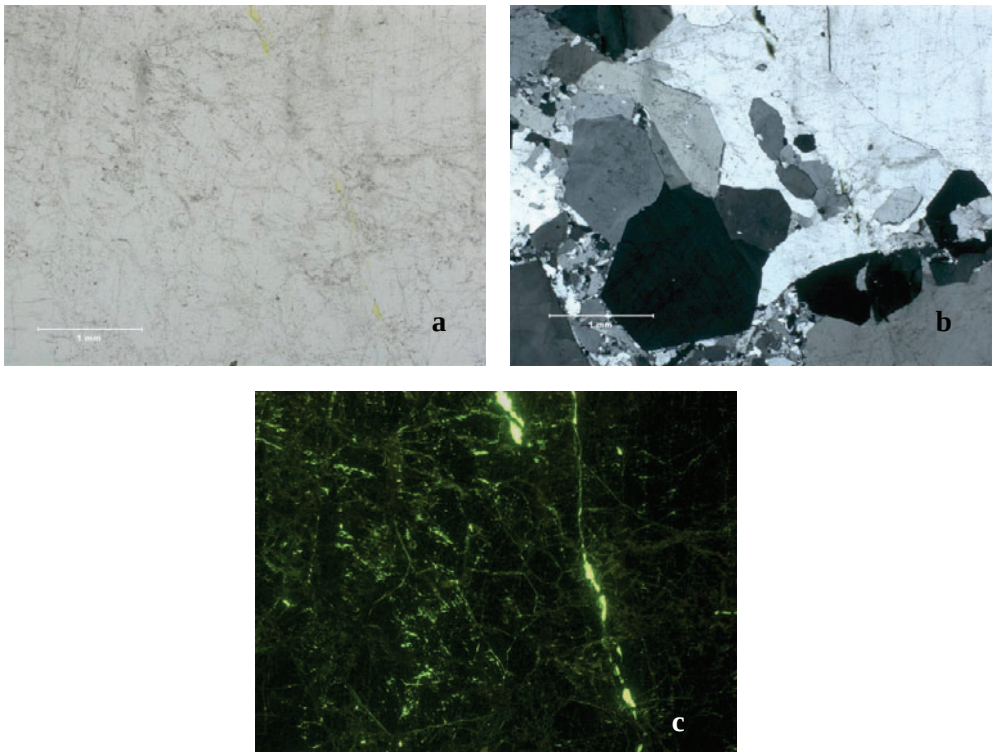

Figure 3-5 Micrographs of Pegmatite D. The large quartz grains show polygonal grain boundaries and subhedral crystal growth whereas the most fine-grained quartz shows lobate grain boundaries and anhedral crystal growth. The largest samples show typical undulating extinction as sign of strain. Micrographs **a** and **b** shows the same area but in ppl and xpl respectively. Micrograph **c** shows the same area in fluorescent light. Note the weak traces of grain boundaries denoting each grain. E.g. the large extinct grain to the lower left in **b** is clearly filled with micro cracks as seen in **c**.

3.6 Quartzite E

3.6.1 Macroscopic description

The sample material contains typically grayish to deep violet fragments (ca 50 to 120 mm), probably originating from different areas of the deposit. The sample is from a rock quartz and resembles a typical quartzite. Quartz is the dominating mineral and no additional minerals can be seen.

3.6.2 Microscopic description

Mineral content: Quartz: 99%; Mica: ~1%; Zircon/monazite: ~0.5%; trace of iron-hydroxides

Quartz: Microscopically, Quartzite E (Figure 3-6a and b) contains mostly relatively equigranular fine-grained (0.2 – 1 mm), rounded quartz grains with little overgrowth. The original clastic grain boundaries may frequently be seen as week traces of iron hydroxide staining ("dust rims") throughout the sample. At some areas, there are signs of weak layering with respect to grain size. The structure resembles a meta-sandstone or very low grade metamorphic quartzite and the clastic rounded grain shape is still present. Some fluid inclusion may be found within some of the clastic grains. Undulating extinction is commonly typically shady but some grains my show sign of subgrain formation.

Mica: Minor mica as small aggregates within grain boundaries and possibly some clay minerals

Zircon/Monazite: Differentiating these minerals in optical microscopy is difficult because of the small grain size. They appear as interstitial grains, approximately 100 μm in size. The interference colors are typically 3rd to 4th order. The presence of both zircon and monazite were confirmed by cathodoluminescence microscopy and spectroscopy (Paper IV).

Iron-hydroxides: Occur as reddish staining between grains and frequently as small particles along the rims between the primary detrital quartz grains and the overgrowth.

3.6.3 Fluorescent light

Fluorescent light microscopy (Figure 3-6c) shows mainly that the grain boundaries are relatively open. It also shows that there are a few cavities in between the clastic grains. However, this may also be result of quartz grains falling out of the sample during sample preparation.

3.6.4 Cathodoluminescence microscopy and spectroscopy

Cathodoluminescence microscopy and spectroscopy (Paper IV) of Quartzite E indicates that there are three main types of sources for the clastic grains. These are related to igneous- and regional metamorphic rocks. However, random grains of quartz from hydrothermal- and volcanic sources are also found.

Cathodoluminescence microscopy and spectroscopy distinguishes zircon and monazite based on the luminescence peaks for REEs in the minerals. Additionally, zircon has higher CL intensity and monazite induce radiation halo in the neighboring quartz grains (only visible in CL).

3.6.5 Conclusion

Quartzite E has the typical texture of low-grade metamorphic quartzite. Initial quartz overgrowth is present however, the shape of the old clastic grains may be recognized and the grain boundaries are relatively open.

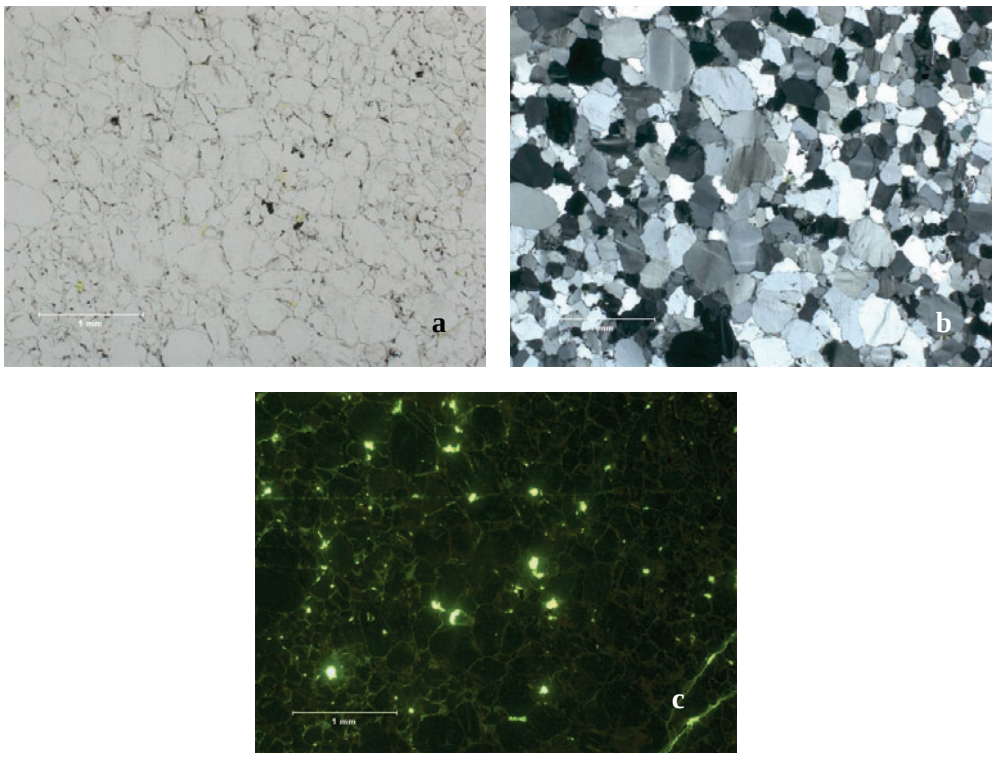

Figure 3-6 Micrographs of Quartzite E shows a typical low-grade metamorphic quartzite or possibly a meta-sandstone (**a** and **b** are under ppl and xpl respectively). The shape of the grains is relatively rounded with only little overgrowth. Some of the grains show primary oriented undulating extinction. Micrograph **c** are under fluorescent light, and shows that the grain boundaries can be followed around each single grain and thus, appears relatively open.

3.7 Gravel F

3.7.1 Macroscopic description

The sample material contains boulders (ca 50 to 100 mm) of typical medium-grained gravel quartz. The color of the investigated specimen is typically rusty-brownish with each grain being difficult to distinguish. Quartz is the dominating mineral and minor mica is seen. Gravel F appears somehow not so massive because of the high amount of iron-hydroxide staining/layering.

3.7.2 Microscopic description

Mineral content: Quartz: 99%; Mica <1%

Quartz: The PTS (Figure 3-7a and b) consists of inequigranular (0.2 – 2 mm) to seriate, anhedral quartz grains with mostly lobate grain boundaries. 120° triple-junctions indicate recrystallization. Some layering is seen with respect to grain size. Some areas show weak preferred orientation with concentrated layers of elongated quartz grains. Only minor amounts of fluid inclusions are observed, these are oriented in trails.

Mica: Mica is disseminated in the sample or as band along grain boundaries.

3.7.3 Fluorescent light

Epoxy occurs all over occupying open grain boundaries and cavities in the rock showing an open grain boundary texture (Figure 3-7c).

3.7.4 Cathodoluminescence microscopy and spectroscopy

No CL on this sample.

3.7.5 Conclusion

It appears that the source for Gravel F is low-grade metamorphic hydrothermal vein quartz.

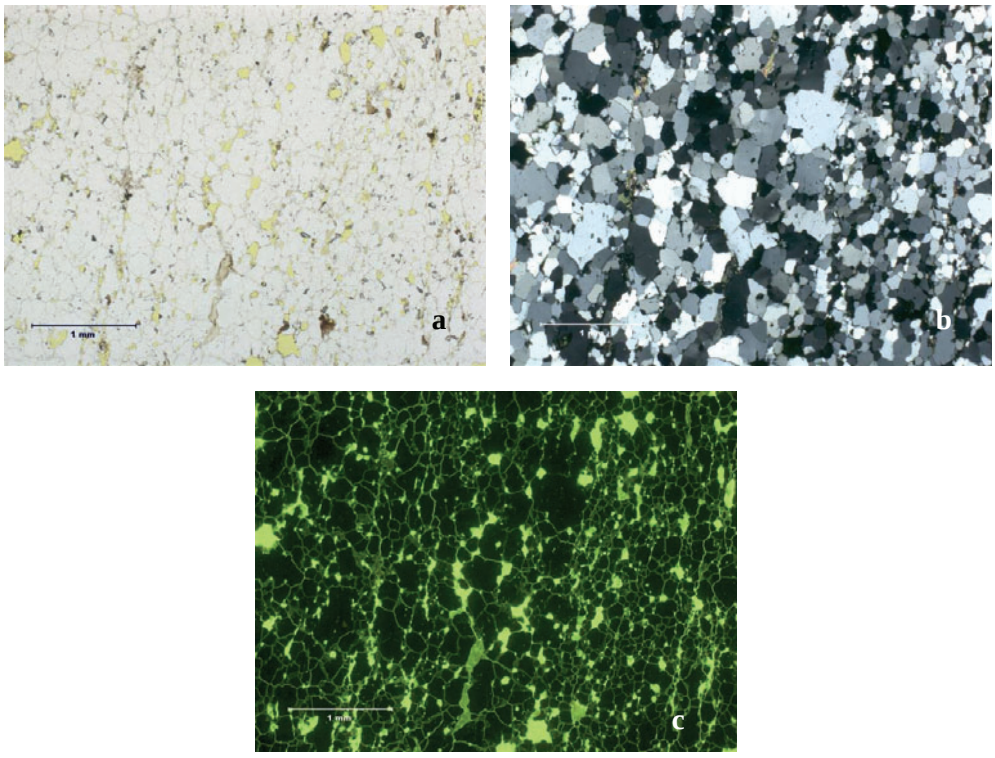

Figure 3-7 Micrographs **a**, **b** and **c** of Gravel F shows the same area however, ppl, xpl and fluorescent light respectively. Although lobate grain-boundaries, 120° triple-junctions are frequent, especially between the largest grains. This is easily seen in micrograph **c.** Note the tendency of layering with grain sizes more fine-grained to the right and more coarse-grained in the middle of the sample area. Fluorescent light microscopy shows that the grain boundaries are relatively open and the single grains can be easily distinguished. Some cavities are seen probably related to loss of grains during sample preparation.

3.8 Gravel F-2

3.8.1 Macroscopic investigation

Gravel F-2 is a typical fine- to medium-grained gravel quartz boulder. It is a well-rounded boulder and the color of the investigated specimen is typically rusty-yellowish on the weathered surface. The sample appears massive, with each grain of quartz being well pronounced as rounded grains. Quartz is the dominating mineral in the specimen.

3.8.2 Microscopic investigation

Mineral content: Quartz: >99%; Mica: <1%

Quartz: The PTS (Figure 3-8 a and b) consists of seriate (0.5 to 5 mm) anhedral quartz with polygonal to lobate grain boundaries. 120° triple junctions are frequent. Some of the coarse-grained quartz shows subgrain formation. Only minor amounts of fluid inclusions are seen.

Mica: A few mica grains are seen along grain boundaries.

3.8.3 Fluorescent light

No fluorescent light microscopy on this sample.

3.8.4 Cathodoluminescence microscopy and spectroscopy

The transient blue CL as described in Paper IV is typical for hydrothermal vein quartz and thus, indicates that the source of the investigated sample is from typical hydrothermal vein quartz.

3.8.5 Conclusion

Sample Gravel F-2 is interpreted to represent metamorphosed hydrothermal vein quartz. The transient blue CL confirms that the investigated sample is of typical hydrothermal vein quartz.

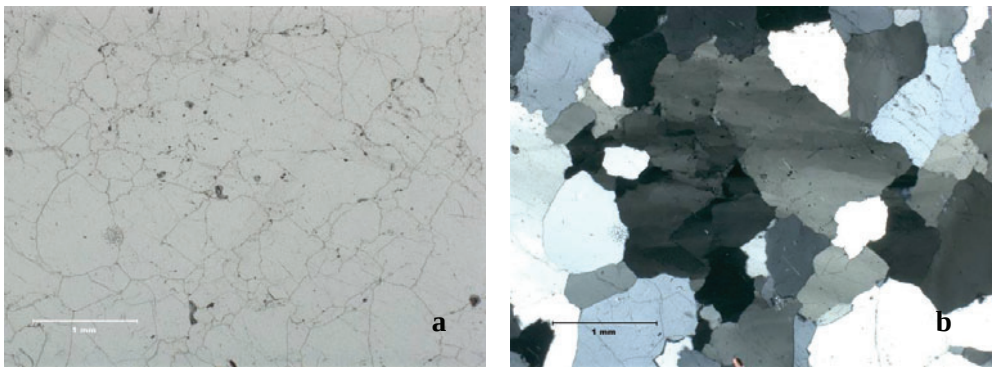

Figure 3-8 Micrographs of Sample F-2 **a** and **b** is ppl and xpl respectively. Lobate to polygonal grain boundaries and some 120° triple-junctions are recognized. The largest (primary) grains show signs of undulating extinction and some sub-grain formation.

3.9 Hydrothermal "Pilot"

3.9.1 Macroscopic description

The Hydrothermal "Pilot" samples are of a smaller fraction (3-25 mm) and represents crushed material from an original 30-120 mm fraction that is used for ordinary silicon metal production. The crushing was according to Myrhaug and Monsen (2002) carried out to achieve the correct size distribution for the pilot scale furnace experiments. Only one PTS was investigated from this sample.

Sample Hydrothermal "Pilot" consists of coarse-grained white (milky quartz) fragments of typical hydrothermal appearance. Quartz is the dominating mineral except a few fragments with minimal iron-hydroxide staining.

3.9.2 Microscopic description

Mineral content: Quartz: ~100%

Quartz: Sample Hydrothermal "Pilot" (Figure 3-9a) consists of inequigranular to seriate fine- to coarse-grained (0.2 – 20+ mm) quartz with polygonal to lobate grain shape. The crystal growth is typically subhedral for many of the intermediate and large grains whereas the fine-grained material is more anhedral. Some of the large, old grains show typical strained quartz with subgrain formation. Some fractures in the large grains contain fine-grained recrystallized quartz. The sample is loaded with fluid inclusion trails.

3.9.3 Fluorescent light

Fluorescent light microscopy (Figure 3-9b) shows that the grain boundaries are relatively open as they can be followed as fluorescent traces between especially the coarser-grained quartz. Few micro cracks can be seen. The cavities are probably related to loss of grains during sample preparation.

3.9.4 Cathodoluminescence microscopy and spectroscopy

No CL investigation of this sample.

3.9.5 Conclusion

Sample Hydrothermal "Pilot" has been interpreted to represent a typical metamorphosed hydrothermal vein quartz.

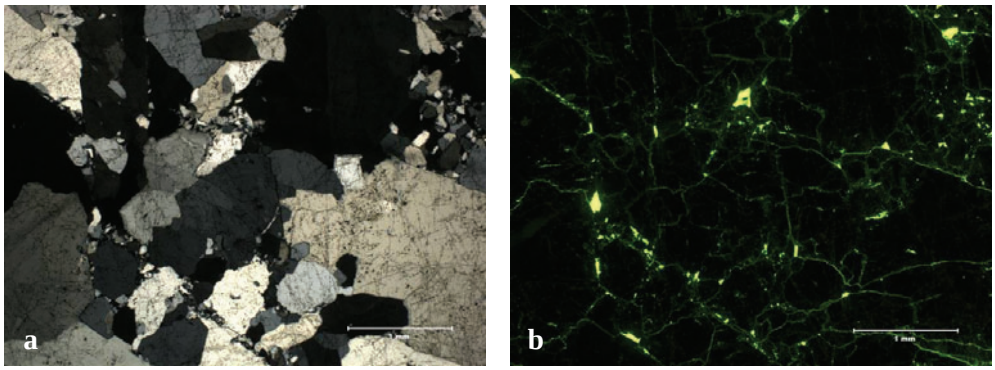

Figure 3-9 Micrographs **a** and **b** shows Sample Pilot under xpl and fluorescent light respectively. Note the relative open grain boundaries seen in fluorescent light. Also some minor micro cracks may be seen.

3.10 Chemical analyzes

ICP-ms analyses on Samples A to F (Table 3-2) was carried out by Elkem Research and presented in Birkeland (2004). Analyses of Hydrothermal "Pilot" (Table 3-3) were performed by MoLab and presented in Myrhaug and Monsen (2002). The analyses show that all quartz types are relatively pure. Hydrothermal C is extremely pure whereas Quartzite E and Gravel F are relatively impure.

Table 3-2 Chemical analyzes of samples investigated. The analyses of Sample A to Sample F were performed by Elkem Research and reported in (Birkeland, 2004).

Enhet	Element	Gravel A	Gravel B	Hydrothermal C	Pegmatite D	Quartzite E	Gravel F
%	Al	0.042	0.074	0.012	0.169	0.212	0.460
%	Ca	0.006	0.003	0.001	0.003	0.003	0.010
%	Fe	0.021	0.031	0.020	0.024	0.084	0.288
%	Ti	0.003	0.004	0.001	0.002	0.020	0.013
%	Co	0.0001	0.0001	0.0001	0.0001	0.0001	0.0001
%	Cr	0.0007	0.001	0.0009	0.0009	0.0015	0.0013
%	Cu	0.0001	0.0001	0.0001	0.0002	0.0001	0.0002
%	Mn	0.0031	0.0052	0.005	0.0041	0.0073	0.0074
%	Ni	0.0001	0.0001	0.0001	0.0001	0.0001	0.0001
%	V	0.0001	0.0001	0.0001	0.0001	0.0002	0.0003
%	Zr	0.0001	0.0001	0.0001	0.0001	0.0045	0.0006
%	Be	0.00001	0.00001	0.00001	0.00002	0.00001	0.00001
%	K	0.003	0.008	0.001	0.017	0.063	0.060
%	Li	0.000	0.000	0.000	0.001	0.000	0.000
%	Mg	0.004	0.003	0.000	0.002	0.005	0.163
%	Na	0.002	0.005	0.002	0.002	0.003	0.006
%	Sum alkali_el.	0.0096301	0.015751114	0.0035378	0.021781462	0.071357518	0.228925576

Table 3-3 Chemical analysis of Sample Pilot performed by MoLab and reported in (Myrhaug and Monsen, 2002).

Enhet	Element	Hydrothermal "Pilot"
%	SiO_2	99.5
%	Al_2O_3	0.36
%	Fe_2O_3	<0.01
%	TiO_2	<0.01
%	MnO	<0.01
%	CaO	0.06
%	MgO	0.02
%	K2O	0.01
%	Na2O	<0.01

3.11 Concluding remarks

The petrographic investigations reveal that most of the quartzes show signs of high strain within the primary, coarse grains. This is seen by the subgrain formation that is present in the primary grains in most samples. Gravel E also shows some signs of strain within single grains but this is probably strain induced before the quartz grain was removed from its original environment by erosion. Recrystallization is mostly related to low temperature regimes and increasing strain rate. Formation of small new grains along fractures and grain boundaries indicates bulging recrystallization (BLG) (Passchier and Trouw, 2005). This is a result of dynamic deformation. Deformation lamella is also seen especially in Samples A to C, where sample C shows the highest content of such lamellas.

The micro textures of the samples investigated varies significantly. Quartzite E differs from the rest of the samples by its fine-grained, well-rounded detrital quartz grains with little overgrowth and open grain boundary textures. The most similar sample is probably Gravel F, with grain size and open grain boundary texture that resembles Quartzite E, however, probably a metamorphosed hydrothermal vein quartz comprising recrystallized quartz grains.

Gravels A and B and Hydrothermal C comprises similar textures with the coarse-grained quartz and sealed grain boundaries. The last group of similar samples includes Gravels B-2 and F-2 and Pegmatite D.

Based on the micro textures, the mechanically and thermo-mechanically strongest samples are probably Quartzite E and Gravel F with its fine-grained and lobate grain boundary textures that will cause fractures to follow the mechanically weakest path through the rock (e.g. Malvik, 1988), which is along grain boundaries. This path will require a long traveling distance and therefore breaking the sample will be difficult. Similarly, the weakest samples are probably the coarse-grained and polygonal grain boundary textured samples Gravels A and B and Hydrothermal C. Here the lack of weak grain boundaries cause the fracture to follow the shortest path straight through each single grain and thus the rock will brake more easily than the fine-grained samples.

4. Methods

This chapter summarizes the experimental and analytical methods used in the research work that make the basis of this thesis. Some of the techniques are standard petrographic tools and described only briefly (e.g. optical microscopy). Other techniques are less common and described in more detail (such as cathodoluminescence and high temperature microthermometry). Relevant methods are also described in the different papers, but often in less detail. Thus, this chapter gives additional detail and collective description to the methods used in the papers in Part 2 of the thesis (Paper III to VI).

The choice of initial methods for the investigations of the thermo-mechanical properties of the quartz was based on earlier work within this field as well as the available material and equipment. Further investigations were based on the results of the initial investigations.

4.1 Optical Microscopy

The optical microscopy (polarized light) investigations were carried out on a Nikon Eclipse E600 microscope. The microscope was equipped with both transmitted and reflected light system. A 2 megapixels SPOT Insight IN320 color digital camera from Diagnostic Instruments Inc. was mounted on the trinocular tube and connected directly to a PC for real-time computer storage and image enhancement using SPOT software.

4.1.1 Fluorescence microscopy

The fluorescence microscopy was carried out on the same microscope as with polarized light microscopy. The microscope was additionally equipped with a Nikon High Pressure Mercury Lamp. Power supply type C-SHG1, mercury lamp type HBO 103/2 HG-100W and Y-FL EPI fluorescence attachment with excitation filter EX 450-490; dicroic mirror DM 505; barrier filter BA 520.

Fluorescence microscopy enables visualization of e.g. micro cracks, grain boundaries and cavities as any such features will be filled with fluorescent epoxy during sample preparation. The fluorescent epoxy will fluoresce when illuminated by UV light from the mercury lamp, as the UV light will excite the epoxy. The filters block any other emitted excitation signals and allow only the emission from

the excited epoxy to pass through to the eyepiece of the microscope. Thus, the fractures, cracks and cavities may easily be seen in the microscope if present.

4.1.2 Sample preparation of polished thin sections

Polished thin sections (PTS) for microscopic investigations were prepared at the sample preparation lab at the Dept. of Geology and Mineral Resources Engineering, NTNU. The samples were prepared as standard 28x48 mm section and approx. 30 μm thick. The PTS were impregnated with Epo-tek 301 from Epoxy Technology before sample preparation. For fluorescence microscopy, Epodye powder from Struers was mixed with the Epo-tek 301 epoxy to give the fluorescence properties.

4.2 High-Temperature Micro Thermometry

A Linkam HTS1500 High Temperature System was used to investigate visible effects during heating of quartz up to temperatures as high as 1350ºC (capacity of 1500 °C).

The stage was mounted on a Nikon Eclipse 600 ME optical microscope with both transmitted and reflected light.

The Linkam TS1500 system consists of:

- TS1500 High Temperature Stage 7/3
- TMS94/ Temperature Programmer
- PSU (Power Supply Unit)
- ECP Water Circulator

The Linkam system was completed with:

- The microscope – Nikon Eclipse ME600 optical microscope – transmitted and reflected light
- Nikon objectives (x10, x20 and x50). Extra long working distance (ELWD) for x20 and x50 objectives.
- Pixelink digital camera (1.3 megapixels)
- PC
- Linksys 32DV software

The PSU, TMS94 Temperature Programmer and the TS 1500 High Temperature Stage are shown in Figure 4-1. The system has the ability to heat small samples from room temperature to 1500 °C at rates from 0.01 to 130 °C/minute. The

programmer can be programmed with 100 ramps for heating or cooling with different rates at different intervals. Additionally the Linksys 32DV software allows for controlling the temperature controller from the PC along with automatic image capture at a preset interval for each temperature ramp.

The sample chamber makes an extra long working distance for the objective lens necessary (minimum 6 mm). In addition, a condenser extension lens (12.5 mm) is necessary for Nikon microscopes (Figure 4-2). This was supplied by Linkam.

Figure 4-1 The Linkam TS 1500 stage connected to the PSU and the TMS 94 temperature controller (photo: www.linkam.co.uk)

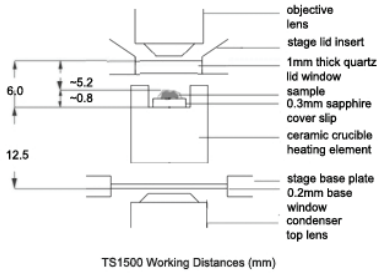

Figure 4-2 Schematics of the working distances for the Linkam TS 1500 stage (illustration: www.linkam.co.uk)

4.2.1 Sample preparation for high-temperature microthermometry

Samples for high-temperature micro thermometry were prepared as polished thick sections. These were prepared as PTS but the thickness of the sections was retained to about 200-250 µm. During preparation, the thick section is mounted on the glass plate using an epoxy easily dissolved using acetone. Thus, the thick section could easily be removed from the glass plate after preparation.

Before investigations in the heating chamber, the size of the sample needed to be reduced to less than 7 mm across to fit inside the furnace. This was made by simply breaking the thick section into smaller pieces. Samples were placed on top of a 7 mm sapphire disc inside the ceramic heating crucible in the heating stage.

4.2.2 High-Temperature Microthermometry

The Linkam High Temperature system (and other high temperature systems) has been reported used for high temperature microthermometry of melt inclusions in magmatic rocks and for use in the study of high temperature investigations of metallurgical and refractory application. However, little work has been reported on the use of such investigations on the behavior of a specific mineral at high temperatures. The only (unpublished) report is that of Birkeland and Carstens (1969). This work has been briefly reviewed in Paper I.

However, the Linkam system should be able to provide a great opportunity to investigate the effects of heating of small quartz samples in real time as well as documentation of all the effects should be taken care of by the Linksys 32DV-system.

4.3 Shock-heating of lump quartz

The shock heating of lump quartz samples was performed in two sequences in an ASEA induction furnace at SINTEF Materials and Chemistry. The furnace is working at 3830 Hz and has a capacity of 50 kg of steel. To monitor the temperature, a thermo element type S was used. A graphite crucible was used to hold the samples in the furnace.

During experiments, SiO_2 based insulation was used to cover the open side (top) of the furnace to prevent heat loss. This contributed to keep the temperature stable during the entire experiment as well as letting the furnace reach the target temperature faster after inserting the sample.

Observations during the heating, such as audible and visual effects, were noted for all samples. After heating, all samples were quenched at room temperature and prepared for further analysis and investigations (e.g. optical microscopy, X-ray diffraction and cathodoluminescence).

4.4 X-ray Diffraction (XRD)

4.4.1 Equipment and procedure

XRD analyses were carried out at the Department of Geology and Mineral Resources Engineering, NTNU, on a Philips PW 1830 XRD with CuK_α radiation at 2-60° 2θ with step size 2° 2θ and 2 sec. per step. XRD samples were first milled in

a laboratory disc mill to approximately -40 μm before pressed to pellets (approx. 5 g sample material) and analyzed.

Alternatively, for experiments presented in Paper VI, small amounts of the samples were scraped off and placed on a glass plate to limit the area of investigation and concentrating on only the interesting material.

4.4.2 XRD on silica polymorphs

The XRD-instrument used in the experiments presented in this thesis was not optimized for silica polymorph discrimination. This is not a problem when using the XRD for qualitative analysis in order to identify different phases present in the samples. However, when using the XRD for quantitative analysis, the lack of standardization routines creates a problem for the precision of the analysis.

4.4.3 Quantitative XRD-analysis and standardization

The cristobalite standard was produced by SINTEF Energy Conversion and Materials from pure Norquartz 60. The quartz was crushed to approximately 1 mm and fired at 1500 °C (ambient pressure) for 48 hours in an Alsint crucible to produce pure cristobalite with final cristobalite concentration measured by XRD to 99%.

Standards for both XRD and DTA were made by mixing pure quartz (from Sample Hydrothermal C) with the cristobalite to a known content of cristobalite and quartz. The material was mixed carefully in an agate mortar to ensure complete mixing of the two materials. Additional pure samples of cristobalite and quartz were used to make a series of 0, 10, 25, 50, 75, 90 and 100% cristobalite.

Quantification of cristobalite and quartz were performed on the standards by normalizing the 0.245 nm peak of quartz and the 0.405 nm peak of cristobalite to 100 %. The deflection of quartz was given a factor of 1.0 as a regular procedure for the XRD instrument used. The cristobalite deflection was given a factor of 0.1 by means of trial and error.

4.5 Differential Thermal Analysis

4.5.1 Equipment and procedure

The Differential Thermal Analysis (DTA) was carried out on a DTA apparatus at the Dept. of Geology and Mineral Resources Engineering, NTNU (as designed by R. Selmer-Olsen in 1957 and with several modifications thereafter). Al_2O_3 was used as reference material.

Analysis were carried out at a heating rate of 10 °C/min from room temperature up to 700 °C. Cooling of the samples was simply done by cutting the power and letting the samples cool at natural rate. Logging was performed during heating and during cooling down to 500 °C. Below this temperature, cooling is too slow to give any comparative reading. The cristobalite content was calculated using the area of the peak of the α-cristobalite to β-cristobalite transformation at approximately 240-270 °C.

This DTA-instrument has a good reputation for its qualities on quantifying quartz contents in rocks for drillability tests (Bruland, 1998).

4.5.2 DTA on silica polymorphs

The analysis presented in this thesis was the first carried out on discriminating silica polymorphs using this DTA equipment. It was early clear that the α-cristobalite to β-cristobalite transformation easily could be detected as the DTA curve showed a nice drop in μV and the hysteresis that always follows the α-cristobalite to β-cristobalite was seen at the expected temperature (between 240 and 272 °C). Unfortunately, due to the set up of the DTA, it was not possible to see the opposite transformation (β-cristobalite to α-cristobalite) since the equipment could not be configured to cool down at a controlled rate to the temperatures needed without significant modifications.

4.6 Cathodoluminescence

4.6.1 Principles of Cathodoluminescence

When a sample is bombarded by an energetic electron beam, the electron beam will, according to e.g. Goldstein (2003), interact with the sample and generate effects such as characteristic x-rays, secondary and backscattered electrons and

cathodoluminescence, as well as heating the sample. The interaction effects are illustrated in Figure 4-3.

The energy of the electron beam is at maximum when entering the sample and decreases with the distance covered within the sample. The cathodoluminescence signal is generated at the low end of the energy scale of the electron beam in semiconductors and insulators (Figure 4-4). Penetration depth of the electron beam and hence excitation depth is dependent on the energy of the electron beam. For electron beam of 10-20 keV, the CL signal is typically generated to depths of 2-8 µm below the sample surface in nonmetallic minerals (Marshall, 1988).

Cathodoluminescence is produced by energetic electrons and is caused by excitation of an electron in the valence band to a higher state. When the electron returns to a state of lower energy, a photon is emitted. This photon is in the UV, visible or IR range. Most frequently, it is observed in the visible range of the electromagnetic spectrum, which is about 400 nm (blue) to 700 nm (red). The photon responsible for generating CL is emitted from the valence band or the molecular orbital (several eV) (Takakura *et al.*, 2005) whereas the photon generating X-rays (detected by WDS (EPMA) or EDS) is emitted from inner shell electrons (100 eV to 10keV).

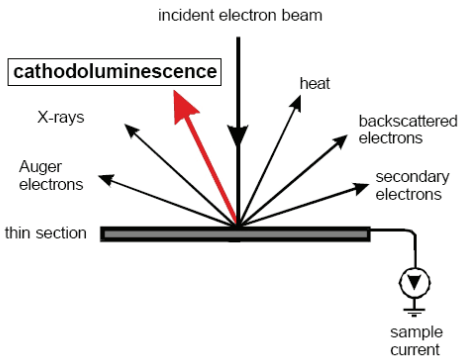

Figure 4-3 Signals generated from interaction between the primary electron beam and the sample (after Müller, 2000)

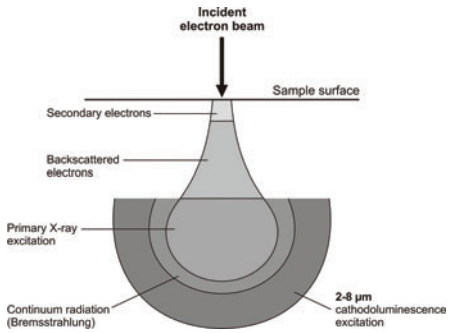

Figure 4-4 Incident electron beam interaction volume. CL signals are produced down to typically 2-8 µm (after Marshall, 1988)

Cathodoluminescence is the least understood method in luminescence phenomena (Townsend and Rowlands, 2000). CL analysis can be carried out on nonmetallic material, either organic or inorganic and the characteristic luminescence is caused by lattice defects derived from chemical substitution or growth related lattice

mismatches, point defects or non-stochiometry. Point defects can be subdivided into 1) extrinsic (trace elements) and 2) intrinsic (lattice defects) as illustrated in Figure 4-5. The trace elements responsible for the extrinsic CL are also called activators.

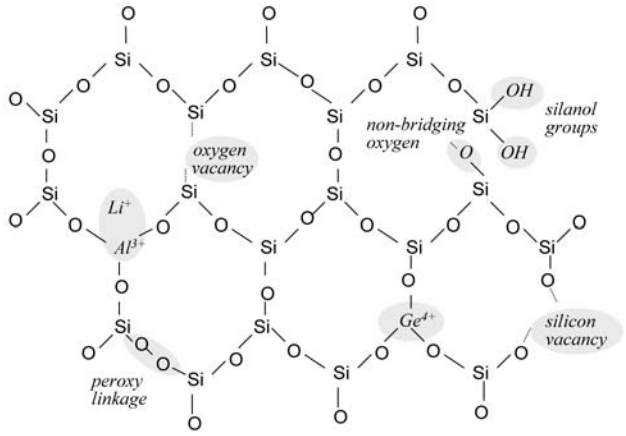

Figure 4-5 Schematic quartz structure showing the most common intrinsic and extrinsic lattice defects (after Götze *et al.*, 2001)

4.6.2 Instrumentation

There are two main types of CL equipment. These are 1) CL connected to a scanning electron microscope (SEM), EPMA or transmission electron microscope (TEM). 2) CL generated by electron gun (or hot cathode) connected to an optical microscope. Here, the stage is mounted on the object table on the microscope and a cold (or hot) cathode generates the electron beam, which then generates the CL signal from the sample.

For the work presented in this thesis, CL data were acquired with a hot cathode CL microscope, HC1-LM as described by Neuser *et al.* (1996). The system was operated at 14 kV accelerating voltage and a current density of about 10 μA/mm^2. Luminescence images were captured "on-line" during CL operations using a peltier cooled digital video camera (KAPPA 961-1138 CF 20 DXC). CL spectra in the wavelength range 380 to 850 nm were recorded with an Acton Research SP-2356 digital triple-grating spectrograph with a Princeton Spec-10 CCD detector attached to the CL microscope by a silica-glass fiber guide. The wavelength of the CL spectrometer was calibrated against an Hg lamp. Each spectrum was obtained with a certain acquisition time, depending on the intensity of the CL emission.

4.6.3 CL on Geological Material

Cathodoluminescence has a wide range of application in geosciences and the technique is widely used for different investigations of geological material. The luminescence is observed as internal zoning or color differences within minerals. The technique is widely used to detect information not available by other analytical methods (e.g. optical microscopy). This includes growth zoning and distinguishing different generations of crystallization. For quartz-arenites and quartzites, different sources for detrital grains and quartz-overgrowth can be revealed with CL.

The main usage is listed below and the minerals in question are mentioned in parentheses (after Pagel *et al.*, 2000b):

– Quantitative separation of Different Mineral Species (e.g. differentiation of calcite and aragonite by the spectral position of the Mn CL band)

– Evidence of different mineral generations from CL Observations (e.g. differentiation of detrital grains in a silicoclastic rock)

– Zonation of Crystals (e.g. sectorial- or intrasectorial zoning in quartz)

– Microfracturing, brecciation, crushing (e.g. existence of a microfractured healed plane in quartz)

– Textural relationships between minerals (e.g. recrystallization grain boundary alteration in quartz)

– Location of trace elements (e.g. REE in carbonates)

– Zone of past α-irradiation (e.g. quartz)

4.6.4 CL on quartz

During the last few decades cathodoluminescence (CL) has proved to be a powerful technique for the investigations of textural features of minerals (e.g. Marfunin, 1979; Remond, 1992; Pagel *et al.*, 2000b). The CL spectra from crystalline and amorphous SiO_2 (silica) polymorphs typically have broad overlapping emissions (Stevens Kalceff *et al.*, 2000). According to Götze *et al.* (2001), the luminescence of SiO_2 is generally weak and the main luminescence bands of the crystalline silica modifications and amorphous silica are similar.

CL investigations of quartz samples may easily detect features that may not be seen in the optical microscope. Examples of such properties are listed above. Distinguishing different sources of clastic quartz grains is one example that was reported in Paper IV. Another is the determination of past α-irradiation of quartz

from neighboring monazite and zircon grains that contains radioactive elements was also reported in Paper IV.

However, the main usage of CL in this thesis is determining and distinguishing the genesis of the different quartz raw materials and were based on published material as reviewed below:

Several investigations have proved that quartz of different types and origin shows distinctive luminescence characteristics during electron bombardment (e.g. Ramseyer *et al.*, 1988; Ramseyer and Mullis, 1990; Watt *et al.*, 1997).

Quartz from igneous and regional metamorphic rocks mostly show characteristic, stable luminescence with two emission bands centered around 450 and 650 nm. Quartz from igneous rocks shows a predominance in the 450 nm band causing different shades of blue CL colors (e.g. Müller *et al.*, 2000; Götze *et al.*, 2001; Müller *et al.*, 2002). The luminescence at 450 nm has been associated with a twofold coordinated Si on an O vacancy (e.g. Skuja, 1998; Fitting *et al.*, 2001). Quartz from regional metamorphic rocks is dominated by the 650 nm emission band causing a reddish to reddish-brown CL color (e.g. Zinkernagel, 1978; Neuser *et al.*, 1989) and this luminescence is related to a non-bridging oxygen hole center, NBOHC (Sigel and Marrone, 1981).

Hydrothermal quartz typically shows short-lived blue or bottle-green CL colors (e.g. Ramseyer and Mullis, 1990). Götze *et al.* (2001)relate the transient blue CL, which changes to brown CL during electron beam irradiation, to the decrease in the luminescence intensity in the emission bands just below 400 nm and/or at 500 nm. Götze *et al.* (1999) detected another yellow CL emission in hydrothermal vein quartz and agate of acidic volcanics. The luminescence emission band is centered at ca. 580 nm. The yellow emission at 560-580 nm was first seen by Rink *et al.* (1993) in TL spectra of natural hydrothermal quartz and interpreted as related to oxygen vacancies.

Götze *et al.* (2005) found that the luminescence of quartz from granitic pegmatite is characterized by a transient bluish-green luminescence emission with bands at around 400 nm and 505 nm.

Some good references for more details on cathodoluminescence are e.g. Marshall (1988), Pagel *et al.*(2000a) and Zinkernagel (1978).

5. Summary of papers

This chapter presents a short summary of the papers presented in Part 2 of the thesis. The summary of the papers is organized in the same sequence as they are presented in Part 2. This sequence is chronological and thus reflects the order of the work through the PhD period.

Papers I-III have been published at conferences with peer review. Paper IV has been submitted for publication in an international peer review journal. The two last papers have been prepared for publication and will be submitted later.

5.1 Paper I

Aasly, K. Malvik, T. and Myrhaug, E. (2006) A review of previous work on important properties of quartz for FeSi and Si metal production. INFACON XI, 1, p. 393-401. February 18-21, 2007 New Dehli, India.

This paper presents a review of the work carried out on the important properties of quartz for FeSi- and Si-metal production. The paper is based mainly on internal- and unpublished reports, but also present results from papers presented in international publications.

The works carried out have mainly focused on the thermo-mechanical properties of the quartz but has also to a certain degree, touched the softening properties of the quartz.

One of the important properties that have been discussed in this review is the volume expansion that takes place between 850 °C to 1000 ºC and results in explosive disintegration for some quartz types. No final and definite conclusions have been made but several reasons have been mentioned: The influence of the phase transformation to tridymite, which takes place within the same temperature interval, has been discussed in several papers. Alkali impurities have been mentioned as a critical factor for this transformation to take place. Other researchers have mentioned mica impurities as a critical factor for the behavior of the quartz at these temperatures and it seems that this is probably the most important factor. Studies of fluid inclusions in quartz was reported in some papers focusing on the volume expansion of these inclusions during heating as a cause for the explosive disintegration of the quartz, especially along planes of healed micro fractures that often contain vast numbers of such inclusions.

Several methods for investigations of the important properties of quartz have been presented and these provide a good basis for the further research on quartz raw materials. This review shows that study of the thermo-mechanical properties of quartz is a complex field and more extensive research is needed to achieve more knowledge about these properties.

5.2 Paper II

Aasly, K. Malvik, T. and Myrhaug, E. (2006) Quartz for carbothermic production of silicon - effect of the process steps, handling and transport from mine to furnace. Silicon for the Chemical Industry VIII, p. 9-18. June 12-16, 2006. Trondheim, Norway.

This paper presents a literature study where the objective was to identify critical factors during production, handling and transport of the quartz raw material for (Fe)Si production from the mine to the furnace. This paper presents a brief literature study to evaluate the importance of the knowledge of the geological history of the quartz deposit. It looks at the importance of using the right extraction methods and that it is important to look at the combined effects of mining and processing to achieve the best possible products. The paper also looks at the transport and storage at the different locations of the raw materials, and especially the significance of the repeated reloading of the materials during transport and storage, and related falls through significant heights.

Careful handling of the materials is important for keeping the required or optimal strength and fragment size of the materials. Gravel- and rock quartz can be useful classification in qualitative terms, as the gravel quartz will be stronger than the rock quartz for two main reasons: Micro cracks are induced in the rock quartz by the blasting operations, and natural selection has left only the mechanically strongest quartz boulders in the gravel deposits. Drilling and blasting combined with the processing (crushing) of the raw materials are important for the generation of fines during further handling and finally inside the furnace. Further, it has been demonstrated that the total number of meters of fall that the quartz has been exposed to is crucial for the increase of fines during material handling. This is a problem on both the mineral production plant in the stages after the crushing and sieving and on the metallurgical plants from the unloading of the ship to the charging on the furnace. Other factors that might influence the final fines content are also mentioned, such as segregation of materials, as well as the effects of outside storage of materials.

5.3 Paper III

Aasly, K. Malvik, T. and Myrhaug, E. (2007) Advanced Methods to Characterize Thermal Properties of Quartz. INFACON XI, 1, p. 381-392. February 18-21, 2007 New Dehli, India.

Paper III reports high temperature experiments on the raw materials that have been investigated with respect to their thermo-mechanical properties. In order to investigate the effect of the thermal shock caused by the rapid heating of quartz when it enters the furnace, two types of high temperature experiments were carried out:

- Heating stage microscopy (high-temperature microthermometry) for in situ observation of heating effects.
- Shock-heating of quartz in an induction furnace

An optical microscope-mounted heating stage was used for in situ observations of the microscopic effects of heating up to 1350 ºC. The effects of heating were observed at different temperature intervals in different samples. The main temperature intervals were below 573 ºC and above 1000 ºC. The cause of the observed effects is interpreted as fluid inclusion decrepitation for T<573 °C and structural implications (micro cracks, grain boundaries and remaining fluid inclusions) at T>1200 °C. Some effects were also seen at temperatures around 573 °C related to the α- to β-quartz transformation. Some of the samples also showed significant effects at 900 to 1000 °C, probably related to mica impurities in grain boundaries.

Shock heating of the samples was carried out in an induction furnace to 1300 ºC for ten minutes. The effects of the heating were studied with different techniques such as direct observation during and directly after heating, optical microscopy (polarized- and fluorescence light) and XRD. Combined polarized- and fluorescence light microscopy indicate that the heated quartz shows an opening of the grain boundaries and evenly distributed micro cracks that were not present in the unheated reference samples. Some of this wide opening of grain boundaries may be related to the same effects seen in high temperature microthermometry caused by mica impurities. Mica was seen along grain boundaries in the corresponding reference samples Pegmatite D and Gravel F. In some of the heated samples, weak generation of cristobalite was detected by XRD. No tridymite was seen in any of the samples.

Tridymite formation, seem to be ruled out as cause for the effects seen around 900-1000 °C, indicated by previous research. On the other hand, mica impurities seem to be confirmed as the cause of these effects.

5.4 Paper IV

Aasly, K. Götze, J. Malvik, T. and Myrhaug, E. (subm.) Application of Cathodoluminescence to evaluate the physical properties of metallurgical quartz. Submitted to Matherials Characterization, December, 2007.

This paper describes cathodoluminescence (CL) microscopy and spectroscopy as a tool for evaluating the physical properties of metallurgical quartz. Cathodoluminescence was used on the products from the shock-heating experiments presented in Paper III.

CL proves that it can be used to define the source of the quartz material, e.g. in Sample Quartzite E, a meta-sandstone, three main types of sources to the detrital quartz grains have been established as well as the rare occurring grains of other sources. One of the sources for the gravel quartz in Sample Gravel B is confirmed as being from hydrothermal vein quartz by the yellowish-green luminescence, which is typical for such type of quartz.

Cathodoluminescence shows that the luminescence of quartz is affected by the shock heating and that most of the obtained spectra are changed as a result of the heating experiments. However, more research needs to be carried out to understand the relationship between the change of the characteristic CL spectra after shock heating and the thermo-mechanical properties of the quartz.

The most interesting discovery was that two of the shock-heated samples show some small red luminescent areas “spotted red CL”. This feature was most pronounced in the most cristobalite rich sample and additionally in a cristobalite-bearing sample. Thus, it has been interpreted as representing cristobalite formation or as effects of the amorphous transition phase that has been stated to occur as an intermediate phase during β-quartz to β-cristobalite transformation.

5.5 Paper V

Aasly, K. Malvik, T. and Myrhaug, E. (in prep) Heating of Quartz and Formation of Cristobalite. Prepared for submission.

Paper V reports transformation of quartz to cristobalite as a result of shock-heating to different temperatures and the relevance of this to the actual process. XRD analysis of the shock-heated samples in Paper III showed that cristobalite was formed in some of the quartz samples after heating to 1300 °C for ten minutes. To investigate the importance of the cristobalite formation on the thermo-mechanical and softening properties of the quartz, new samples from each of the quartz types were shock-heated in the same induction furnace. Target temperatures ranged from 1250 to 1550 °C at 50 °C intervals. As for the previous shock-heating experiments, the samples were heated for ten minutes before cooled at room temperature. Additionally, the two most different samples from these experiments, with respect to cristobalite formation, were heated to 1550 °C for five hours to investigate the differences in cristobalite formation and transformation rates at prolonged heating at elevated temperatures. The products from the shock heating were prepared for XRD and DTA analysis of the cristobalite content.

Vast differences were seen in the amounts of cristobalite formed during 10 minutes at different temperatures. The highest amount of cristobalite formed was seen in Sample Quartzite E with up to 9.8% cristobalite, whereas Sample Hydrothermal C only showed minor cristobalite formation (0.3%). However, prolonged heating of these two samples showed that the rates of transformation are leveled out and after five hours at 1550 °C, the amount of cristobalite formed was 77.6% and 80.7% respectively. No tridymite was seen in any of the samples after the shock heating.

These results indicate that the quartz have different properties with respect to cristobalite formation and that these differences most probably are significant for the thermo-mechanical properties of the quartz raw materials for the (Fe)Si process. However, further work is required to find the relationship between the TSI and the phase transformation from quartz to cristobalite.

5.6 Paper VI

Aasly, K. Malvik, T. and Myrhaug, E. (in prep) Quartz in the Silicon Furnace. Prepared for submission.

This paper presents investigations of samples from two different furnaces. The sampled materials were made available for this project from Elkem AS. Drill cores were drilled from an operational scale FeSi furnace and from a pilot scale Si furnace. The two furnaces were producing ferrosilicon and silicon metal respectively, from quartz raw materials of different qualities. XRD analyses were performed on scrape-off material from quartz or SiO_2 fragments in the drill cores aiming at describing the silica phase transformation and the alteration of the quartz on its way through the furnaces. Additionally, some of the samples were investigated by optical microscopy.

The XRD-analysis from the FeSi-furnace showed that mainly cristobalite was present in both furnaces as the main silica phase. In some samples, cristobalite was accompanied by minor amounts of quartz. However, in one drill core, containing the most unaltered charge material with typical fresh lumpy quartz, (α-)quartz was the main or only silica phase. Quartz was accompanied by cristobalite only in some of the samples. Typically, cristobalite takes over as the dominating silica phase in the lower sections of this drill core.

Tridymite was not expected to form within the furnaces from the results presented in previous papers (Paper III and V). However, tridymite was seen in samples from two drill cores accompanied by cristobalite or by cristobalite and quartz.

Samples from the pilot scale Si-furnace shows that cristobalite is the dominating silica phase in all the samples, accompanied by quartz only in two of the samples in the top of the charge, closest to the electrode.

Cristobalite transformation seems to be achieved rather quickly inside the furnace, with cristobalite mainly formed in the top of the charge, whereas quartz is present to a certain degree in the top of the charge closest to the electrode. This is mainly because of the relatively high temperatures leading to increased mass flow and shorter retention time near the electrodes compared to further away from the electrodes. Thus, cristobalite formation is not achieved until further down the charge.

Tridymite seem to form in the FeSi furnace but not in the Si furnace. The most obvious reason must be the content of certain impurity elements in the FeSi furnace compared to the Si furnace.

6. Discussion and conclusion

The work presented in this PhD-thesis has emphasized two main goals:

1. Investigating important properties for the quartz as a raw material for production of (Fe)Si
    a. Define mechanical properties for quartz that are important for the size reduction experienced during transport and storage.
    b. Define thermo-mechanical properties for quartz that are assumed important for the melting behavior on the furnace.
    c. Additionally, the softening properties have been briefly discussed in some of the papers.
2. Testing analytical and experimental methods for investigating these properties.

Previous work on quartz raw material for production of (Fe)Si has been reviewed in Paper I. This paper will not be further discussed in detail, but will be referred to in discussion of the results presented in the other papers.

The lack of available research material that has been published in scientific journals or on conferences is striking. Almost no available literature is found in such forums, except a few journal- and conference papers. Most of the literature originate from research organizations and made available through NTNU or Elkem AS. The reason for the difficulties finding published research on this topic is probably related to the confidentiality policies within the companies in combination with very little attention on increasing basic knowledge of quartz properties and behavior in (Fe)Si furnaces.

Much of the literature that has been cited is from Norwegian research projects. This is probably related to the fact that Norway has been the leading (Fe)Si producer. Thus, the majority of the research has been carried out in Norway as well. However, significant research has probably been carried out by the different companies, but as a consequence of the factors mentioned above, this research has not been published.

Some important factors that will be discussed in this section are:

– Production and handling of quartz and its importance for the generation of fines

– Micro textures of quartz and its importance to the mechanical and thermo-mechanical properties

– Mica or tridymite as the cause of the effects of heating seen at 900-1000 °C

– Cathodoluminescence as a tool for investigating thermo-mechanical properties of quartz

– Silica phase transformations and its significance to the thermo-mechanical properties of the quartz raw material with emphasis on the cristobalite formation

– Behavior of quartz in the furnace with emphasis on the phase transformations

6.1 Fines generation and mechanical properties of quartz outside furnace

The fines content in the raw materials is an important contribution to some of the problems seen in furnaces as the charge is clogged and the gases produced in the furnace is blocked from emerging evenly upwards in the furnace to react properly with the materials higher up in the furnace and thereby escaping the furnace unreacted to the off-gas system.

Schei *et al.* (1998) defines the general requirements to the sizing of the quartz as a raw material for (Fe)Si-production to between 10 to 150 mm. However, the absolute requirements from various silicon plants may vary within this interval. In this context, fines can be defined in two ways: Fines can be all material below the specifications from the (Fe)Si producer (e.g. 10 mm according to Schei *et al.* (1998)). However, the fines that are critical for the process performance are fines that are below 2 mm. This size fraction is the one that creates problems in the furnace. The production of excess amount of fines is also a problem for the producer, since the market potential usually only covers a small fraction of the produced fines.

The results in Paper II show that it is established that the origin of the quartz is important for the mechanical strength. This is supported by e.g. Jern (2004) and Malvik (1986a; 1988) who stated that the cohesion factor between the grains is important. Malvik (1986a; 1988) showed by a case study of one “good” and one “bad” thermal quartzite, that the cohesion between grains and the ratio of cement to

clastic material should be as high as possible. However, the natural quality of the raw materials can be insignificant if the production in the mine and processing plant is not optimized. This has been shown for different ores and industrial minerals by e.g. Nielsen and Malvik (1999) and Nielsen (1999b, a). Nevertheless, Jern (2004) showed that producing two types of aggregate raw materials by identical drilling and blasting conditions does not give the same damage on different types of rocks. This is caused by textural differences within the rocks. These results shows that mining (and processing) of quartz must be planned according to the properties of the deposit to be able to produce the best possible raw material with respect to mechanical (and thermo-mechanical) strength.

The effects of drilling and blasting of ores and industrial minerals (e.g. quartz) generates a halo around the drill hole that contains vast amounts of micro cracks that lowers the mechanical resistance of the produced material (e.g. Nielsen and Malvik, 1999; Nielsen, 1999b). The size of the halo and frequency of the micro cracks are related to several factors such as drill hole pattern and -deviation as well as the amount and type of explosives used.

A raw material that has been blasted with excessive amounts of explosives will leave a material for crushing that will easily break and cause too much fines in the product. The material that is still within specifications will probably contain a significant amount of micro cracks causing the mechanical strength of the material to be reduced.

For an optimal production, these factors should be adjusted in cooperation with the processing plant, i.e. crushing works (e.g. Nielsen and Malvik, 1999; Nielsen, 1999b). The optimal raw material that are still within specifications from the customer should contain a minimum of fines after crushing and simultaneously the number of micro cracks remaining in the product should be minimal. This can only be achieved by close cooperation between the two departments or steps in the production chain.

During transport and storage of the raw materials, the rocks are subject to mechanical wear by different sub-processes related to the handling of the material. The most important factor related to the handling is reloading of the raw materials. During reloading e.g. from the vessel to the conveyor belt or between conveyor belts, the raw materials experience height differences in single points that involve heights of fall up to 20 m (Tveit and Valderhaug, 1993). Accumulated heights of fall are known to be as much as 70 m over several drop points in a transportation

system (pers. com. H. Tveit, 2004). These factors related to the handling of the raw materials are shown to increase the fines content as presented by (e.g. Tveit and Valderhaug, 1993; Forjàn, 1999).

6.2 Thermo-mechanical properties of quartz

The mechanical and thermo-mechanical properties of the quartz raw material are probably related. Certainly, badly produced quartz containing vast amounts of micro cracks is likely to disintegrate easily when it experiences shock heating within the furnace. High-temperature microthermometry shows there are several temperature intervals that involve fracturing of the samples, as reported in Paper III. The fracturing is more or less destructive and some of the temperature intervals involve fracturing in all samples, such as the low temperature interval below 573 °C, where the most significant cause of the fracturing seems to be the decrepitation of fluid inclusion and some opening of micro cracks or grain boundaries. Naturally, all samples show an effect of the α- to β-quartz transformation at 573 °C. At the highest temperature interval, above 1200 °C, most samples show more or less destructive fracturing. In the worst cases (Gravel F), the samples suddenly moved out of position inside the heating chamber. Some of these samples are split into two or more pieces, while most of them only shifted position probably because of abrupt movements internally in the sample or because of thermal drifting. The most crucial temperature interval seems to be between approximately 900-1000 °C. Sample Gravel F and one run on Sample Pegmatite D showed moderate to high activity in the temperature interval that started just below 900 °C.

The microthermometry experiments mainly confirm the findings by Birkeland and Carstens (1969). However, they did not mention any strong effects at high temperatures (>1000 °C) similar to those reported in Paper III in this thesis. Birkeland and Carstens (1969) carried out their experiments up to 1300 °C and combined with the thicker samples investigated, their peak temperature may have been too low, causing the high temperature effects not to be observed.

Shock heating of quartz samples in the induction furnace provided a good base for investigation the quartz after shock heating. However, some effects could be observed during the shock heating as well. This was especially related to the degree of fracturing after heating and some audible effects during the heating (although subjective observations). This was observed in Sample Hydrothermal C where an intense crackling was heard from the crucible just after insertion of the sample.

This observation coincided with the extreme fracturing of the sample. In Sample Gravel F, only a small degree of fracturing was seen after the shock heating. Other samples appeared to have high degree of fracturing but released no or very limited audible effects during heating.

However, after sieving the materials from the shock heating on a -1.651 mm sieve, Sample Gravel A and Gravel F showed a higher content of fine material (1.41 and 1.14% respectively) whereas Gravel B and Hydrothermal C showed low content of fines (1.00 and 1.05% respectively). This is in contrast to the observations immediately after heating where Sample Hydrothermal C was heavily fractured and Sample Gravel F was only weakly fractured.

Sample Pegmatite D showed the lowest amount of fines (0.71%). However, this sample was smaller than the other samples, which could be significant for the lower content of fines material.

Further investigations after the shock heating show many characteristics of the different types of quartz. However, some reservations must be made when interpreting the results of the investigations carried out after cooling of the samples. High temperature microthermometry showed that most of the effects were observed during heating, however, some additional fracturing and changes in the samples were also observed during cooling. This is a result of the relatively rapid cooling of the samples. Therefore, it cannot be excluded that some of the fracturing etc. observed in the shock-heated samples are results of quenching effects.

From the shock heating of quartz samples to 1000 °C carried out by Birkeland and Carstens (1969) they stated that the fluid inclusion planes were of no significance for the fracturing of the samples. Their interpretation was that the fluid inclusions as well as the micro fracturing of the samples had no “qualitative significance”. However, the investigations by microscopic methods of the shock-heated samples presented in this thesis (Paper III) showed that the heating of the samples introduced an opening of the grain boundaries in most samples accompanied by the development of micro cracks, either as short disconnected cracks in a dense pattern or as a network of connected micro cracks. The fluid inclusion planes also show networks of micro cracks that probably are a result of the decrepitation of the fluid inclusions. This is in contrast to the observations made by Birkeland and Carstens (1969). Martinsen (1987) showed that the properties of fluid inclusions may be important for the thermo-mechanical strength of quartz. By measuring salinity and

homogenization temperature of (secondary) fluid inclusions in quartz, the “good” quartzes plotted together when plotting salinity vs. homogenization temperature.

The mica seen along grain boundaries in reference Samples Cold Gravel B and Cold Gravel F, which were not seen at all in the heated Samples Warm Gravel B and Warm Gravel F, indicates that mica is responsible for the fracturing of the samples. However, there was no possibility to confirm the presence of the mica in the investigated samples before heating, since the PTS were prepared after the heating. The role of the mica is also supported by the high-temperature microthermometry investigations, especially for Sample Gravel F, where moderate activity was seen at the temperature interval around 900 - 1000 °C, which is also the conclusion by Malvik and Lund (1990). Although no mica was seen in the thick sections that were investigated, the thickness of the samples and the resolution of the microscope and camera, may have suppressed the visibility of microscopic mica grains. Mica minerals will dehydrate and decompose at temperatures near those discussed here (e.g. Deer *et al.*, 1962 and references therein). Malvik (1986b) carried out dilatometry investigations of quartzites and mica separated from the grinded quartzites. The pure mica samples showed strong effects at temperatures 700 to 1000 °C. This was interpreted as indicating that mica has an importance for the thermo-mechanical strength of the quartz.

Early investigations (e.g. Nervik in Geiss, 1977) indicated that tridymite has significance for the discussed temperature interval. XRD investigations of heated quartzites showed weak formation of tridymite (Geiss, 1977). However, the XRD analysis of the shock-heated samples presented in this thesis (Paper III) indicates no formation of tridymite in any of the samples. Together with earlier investigations (e.g. Malvik, 1986b), this seems to confirm that tridymite formation can be ruled out as a cause of these effects. The absence of the tridymite formation is most probably related to the purity of the quartz, which is such that the required catalyst elements are not present in sufficient amounts, but also the short retention time at 1300 °C.

The low degree of fracturing in Sample Gravel F may be contradicting the role of mica. However, when looking at the fines index, defined as the weight percentage below 1.651 mm (Paper III), Sample Gravel F shows a high content of fines, such that the mica may still be the reason for the fines generation.

The crucial impurity content related to the thermo-mechanical properties of the quartz has previously been related to Al_2O_3 and K_2O through the correlation

between one or both of these elements and the dilatometry deflections. Al and K are the main elements in muscovite together with Si, but have also been shown to be important catalyst elements for the formation of tridymite. However, the ratio between Al_2O_3 and K_2O indicated that it originates from muscovite (Malvik and Lund, 1990).

A correlation of thermal strength index (TSI) and impurity content is difficult as Sample Gravel F shows high TSI, but is the most impure quartz whereas Sample C is the purest quartz but shows the second lowest TSI.

The microthermometry technique is an important technique for investigating the microscopic in-situ effects of heating. By carrying out a series of tests on significantly different quality quartz, this technique certainly is at least capable of indicating the thermo-mechanical quality of quartz. However, for more comprehensive investigations, the shock-heating test has a wider capacity as the test can be carried out on larger fragments that correspond with the size of the actual raw material. Further, the tested material can be investigated by different techniques after heating, although the findings cannot be related back to specific temperatures. Thus, the combined use of the two methods is recommended.

6.3 Cathodoluminescence on thermo-mechanical properties of quartz

Paper IV presents the use of cathodoluminescence (CL) to characterize the thermal properties of quartz. The paper confirms that using CL to characterize different types of quartz gives a good indication of the geological origin of the quartz. It also gives an indication of the metamorphic state of the quartz.

However, using CL directly to indicate the quality of the quartz related to silicon production needs further investigations. It is clear from the results presented in Paper IV that CL gives unique results for different types of quartz but further research must be carried out to understand the cause of the altered CL spectra after shock heating. However, the shock heated Samples Quartzite E and Gravel F shows an interesting CL signature ("spotted red CL"). This feature was seen related to micro fracturing and grain boundaries in the two samples, although most pronounced in Sample Quartzite E. This CL signature has been interpreted to represent silica phase transformation. Although cristobalite previously has been reported showing blue CL (e.g. Marshall, 1988), it cannot be excluded that this red CL is caused by newly formed cristobalite. However, the red CL may also

represent the amorphous intermediate phase that has been reported to occur during transformation of quartz to cristobalite (e.g. Chaklader and Roberts, 1961; Chaklader, 1963). The possibility of cristobalite or amorphous intermediate phase as cause of the red CL is supported by XRD investigations of the samples after heating (Paper III) confirming that Sample Quartzite E contains significant cristobalite and Sample Gravel F contains minor cristobalite. Further investigations of cristobalite formation in the samples, are presented in Paper V and confirm the same with Sample Quartzite E, showing major cristobalite formation while Sample Gravel F shows minor content of cristobalite at 1300 °C. Another important indication is that the spectra from the red CL with main peak at 650 nm represents none-bridging oxygen hole centers caused by breaking of Si-O bonds (Sigel and Marrone, 1981). This bond breaking is necessary for the transformation from quartz to cristobalite and must be occurring as a result of the intermediate amorphization of the quartz structure.

6.4 Silica phase transformation

Shock heating of quartz to temperatures ranging from 1250 to 1550 °C at 50 °C intervals for 10 minutes shows that cristobalite formation is extensive in some of the quartzes, especially Sample Quartzite E with almost 10 %. For the other samples, the maximum cristobalite content ranges from 0.3 to 1.5% at 1550 °C.

Although the samples are at ambient temperature when analyzed to find the cristobalite (and tridymite) content, the quenching of the samples after heating causes the meta-stable silica phases to remain present in the samples and not transform back to quartz.

The micro cracks and grain boundary openings observed after the shock heating (Paper III) may have been caused by generation of cristobalite or the amorphous intermediate phase. This is justified by the fact that cristobalite at approximately 1000 °C has a specific volume 15.2% higher than quartz (Salmang and Scholze, 1982). This will result in severe fracturing, especially in rocks with relative dense grain boundaries. As the quartz lattice is broken and the volume increases as result of amorphization and formation of cristobalite, this will lead to distortion of the texture of the rock and therefore lead to the severe fracturing of the rock seen after shock heating. For rocks originally comprising a more fine-grained and open grain boundary texture, the increased specific volumes will not necessarily lead to as severe fracturing. The open grain boundary texture gives room for at least some of

the additional volume expansion that follows the phase transformation, and therefore the rock will not be exposed to the same stress as rocks comprising less open and possibly fewer grain boundaries.

Prolonged heating of the samples showing most and least cristobalite formation, respectively (Samples Quartzite E and Hydrothermal C), shows that the amount and rate of cristobalite transformation are leveled out during extended time of exposure to the high temperatures. This is important knowledge when considering differences with respect to the retention time for quartz in the furnace before it melts. Extended time of exposure to high temperatures as crystalline phase will give more fracturing from the phase transformation than shorter exposure time to the same temperature before melting.

Investigations of the significance of silica phase transformations in quartz showed that no tridymite is formed during shock heating of the different quartz types, not even at prolonged heating.

The XRD analysis were carried out on the XRD equipment at the Dept. of Geology and Mineral Resources Engineering at NTNU, and the quantification of different silica polymorphs were carried out as described in the Methods chapter. This quantification is probably not precise and therefore the content of different polymorphs is more an indication of relative differences than absolute. This is because the standardization routines are optimized only for petrographic analysis and therefore only the main rock forming minerals. However, the results obtained from the XRD analysis were more or less within the expected range for all samples. Compared with the DTA analysis, the XRD analysis shows an increase in the cristobalite content with temperature that is more gradual. DTA shows agreement with the XRD results at some temperatures, but deviate from the XRD analysis at other temperatures. The agreement is related to qualitative observations. For quantitative DTA observations however, the amounts are more than doubled where cristobalite is seen for Samples Gravel A, Gravel B and Hydrothermal C. DTA analysis of Sample Quartzite E is more similar to XRD analysis. The deviating results between XRD and DTA may be an indication of detection limits for DTA analysis compared to XRD.

Previous research on the quartz-cristobalite transformation, as well as results presented in this thesis, has shown that the phase transformation of quartz to cristobalite may be the reason why some quartz shows high degree of disintegration at the highest temperature. Comparing the amount of cristobalite

formed at 1300 °C from the experiments in Paper V and the fines index calculated in Paper III, these two parameters seems to correlate well (Figure 6-1). However, Sample Quartzite E does not show as high fines index as expected compared to the other samples.

Sample Quartzite E is not included in the calculation of the regression line in Figure 6-1, as the micro textures of this sample is very different from the other samples, although Samples Gravel A, Gravel B and Hydrothermal C are coarser grained than Samples Pegmatite D and Gravel F. The extremely high cristobalite content in Sample Quartzite E may be a result of the open grain boundaries and small grain size.

In Figure 6-1, the different groups of samples with similar micro textures are plotted so they can be distinguished. When leaving Sample Quartzite E out of the discussion, it seems that there is a correlation between fines index and cristobalite content. However, this must be investigated further as the number of tests presented here are too low to be statistically significant.

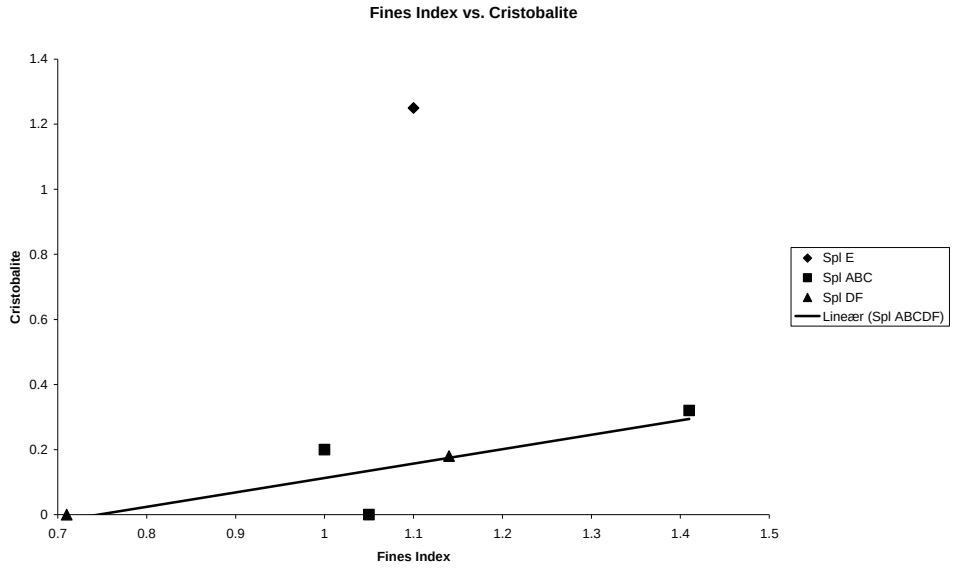

Figure 6-1 Correlation between fines index (w% less than 1.651 mm after shock heating) and cristobalite content at 1300 °C for Samples A to F. The different samples are grouped according to their micro-textural properties. Sample Quartzite E is left out of the calculation because of its totally different micro-textural properties.

6.5 Investigations of quartz from furnaces

Paper VI presents investigations of samples of quartz from different stages inside two operated furnaces. The furnace materials represent one operational scale FeSi-furnace and one pilot scale Si-furnace. The materials were made available from other projects, and gave the opportunity to investigate what the quartz goes through during the production process.

Because of the risk of dilution or contamination of the silica phases from the furnace samples, the sampling was carried out by scraping off the material, which by visual observation was interpreted as silica phases. This secures good detection of the different silica phases and increases the chances of detecting even small amounts of a silica phase among large amounts of other silica phase(s). However, this is not always considered proper procedure for sampling, but in this case, the aim of the sampling is assumed to justify the method. Reproducibility is confirmed by re-analyzing all samples from the FeSi-furnace by scraping off new material from the same sample surface.

The size difference of the two furnaces may give some differences in the results. However, Schei (1977) states that the small-scale pilot furnaces can be used to collect experience for new areas and knowledge. Thus, comparing the two furnaces investigated in Paper VI should be highly valuable when done with care.

Investigations of quartz samples from the two furnaces give some interesting results. As expected, cristobalite is formed relatively early after charging the quartz. Most samples analyzed actually contain cristobalite sometimes followed by minor amounts of quartz. A surprising discovery when considering the results from the shock heating experiments discussed earlier is that tridymite is actually formed inside the furnace. However, only inside the FeSi-furnace since no tridymite was found in samples from the Si-furnace.

Quartz is mainly present in the charge top together with cristobalite. In the Si-furnace, this quartz is found in the samples located closest to the electrodes whereas the cristobalite is found in the samples more distant from the electrode. The quartz seems to be converted to cristobalite before it moves further into the furnace. However, some quartz was found in the deeper parts of the FeSi furnace, but is probably related to cavities letting the quartz fragments fall down during drilling of the cores or as a result of the drill core collection. Tridymite seems to be present in the rather inactive parts of the furnace, indicating that only the quartz

with long exposure time to high temperatures in the furnace converts to tridymite. It may also indicate that there is some accumulation of the important impurities in this area although this has not been confirmed.

The most surprising result of the furnace investigations was to find tridymite in the furnace. Although finding tridymite only in the FeSi-furnace is easier to explain than if only found in the Si-furnace. This is related to the impurity content in the different furnaces. The less impure quartz used in the FeSi-furnace than in the Si-furnace does not explain the tridymite formation in the FeSi-furnace alone, since no tridymite was formed from this quartz after 10 minutes at 1300 °C or even 5 hours at 1550 °C. Thus, the impurity content in the quartz alone is not high enough to allow tridymite formation. This indicates that the impurity contents from other raw materials also may be important. For FeSi-production, the impurity content of the raw materials is generally higher than for Si-production. Additionally, FeSi-production implies adding iron to the system, and the iron sources contain significant amounts of impurities. The impurity level may therefore be high enough to catalyze the quartz-tridymite phase transformations. Additionally, the investigations indicate that tridymite is found only in the more inactive parts of the furnace where the raw materials has a significantly longer exposure time to high temperatures than in the more active parts of the furnace. This allows extra time at high temperature, which may contribute to make the tridymite transformation possible.

Although XRD is a good method for detecting silica phase transformation in the samples from the furnaces or from shock heating experiments, the method is not able to tell anything about how and where within the quartz the phase transformation occurs. By using electron backscatter diffraction (EBSD), mapping the occurrence of the different silica phases within a sample should be possible. Unfortunately, this was not achieved for the investigations for this thesis. When using the EBSD technique, further investigations of the samples from the microthermometry is also possible. The size of these samples makes XRD and other techniques difficult, but for EBSD the size is more than sufficient. The observations of cristobalite or intermediate phase in Samples Quartzite E and Gravel F by CL (Paper IV) may be confirmed by EBSD, the CL technique may also be a possible method for mapping the different silica phases in the samples. If this is the case, combining CL with electron probe micro analyzer (EPMA), makes it possible to relate the silica phases to impurities in the samples.

6.6 Other aspects

As discussed briefly earlier, the quenching of the samples after heating makes the meta-stable cristobalite (and potential tridymite) remain in the sample and not transform back to quartz but remains as the respective low temperature versions. Naturally, the temperatures in the furnaces do not decrease as rapid as is the case for the shock-heated samples quenched at ambient temperature. However, it is assumed that the different high temperature silica polymorphs in the furnaces do not transform back to quartz, but that these also remain as the low temperature version. Thus, it should be possible to detect all the high temperature polymorphs generated inside the furnace by XRD and DTA investigations.

The transformation of quartz to cristobalite may cause severe fracturing due to the breaking of Si-O bonds during the transformation process. This may contribute to the generation of critical fine material inside the furnace as the volume expansion that follows the transformation will contribute to severe fracturing of the samples. However, differences in the degree of fracturing as result of the phase transformation are likely to occur between the quartz types. This is probably because of the differences in micro textures. As discussed above, quartz comprising an open grain boundary texture will probably not experience as severe fracturing as quartz with sealed or tighter grain boundaries. This is explained by the free volume that will compensate for parts of the volume expansion experienced. The size of the total grain boundary area will probably also be critical for this volume expansion.

The amount of cristobalite formation is the highest in Sample Quartzite E according to the analysis in Paper III and Paper V. This may be caused by the relatively fine-grained and open grain boundary texture of the rock, which allows for more rapid transformation. For rocks comprising an open grain boundary texture, the surface area for the initial transformation of quartz to transition phase is larger than for rocks with sealed grain boundaries. Therefore, the formation rate of transition phase is higher for quartz comprising open grain boundary textures. The transformation from quartz to cristobalite is therefore more rapid, at least in the initial phase of phase transformation. As the transition phase propagates through the sample, more fracturing occurs and allows for increased reactive surface area.

6.7 Overall conclusion

The results and conclusions presented in this thesis is a result of different kinds of work. First of all the two first papers presented are based on literature studies and especially the results in Paper II are previously known but presenting these work together shows the complexity of how to achieve a mechanically stable quartz raw material. Further, the results and conclusions of Papers III – VI are based on work with different methods and equipment with the aim to obtain improved characterization of the material properties and expected behavior on the furnace as well as increasing the knowledge about these properties.

It is important to understand that the research presented in the thesis is a result of work that often has been located on the border between process metallurgy and mineralogy. This work has been challenging in the way that to understand the mineralogical properties of quartz, it has also been necessary to understand the principles of the silicon furnace and the reactions within. Many of the subjects that have been studied are related to factors that are not relevant in geological environments and thus never been studied by mineralogists. However, the results from this thesis may, hopefully, provide some additional knowledge to the mineralogy of quartz.

The most important results presented in this thesis are:

– For best possible mechanical strength of the raw material, production in the mine and processing plant should be carefully planned to minimize amount of blast-induced damage in the rock

– The amount of fines can be minimized by controlling the handling of the raw materials during the transport and storage. It is especially important to avoid high drops, both high single drops and accumulated height of all the drops in total.

– Mica as a cause of the strong effects at 900-1000 °C seems to be confirmed, although it has been shown that tridymite actually can form inside the furnace. This phase transformation may contribute to the effects seen at these temperatures.

– Combined use of shock heating and high-temperature microthermometry may contribute with important information about thermo-mechanical properties of the quartz and relate these to specific temperature intervals.

– Cristobalite may be an important factor for the generation of fines in the FeSi furnace. It is shown that the cristobalite formation may be a cause for the disintegration of quartz in the furnace.

– The fines index correlated with cristobalite content may be used to say something about the importance of the cristobalite formation on the disintegration of quartz inside the furnace.

– Cathodoluminescence has proved to be a promising tool for petrographic description of quartz. The investigations of shock-heated quartz also show that it could be used to indicate the thermal properties of the quartz as well. However, more research needs to be carried out to understand the cause of the changed luminescence characteristics after heating.

– This work has mainly given an overview of possible techniques that can be used for further investigations of thermo-mechanical properties of quartz. It has also contributed with new knowledge about the importance of the cristobalite formation on the thermo-mechanical properties.

7. Further work

Polarized light microscopy and XRD has given a good indication to what happens to the quartz material in the silicon furnace. However, these results are based only on samples from two different furnaces and the use of two quartz types. In order to get a better overview, more furnace material should be studied where other types of quartz has been used. This will allow for a more diversified interpretation of what happens within the furnace. One needs to keep in mind that the experiences from furnace operations have shown that different types of quartz may give differences in furnace operations.

XRD is a powerful technique to identify the different crystalline phases that are present in a sample. However, it gives only information on the bulk material. By using electron backscatter diffraction (EBSD), it is possible to map areas of polished samples to investigate the actual spatial distribution of the different mineralogical phases within an area of the sample. Then it is possible to see how for example quartz, cristobalite and tridymite are related to each other down the furnace.

The investigations of the significance of the cristobalite formation on the disintegration of quartz at high temperatures should be continued. The results discussed in this thesis indicate that there are some correlation between the fines index and the cristobalite content. This should be investigated further by heating quartz samples to e.g. 1300 °C for ten minutes and further correlate the weight percent fraction below 1.651 mm and the cristobalite content. An alternative method is by correlating one of the existing thermo-mechanical tests (either the TSI or the HI) with the cristobalite content.

Cathodoluminescence is a tool that can give additional petrographic information, as well as having the potential of being an important tool for investigating thermo-mechanical properties of the quartz. However, a lot of work remains for this being possible. A study of the cause of the change in luminescence characteristics of quartz after heating is highly recommended.

Fluid inclusion study as presented by Martinsen (1987) indicates a correlation between salinity and homogenization temperature for the thermo-mechanical properties of quartz. This should be studied further by a detailed study of the fluid inclusions in different types and quality of quartz raw material. This is important as

micro cracks are occurring as result of decrepitation of fluid inclusions as shown in Paper III.

Another technique that should be tested is the investigation of softening properties of quartz by studying the melting progress in a wettability furnace. Here, the sample is photographed during the heating progress and the temperature for initial softening and melting can be read directly by observing when the sample starts to change form. Such equipment exists at SINTEF Materials and Chemistry and is capable of heating samples to above the melting point of quartz.

8. References

Aasly, K., Malvik, T., and Myrhaug, E. 2006: Quartz for Carbothermic Production of Silicon - Effect of the process steps, handling and transport from mine to furnace. *Silicon for the Chemical Industry VIII*, p. 9-18, Trondheim.

Aasly, K., Malvik, T., and Myrhaug, E. 2007: A review of previous work on important properties of quartz for FeSi and Si metal production. *Innovation in the Ferro Alloy Industry (INFACON XI)*, **1**, p. 393-401. MacMillan, New Dehli, India.

Alnæs, L. I. 1986: A geological and mineralogical investigation of the Mårnes quartzite in Gildeskål, Nordland (in Norwegian), **MSc**. Unpublished Thesis, NTH, Trondheim.

Birkeland, R. 2004: *Optimal quartz properties - method evaluation part 1, report no F10/03, Internal Report, With permission from Elkem (in Norwegian)*. 25 p. Elkem Research, Kristiansand.

Birkeland, T. 1975: Subject: Thermal stability of quartzite. Unpublished work note.

Birkeland, T., and Carstens, H. 1969: Preliminary report on high temperature investigations of natural quartz, NGU Project B 2006 (in Norwegian).

Bruland, A. 1998: Hard rock tunnel boring. *Deparment of Civil and Transport Engineering*, **1998:81**, p. 10 b. Norwegian University of Science and Technology, Trondheim.

Chaklader, A. C. D. 1963: X-Ray Study of Quartz-Cristobalite Transformation. *J. Amer. Ceram. Soc.*, **46**, 66-71.

Chaklader, A. C. D., and Roberts, A. L. 1961: Transformation of Quartz to Cristobalite. *J. Amer. Ceram. Soc.*, **44**, 35-41.

Craig, J. R., Vaughan, D. J., and Skinner, B. J. 1996: *Resources of the Earth: Origin, Use and Environmental Impact*. Prentice-Hall, Inc., Upper Sadle River, New Jersey 07458.

Deer, W. A., Howie, R. A., and Zussman, J. 1962: *Sheet silicates*.

Deer, W. A., Howie, R. A., and Zussman, J. 1992: *An introduction to the rock-forming minerals*. XVI. Longman Scientific & Technical, Harlow, Essex.

Evans, A. M. 1997: *An introduction to economic geology and its environmental impact*. IX. Blackwell Science, Oxford.

Fenner, C. N. 1913: The Stability Relations of the Silica Minerals. *Am. Jour. Sci.*, **XXXVI**, 331-384.

Fitting, H. J., Barfels, T., Trukhin, A. N., and Schmidt, B. 2001: Cathodoluminescence of crystalline and amorphous SiO2 and GeO2. *Journal of Non-Crystalline Solids*, **279**, 51-59.

Floerke, O. O. W. 1957: Structural anomalies in tridymite and cristobalite. *Amer. Ceram. Soc. Bull.*, **36**, 142-148.

Forjàn, C. 1999: Fines Created by falling, p. 18. Internal report.

Foss, B., Halfdanarson, J., and Wasbø, S., 2000: "Dynamc Si-model - Simon v. 1.50", Technical Report, SINTEF-report no STF72 F00307 (in Norwegian).

Geiss, H. P. 1977: High temperature investigations with quartzite from the Gulodden quarry at Kragerø (in Norwegian). Report to Fesil & Co.

Goldstein, J. I. 2003: *Scanning electron microscopy and X-ray microanalysis*. Kluwer Academic/Plenum Publishers, New York.

Grådahl, S., Johansen, S. T., Nubdal, G., Ravary, B., Laclau, J. C., Vassbotn, T., and Hellevik, L. R. 2000: Environment and furnace processes part III (in Norwegian). SINTEF Report no. STF24 F00600, Trondheim, Norway.

Götze, J., Plötze, M., Fuchs, H., and Habermann, D. 1999: Defect structure and luminescence behaviour of agate - results of electron paramagnetic resonance (EPR) and cathodoluminescence (CL) studies. *Mineralogical Magazine*, **63**, 149-163.

Götze, J., Plötze, M., and Habermann, D. 2001: Origin, spectral characteristics and practical applications of the cathodoluminescence (CL) of quartz - a review. *Mineralogy and Petrology*, **71**, 225-250.

Götze, J., Plötze, M., and Trautmann, T. 2005: Structure and luminescence characteristics of quartz from pegmatites. *American Mineralogist*, **90**, 13-21.

Harders, F., and Kienow, S. 1960: *Feuerfestkunde: Herstellung, Eigenschaften und verwendung feuerfester Baustoffe.* Springer, Berlin.

Holmquist, S. B. 1961: Conversion of Quartz to Tridymite. *J. Amer. Ceram. Soc*, **44**, 82-86.

Jern, M. 2004: *The Geological Conditions for Aggregate production, with special focus on blasting and fines production*. Chalmers Unicersity of Technology, Göteborg, Sweden.

Johannesen, U. 1998: A geological and mineralogical investigation of the quartzite deposit at Tananeset, Finnmark (in Norwegian), **MSc**. Unpublished Thesis, NTNU, Trondheim, Norway.

Kallfelz, P. L. 2000a: Quartz for Production of Silicon Metal - Criteria for the Right Choice. Internal report. Elkem ASA, Silicon Division.

Kallfelz, P. L. 2000b: Quartz for production of silicon metal - criteria for the right choice. Study for Elkem Si-div, Internal report, With permission from Elkem.

Klein, C., and Hurlbut, C. J. 1993: *Manual of Mineralogy, 21st edn*. John Wiley, New York.

Malvik, T. 1986a: Method for characteizing grain boundaries/cementation in quartz materials, SINTEF internal report, Project title: Thermal properties of quartz, work note 4/23; Project no: 363023 (In Norwegian). Trondheim.

Malvik, T. 1986b: Working paper: The importance of mica on the thermal shock properties of quartz materials, SINTEF internal report, Project title: Thermal properties of quartz, work note 3/23; Project no: 363023 (in Norwegian). Trondheim.

Malvik, T. 1988: Relations between mineralogical texture and commintion characteristics for rocks and ore. In E. Forssberg, Ed. *XVI International Mineral Processing Congress*, **XVI**, p. 257-270. Elsevier Science Publisher B. V., Amsterdam.

Malvik, T., and Lund, B. 1990: Problems involved with quartzite as a raw material for FeSi and Si metal production. *Process Mineralogy IX, The Minerals, Metals & Materials Society*, **IX**, 499-508.

Marfunin, A. S. 1979: *Spectroscopy, Luminescence and Radiation Centers in Minerals*. Springer-Verlag Berlin Heidelberg New York.

Marshall, D. J. 1988: *Cathodoluminescence of geological materials*. Unwin Hyman, Boston.

Martinsen, M. 1987: Report in the open SINTEF-project: Fluid inclusions in quartzites, SINTEF internal report, report no. 363030 (in Norwegian).

Mitra, S. 1977: Kinetics of Quartz-Cristobalite Transformation. *Brit Ceram Trans J*, **76**, 71-74.

Moen, K., and Malvik, T. 2002: A brief investigation of optimal quartz for Elkem Silicon, Internal report, With permission from Elkem (in Norwegian). NTNU.

Monroe, J. S., and Wicander, R. 1994: *The Changing Earth- Exploring Geology and Evolution*. West Publishing Company, St. Paul, MN.

Müller, A. 2000: Cathodoluminescence and characterization of defect structures in quartz with applications to the study of granitic rocks. University of Göttingen, Göttingen.

Müller, A., Lennox, P., and Trzebski, R. 2002: Cathodoluminescence and micro-structural evidence for crystallisation and deformation processes of granites in the Eastern Lachlan Fold Belt (SE Australia). *Contributions to Mineralogy and Petrology*, **143**, 510-524.

Müller, A., Seltmann, R., and Behr, H. J. 2000: Application of cathodoluminescence to magmatic quartz in a tin granite - case study from the Schellerhau Granite Complex, Eastern Erzgebirge, Germany. *Mineralium Deposita*, **35**, 169-189.

Myrhaug, E., and Monsen, B. 2002: Silisiumsmelteforsøk i 150kW pilotovn høsten 2001. "Bruk av biokarbon i norsk ferrolegeringsindustri". SINTEF, Trondheim, Norway.

Neuser, R. D., Bruhn, F., Götze, J., Habermann, D., and Richter, D. K. 1996: Cayhodoluminescence: method and application (in German). *Zentralblatt für Geologie und Paläontologie*, **1995**, 287-306.

Neuser, R. D., Richter, D. K., and Vollbrecht, A. 1989: Natural quartz with brown/violet cathodoluminescence - Genetic aspects evidence from spectral analysis. *Zentralblatt für Geologie und Paläontologie Teil 1*, **7/8**, 919-930.

Nielsen, K., and Malvik, T. 1999: Grindability enhancement by blast-induced microcracks. *Powder Technology*, **105**, 52-56.

Nielsen, K. O. 1999a: The Economic Consequences of Drill Hole Deviation in Crushed Aggregate Production. *Explo '99*, 9-13.

Nielsen, K. O. 1999b: Economic effects of blasting on the crushing and grinding of ores. *South African Institute of Mining and Metallurgy*, 251-255.

Pagel, M., Barbin, V., Blanc, P., and Ohnenstetter, D. 2000a: Cathodoluminescence in Geoscience. Springer Verlag, Berlin.

Pagel, M., Barbin, V., Blanc, P., and Ohnenstetter, D. 2000b: Cathodoluminescence in Geoscience: An Introduction. In M. Pagel, V. Barbin, P. Blanc, et al., Eds. *Cathodoluminescence in Geoscience*, p. 1-21. Springer Verlag, Berlin.

Passchier, C. W., and Trouw, R. A. J. 2005: *Microtectonics*. Springer, Berlin.

Ramseyer, K., Baumann, J., Matter, A., and Mullis, J. 1988: Cathodoluminescence Colors of Alpha-Quartz. *Mineralogical Magazine*, **52**, 669-677.

Ramseyer, K., and Mullis, J. 1990: Factors Influencing Short-Lived Blue Cathodoluminescence of Alpha-Quartz. *American Mineralogist*, **75**, 791-800.

Remond, G. G. 1992: Cathodoluminescence applied to the microcharacterization of mineral materials: a present status in experimentation and interpretation. *Scanning microscopy*, **6**, 23-68.

Rink, W. J., Rendell, H., Marseglia, E. A., Luff, B. J., and Townsend, P. D. 1993: Thermoluminescence Spectra of Igneous Quartz and Hydrothermal Vein Quartz. *Physics and Chemistry of Minerals*, **20**, 353-361.

Salmang, H., and Scholze, H. 1982: *Keramik*. Springer, Berlin.

Schei, A. 1977: Ferrosilisiumprosessens metallurgi. Elkem Spigerverket a/s, R & D Center for A/S FESIL & CO.

Schei, A., Tuset, J. K., and Tveit, H. 1998: *Production of High Silicon Alloys*. Tapir Forlag, Trondheim.

Seltveit, A. 1992: *Refractories (in Norwegian)*. Tapir Forlag, Trondheim.

Senapati, D., Uma Maheswar, E. V. S., and Ray, C. R. 2007: Ferro Silicon Operation at IMFA - A Critical Analysis. *INFACON XI*, **1**, p. 371-380. MacMillan, New Delhi, India.

Shoval, S., Champagnon, B., and Panczer, G. 1997: The quartz-cristobalite transformation in heated chert rock composed of micro and crypto-quartz by micro-Raman and FT-IR spectroscopy methods. *J Therm Anal*, **50**, 203-213.

Sigel, J. G. H., and Marrone, M. J. 1981: Photoluminescence in as-drawn and irradiated silica optical fibers: an assessment of the role of non-bridging oxygen defect centers. *Journal of Non-Crystalline Solids*, **45**, 235-247.

Skuja, L. 1998: Optically active oxygen-deficiency-related centers in amorphous silicon dioxide. *Journal of Non-Crystalline Solids*, **239**, 16-48.

Stevens Kalceff, M. A., Phillips, M. R., Moon, A. R., and Kalceff, W. 2000: "Cathodoluminescence Michrocharacterisation of Silicon Dioxide Polymorphs." *"Cathodoluminescence in Geoscience."*. Springer Verlag, Berlin Heidleberg.

Stevens, S. J. 1997: Temperature dependence of the cristobalite alpha-beta inversion. *J Therm Anal*, **49**, 1409-1415.

Stevens, S. J., Hand, R. J., and Sharp, J. H. 1997: Polymorphism of silica. *J Mater Sci*, **32**, 2929-2935.

Takakura, M., Notoya, S., and Takahashi, H. 2005: *Application of Cathodoluminescence to EPMA. Retrieved January 2005, from* *http://www.jeol.se/JEOL%20News/news36E/NEWSHOME/News%20home/35/index.html*.

Townsend, P. D., and Rowlands, A. P. 2000: Information Encoded in Cathodoluminescence Emission Spectra. In M. Pagel, V. Barbin, P. Blanc, et al., Eds. *Cathodoluminescence in Geoscience.*, p. 41-58. Springer Verlag, Berlin Heidleberg.

Tveit, H., and Valderhaug, A. 1993: *FeSi 8000 Final Report*. Elkem Internal Report.

Watt, G. R., Wright, P., Galloway, S., and McLean, C. 1997: Cathodoluminescence and trace element zoning in quartz phenocrysts and xenocrysts. *Geochimica Et Cosmochimica Acta*, **61**, 4337-4348.

Zinkernagel. 1978: Cathodoluminescence of quartz and its application to sandstone petrology. In H. Füchtbauer, A. P. Lisitzyn, D. Milliman, et al., Eds. *Contributions to Sedimentology*, **8**. E. Scweizerbart'sche Verlagsbuchhandlung (Nägele u. Obermiller), Stuttgart, Germany.

Part Two

Paper I

A REVIEW OF PREVIOUS WORK ON IMPORTANT PROPERTIES OF QUARTZ FOR FESI AND SI METAL PRODUCTION

K. Aasly, T. Malvik and E.H. Myrhaug[1]

Department of Geology and Mineral Resources Engineering, NO-7491 Trondheim, Norway
[1]Elkem ASA, Silicon Division, Alfred Getz vei 2b, NO-7465 Trondheim, Norway
E-mail: kurt.aasly@ntnu.no, terje.malvik@ntnu.no, [1]edin.myrhaug@elkem.no

ABSTRACT

Quartz is one of the main raw materials for the carbothermic production of ferrosilicon and silicon metal. The ideal process is written:

$$SiO_2 + 2C = Si + 2CO$$

The real process is much more complicated, depending on the quality of the raw materials. Several research projects have been carried out on quartz for the (Fe)Si process during the last 50-60 years.

One of the important properties that have been discussed in this review is the volume expansion that takes place between 850 °C to 1000 °C and explosive disintegration for some quartz types. No final and definite conclusions have been made but several reasons have been mentioned: The influence of the phase transformation to tridymite, which takes place within the same temperature interval, has been discussed in several papers. Alkali impurities have been mentioned as a critical factor for this transformation to take place. Other researchers have mentioned mica impurities as a critical factor for the behavior of the quartz at these temperatures. Studies of fluid inclusions in quartz was reported in some papers focusing on the volume expansion of these during heating as a source of explosive disintegration, especially along planes of healed micro fractures that often contain vast numbers of such inclusions.

Several methods for investigations of the important properties of quartz have been presented and these provide a good basis for the further research on quartz raw materials.

1. INTRODUCTION

Many of today's advanced materials depend on quartz as a raw material. Either as processed quartz or as silicon metal produced from quartz. Examples of such advanced materials are the computer chips that are used in all kinds of electronic equipment such as computers, mobile phones, refrigerators, etc., which all use silicon and quartz as raw material. Another important consumer of silicon metal is the photovoltaic industry that is growing fast. The silicon demand from the solar cell industry is rising and the challenge of the shortage of silicon with the right price and purity is already here. Silicon metal is also used as a raw material for the chemical industry in e.g. silicones. Ferrosilicon is used in steel making for desoxidation and alloying.

Silicon is produced industrially by reduction of silicon dioxide with carbon in an electric arc furnace at temperatures higher than 2000 ºC in the hottest parts, by a reaction that can be written ideally as:

$$SiO_2 + 2C = Si + 2CO \quad (1)$$

Quartz and quartzite are the source for Si in the carbothermic process for ferrosilicon and silicon metal ((Fe)Si). The industry has defined a list of absolute requirements to the raw material that must be achieved in order for the process to be optimized e.g. Schei et al. [1]:

– Chemistry (trace element content, e.g. Al, Ti, B, P, Fe, Ca))
– -Lump size (typical 10 – 150 mm)
– -Mechanical strength
– -Thermal strength
– -Softening properties

This review will focus on the work carried out with respect to the thermal strength of the quartz. This is important for the behavior of the quartz inside the furnace. Especially for how the quartz reacts to the sudden rise in temperature when it is fed to the furnace. If the heat makes the quartz disintegrate, the resulting fine-grained particles will create problems for the gas flow inside the furnace.

The quality of the raw materials is important for the quality of the final products from the (Fe)Si furnace. The industry has so far been most concerned about the quality of the black (carbon) raw materials. Consequently, research on the quartz raw materials has had low priority. However, several smaller and larger projects have been carried out with respect to the quartz raw materials during the last fifty years. Most of the available literature comes from projects carried out in Norway. There may be many reasons for this, but the major reason is that Norway has been the world's leading producer of FeSi and Si metal. This will of course be reflected in the available research material. Another factor is the secrecy around the process that can be seen within the industry. When one company has found a way of improving the process, this is kept as an industrial secret in order to achieve a competitive advantage. Therefore, the following review is based only on literature that has been published, or has recently been made public by the industry.

Knowledge about the raw materials becomes more important when the requirements to product quality increase. Therefore, an overview of the knowledgebase of characterization methods and results is important.

2. WORK ON QUARTZ FOR SI-METAL

2.1 Work up to the mid 1960's

According to Geiss [2], the Norwegian FeSi producers started to show interest in the cause of the behavior of the quartz/quartzites in the furnace towards the end of the 1950's. It has been difficult to find literature on the earliest work mentioned, thus only descriptions provided by Geiss [2] are available. During the late 1950's industrial tests were carried out by "Electrochemical Research Station" at Fiskaa on different Norwegian quartz and quartzite. These samples were heated to 1250 °C; and after heating, changes in the density of the samples were recorded. The conclusion of these investigations, based on the changes in density, was that some of the quartz had been transformed to tridymite. However, according to Geiss, later investigations on different quartz types made modifications of the conclusion necessary.

Geiss [2] also refers to T. Nervik, who studied the transition from quartz to cristobalite and its influence on the thermal strength of the material. Quartz, cristobalite and a glass phase were separated and identified by differential thermal analysis (DTA) and buoyancy in liquid (the type of liquid is not specified). According to Geiss, these results only exist as a manuscript and the work seems to have never been finished. Thus, the only conclusion available from this work is that different pegmatite quartz samples were weakened by the α- (low)/β- (high-) quartz phase transformation. The fact that the heating weakens different types of quartz has been confirmed in later work. However, different authors give different answers to this effect, and Nervik is the only who blames the α- / β-quartz phase transformation for all the effects. Later work, as will be shown in another section, uses more combined investigations and sees things in another perspective. Nervik would perhaps have given more specified arguments if the manuscript had been completed.

2.2 Work from the late 1960's to mid 1970's

In the 1960's and through the 1970's there were several Norwegian projects related to the problems with quartz raw materials. Many of these small projects showed some interesting conclusions based on the continuation of other work. It is not clear, if the different research groups knew about each other's work or if the projects were completely independent. However, the conclusions overlap to a certain degree and give new

answers to some questions. These reports have not been found, so these comments are, as for the previous paragraphs, based on the report from Geiss [2].

During the 1960's, a group of researchers at the Norwegian Geological Survey (NGU) worked on the significance of the defects on the thermal decrepitation of natural quartz. According to Birkeland and Carstens [3], this was a result of several meetings between NGU, "Metallurgical committee" and "Norwegian Ferrosilicon Producers' Central Committee". As a result of these meetings, NGU found this work to be its responsibility. The report presents three parts where the first part considers thin-section investigation of quartzites before and after heating. Three samples of each quartzite were cut into 1x5x5 cm. Two of these were heated in a furnace to 1000 ºC with different heating rates: One sample was introduced to the furnace at room temperature and heated to 1000 ºC over a period of 20 min, while the other sample was introduced directly to the furnace at 1000 ºC. Both samples were slowly cooled (2-3 hours), however, there are no specifications of how long the samples were kept at 1000 ºC. The third sample was used as an unheated reference. The three samples were then prepared as polished thin sections and studied by optical microscopy. Some interesting observations were made: The authors were surprised that the traces of fluid inclusions did not seem to be important for the fracturing of the sample. Deformation structures like undulate extinction, sub-grain segmentation, deformation lamellae and deformation bands, and most of the inclusion planes, seem unaffected by the heating. Birkeland and Carstens [3] observed that the heated rocks were more fractured than the unheated rocks and there were indications that the cracks tend to pass through each single grain. The fracturing was interpreted to be non-qualitative. The fractures were of the same type and distribution as in the fresh rocks. Birkeland and Carstens [3] also discussed the outcome from potential similar tests on smaller samples and concluded that such samples would probably show more and different fracturing. They also discussed the outcome of heating the samples to different temperatures and thought that different temperatures would give different results.

Part two presents microscopy of quartzites and single-crystal quartz in a heating stage microscope. The samples were prepared as 1 mm thick and 6 mm diameter cylindrical slices, polished on both sides. The apparatus used was a Leitz 1350 heating stage mounted on a Leitz Ortholux transmitted light microscope. The heating occurred over five to ten minutes up to 1300 ºC. The heating was carried out stepwise in order to lower the heating rate. This gave, according to Birkeland and Carstens [3], an irregular heating rate. Results were recorded as visual observations of differences in the temperatures when cracking occurred during heating. In most samples, cracking appears at 300 °C – 400 ºC. This seems to be related to fluid inclusions and sometimes to grain boundaries. The cracking seems to increase in most of the samples towards the transition from α-quartz to β-quartz at 573 ºC. After 600 ºC usually nothing happens and the samples show some sort of relaxation of the samples up to 900 ºC. Above 900 – 1000 ºC, there is regenerated activity in several samples. The authors describe the activity as explosions that destroy the samples. Birkeland and Carstens conclude that this type of explosion is of importance for the strength of the quartzite. However, there is no discussion around the difference between the small sample size used in the investigations compared to the larger material sizes used in the actual process.

This study is advanced to a degree that even today's technology seems to have stalled on this level. The heating stage investigation presents some interesting observations, although these are based only on visual observation and are difficult to quantify. Today's technology is more advanced in the way that images can be captured sequentially (or even recorded on digital video) such that the observations can be better illustrated.

The third part of the report consists of comments to numerous specialty investigations. One of the techniques mentioned here is the so-called decreptiograph or better known as thermosonimetry (TS) of minerals. The equipment has not been used in this project but the theory around it is briefly described. It is mentioned that the project initiated the construction of one such decreptiograph at the Dept. of Physics at the Norwegian School of Technology (NTH, now the Norwegian University of Science and Technology (NTNU)). This equipment has later been described and tests carried out by Lønvik [4-6] and Lønvik and Smykatz-Kloss [7] among others.

Lønvik [4, 5] investigated different types of quartz by thermosonimetry. Samples of the rock were made by drilling cylindrical cores with approximately 8-12 mm diameter (varying) and around 3 - 4 grams. These sam-

ples were then analyzed in a chamber capable of heating to ca 1000 °C and a stethoscope mounted in the sample chamber recorded the acoustic effects from the sample during heating. Lønvik [4, 5] proved that the equipment was capable of measuring the acoustic effects, and the intensity of these, created in the samples during heating.

Peaks at 550 °C to 580 °C represent the phase transformation from α- to β-quartz. Peaks also occurred at 870 °C and 960 °C that were interpreted as representing the quartz – tridymite transformation. These peaks were not present in all the samples, indicating that tridymite transformation is present in only some of the samples.

2.3 Work during the late 1970's

Lønvik also carried out investigations reported by Geiss [2] on two samples from that project. These results gave the same conclusion as the earlier TS investigations mentioned above. However, Geiss mentioned an important drawback: This method is only capable of heating samples to 1000 °C, which is too low to confirm the effects of heating described by others e.g. [3] at temperatures higher than 1000 °C. Thus, he argued that dilatometry is more useful because it has a higher temperature range, and can be handled more quantitatively.

In a letter to various people, Birkeland [8] summarized some of the work he carried out at the Norwegian Geological Survey (described by e.g. Birkeland and Carstens [3]). He also made comments on work carried out by the Metal Properties Group at Niagara Falls (reference not available) which concluded that "cracking is caused by and correlated to the amount of optical visible mica (at 10x magnification) and $Fe(OH)_3$". Birkeland disagreed with these conclusions based on the fact that high amounts of mica are observable only if the quartzite is coarse-grained and of relatively high metamorphic state. The coarse-grained fabric and high metamorphic state were also thought to be a reason for low thermal stability, such that no conclusions can be drawn to the mica itself. He also referred to his own work with the Kragerø quartzite [3] that had no visible mica or $Fe(OH)_3$, but still disintegrated heavily when heated to 1000 – 1100 °C. At the end, Birkeland concluded that one has to distinguish between different types of cracking. Birkeland believed that cracking could be both "dangerous" and "unimportant". He probably related this to the observation of large grains (flakes) of mica, which will create cracking along its boundaries with certain effects as described by Mrs. Faulring (Birkeland gives no reference but she probably belongs to the Niagara Falls group). Birkeland questioned if these effects are dangerous.

Geiss [2] presented a high temperature investigation of quartzite from the Gudvangen deposit, Kragerø, Norway. This is a comprehensive report with considerations made around the different methods used and the comparisons between different types of equipment for each of the methods. Geiss considered such as regular optical microscopy and fluid inclusion studies as well as more advanced techniques such as differential thermal analysis (DTA), TS, dilatometry, high-temperature XRD and softening point measurements (by use of compressive strength measurements).

Optical microscopy showed that the samples were coarse crystalline, completely recrystallized quartzites that had undergone plastic deformation. Numerous fractures were healed and the samples contained three generations of fluid inclusions. The rocks looked very similar and they could not be easily separated into "good" and "bad" quartz based on microscopy itself.

The DTA analysis was carried out on three different types of equipment (own equipment, by Birkeland and test analysis by two instrument manufacturers). Birkeland carried out the most extensive investigations with regards to the amount of samples, while the other equipment were tested on two of these samples. Geiss [2] showed that the equipment gave more or less the same results when the analyses were carried out with the same heating rate and paper speed (the paper speed determined the resolution of the results). He also stated that reanalyzing already heated samples might give interesting additional information, especially about the generation of cristobalite (and Tridymite) from the initial analysis. Geiss also concluded that Al_2O_3 should be used as standard. The analysis carried out by Birkeland showed, except for the α- to β-quartz phase transfor-

mation, zero to one peaks for "good" quartz and one to several peaks for "bad" quartz. This may be interpreted as a criterion for distinguishing "good" and "bad" quartz samples.

Dilatometry analysis was also carried out in the project reported by Geiss [2]. These were as the DTA, carried out on three different dilatometry equipment. Geiss [2] concluded that the best results were obtained by using relatively coarse and compressed diagrams and summarized the results to say that "good" quartz shows little or no effect between 800 °C – 965 °C and "bad" quartz shows strong effects in the same interval. Geiss [2] related this to the generation of tridymite and said that the effects between 800 °C and 965°C increased at alkali content above 0.15%. However, he made this as an assumption and stated that the generation of tridymite had not yet been proved. This has to be done by using, for instance, XRD or optical microscopy of thin sections. Still, he concluded that the content of alkalis seem to have a crucial influence on the fracturing of the rock during heating.

The softening point of quartz was measured using "standard" equipment at SINTEF Metallurgy. Samples from each piece of quartz were made as cylinders with diameter 31.6 mm and height 31 mm. The cylinders were exposed to a load of 2 kp/cm^2 and the temperature was recorded at 0.6 % and at 40 % compression of the samples (for complete method description, see e.g. Seltveit [9]). The analyses showed that the softening interval were as narrow as 10 °C. The chemical analyses with respect to Na2O were extremely high in some of the samples, up to ten times the value in average samples. Visual observations of changes (fracturing and dark spots) were made as well. The conclusion from this work stated that there were no significant differences between the different quartz samples. The reason Geiss [2] carried out these investigations was that this was the only method capable of giving results up to the smelting point of quartz.

In an oral communication with Geiss [2], Birkeland described x-ray diffraction (XRD) on quartz samples that initially were heated (temperature and other vital details were not reported) and further cooled and crushed. According to Geiss [2], Birkeland reported that only high-quartz was detected. These analyses were carried out on pulverized rock. Geiss' [2] hypothesis was that the crushing alters the lattice tension and thus leads to different reactions to the heating. He believed this was the reason that only quartz was found and no tridymite, as were interpreted to be the cause of fracturing in other tests. In order to check this hypothesis, Geiss [2] carried out high-temperature XRD analyses on larger pieces of quartz. Samples were sent to three different laboratories. He concluded that all of the analyses were more or less unsuccessful and did not confirm the possible generation of tridymite in the most alkali rich samples that were seen from the dilatometry investigations. Tridymite (and cristobalite) were found only in samples heated to 1200 °C and higher. Samples cooled to 80 °C showed cristobalite, tridymite, and only weak deflection for quartz. Analysis of the same samples after crushing showed quartz, cristobalite and possibly tridymite. According to Geiss [2], the absence of tridymite in the samples after crushing was caused by the crushing, which seemed to alter the SiO_2 lattice. He concluded that as long as the samples had not been accidentally switched, the generation of tridymite could not be the reason for the heavy fracturing seen between 800 and 965 °C in dilatometry investigations (e.g. Geiss [2]). Geiss wrote that he intended to do more of these investigations and even described the procedure he was planning. However, no reference has been found to these further investigations.

2.4 Work during the 1980's

Seki et al. [10] discussed the influence of raw materials on the production of 75% ferrosilicon. The paper considered the influence of all raw materials and referred to observations of a furnace and investigations made during excavation of a furnace. These investigations gave interesting observations and statements for the requirements to the quartz raw materials but the only test method mentioned was the Seger Cone test (cone test for refractoriness). This test were carried out on the considered raw materials but the theory and methodology were not discussed in the paper (see e.g. Seltveit [9] for method description). This is the only reference to the use of this method on this type of material that has been found. However, according to Kallfelz [11] this is an interesting method for testing the softening properties of quartz and can possibly be compared with results from dilatometry.

Malvik and Vokes [12] summarized research on the liberation of minerals by comminution. This research was concentrated on Norwegian raw materials for the metallurgical industry with emphasis on dolomite. However, quartzite was also tested to certain degree. Image analysis was carried out to determine the form factor and cohesion factor of the rock. The Norwegian Tana quartzite (regarded as having good thermal properties) and the Finnish Nilsiia quartzite (bad thermal properties) were investigated. The results show that even if the form factors are almost identical, the cohesion factors can be used. The Tana quartzite had a much better cohesion factor than the Nilsiia quartzite along the grain boundaries. Thus, this may explain the differences in thermal stability.

Lønvik and Smykatz-Kloss [7] compared the DTA and the TS techniques. The results confirmed the agreement of the main features of TS to those of DTA. They emphasized the higher resolution of TS in case of overlapping effects compared to DTA analysis.

Malvik [13] discussed earlier quartz investigations and listed possible parameters that influence the thermal properties of the quartz. These parameters are listed in Table 1.

Table 1: Parameters influencing the thermal properties of quartz (after Malvik, 1986a)

A	Internal parameters in quartz	Grain structure	Size
			Shape
			State of recrystallisation
			Grain bonding
		Fluid Inclusion	Amount
			Type
			Composition
		Chemistry	Foreign ions
			Trace elements
		Strain conditions	
		Elasticity module	
		Crystal structure	
B	Effect related to foreign minerals	Type of minerals	Mica most important
		Amount of minerals	
		Grain-size	grain size distribution
		Composition of other minerals	
C	Effect of the total chemistry	Diffusion of elements into quartz	Negative influence

Malvik [13] emphasized the fact that the TS technique had been further developed to be capable of heating to 1650 °C, something that gave the method a higher capacity, especially as the higher temperature enables the TS technique to detect acoustics in the entire interval that also is covered by dilatometry.

Malvik [13] reported investigation methods that he proposed for different types of quartz to see what causes the deflection between 850 and 1000 °C. As he interpreted the results, this is caused by mica impurities and/or tridymite formation catalyzed by high content of impurities. The types of quartz to be investigated were also specified: Malvik [13] proposed a limited selection of bad thermal quartzes and a reference sample of good thermal quartz.

Malvik [14] performed further investigations on the role of mica on the thermal properties of quartzite. This was carried out on two of the quartz samples used by Geiss [2] and two other samples. Malvik carried out additional dilatometry on one sample (the others were already analyzed by Geiss [2]) and TS on all the samples. TS was carried out on different types of prepared samples: powder of unsorted samples, on samples consisting of mica separated from the rock and the quartz resulting from the extraction of mica. In addition, analyses were carried out on different grain size fractions of the crushed material. Malvik [14] concluded that the mica is the cause of the large effects seen in dilatometry and TS, thus mica plays an important role for the thermal stability of the quartzite. However, Malvik [14] made reservations to the type and occurrence of the

mica. Thus, he disagreed with the critical comments made by Birkeland [8] on the conclusions made by the research group at Niagara Falls.

Lønvik [6] discussed the theory around the TS technique. He presented data around the phase transformation from high-quartz to high-cristobalite. Constant firing time at 1470 °C for one hour prior to the investigations showed that quartz of different origins were transformed to cristobalite with different transformation rates. Thus, he concluded that the grain size and the presence of impurities influence the transformation rate.

Martinsen [15] studied the fluid inclusions in different quartzes and compared these with regard to the classification of the quartz as having "good" or "bad" thermal properties. Martinsen observed only secondary fluid inclusions in most samples except one quartzite that contained pseudo secondary inclusions. By plotting the data collected in a diagram (see Martinsen [15] fig. 8) as homogenization temperature vs. salinity, the two types of quartz regarded as having very good thermal properties, plot together. Martinsen concluded that the amount of samples and data in his investigation was too limited to give a final answer, but that it was reasonable that the fluid inclusion composition in the quartz could say something about its quality as a raw material for the (Fe)Si process. This seems to have been a more advanced fluid inclusion study than the one by Birkeland [2]. Birkeland studied only the shape and visual content of the inclusions by ordinary optical microscopy, while Martinsen [15] used a freezing and heating stage to study smelting temperatures (water and solid phases) and the homogenization temperature for the inclusions. Thus, Martinsen could say more about the properties of the fluid inclusions than Birkeland. Fluid inclusion studies on quartz for the glass industry have been reported by e.g. Gemeinert et al. [16]. He demonstrated that the properties of the fluid inclusions determine the behavior of the raw material during phase transformation and smelting process. The conclusion states that low-hydrothermal samples of quartz show high speed of phase transformation from β-quartz to β-cristobalite, which causes a release of the inclusion contents. This is regarded as positive for the production of silica glass, in order to avoid gas bubbles in the glass. These observations can also be relevant for quartz for the (Fe)Si industry. It certainly indicates that fluid inclusion is important for the cristobalite formation and, thus, also for the heating rate of the material.

Malvik [17] discussed the relationship between mineralogical texture and comminution characteristics for rocks and ores. He used several case examples and one of these was the grain structure of quartzite. Malvik investigated two quartzites of different thermo mechanical properties: The Tana quartzite ("good") and the Nilsiia quartzite ("bad"). Investigations were carried out using a technique developed by Boasen and Fjerdingstad [18], combining backscattered electrons (BSE) and cathodoluminescence (CL) images, to give an indication of the cohesion between the different quartz grains. These results were also discussed by Malvik [19]. Quartzites that are of low recrystallization and low metamorphic grade show differences in luminescence brightness in the different generations of quartz. The silica cement and the recrystallized quartz will have less luminescence than the low luminescence recrystallized quartz. In completely recrystallized quartzites, there will be no contrast between different quartz grains. The author concluded that it is important that the ratio cement/clastic materials is highest possible if one wants to avoid the collapse of the grain structure when heating the quartzite. The discussion around CL as a method for characterizing quartzite raw materials was continued in a paper presented by Malvik and Lund [20]. This paper defines problems involved with quartzite as a raw material for (Fe)Si metal production. In this report, the authors describe several test methods that can be used in the field when searching for new deposits, and further in the process of testing possible methods. Most of these methods have been described earlier, such as CL (e.g.[17, 19]), Dilatometry (e.g. [2]) and TS (e.g. [4-6] and [7]).

2.5 Recent work on quartz

During the 1990's several people within Elkem ASA Silicon Division have been engaged in work on quartz raw material. Unfortunately, most of this work exists either as confidential reports or as memos (e.g. [21]).

At NTNU, two different quartz related projects have been carried out during recent years: At the Department of Geology and Minerals Resources Engineering, professors, post docs and PhD-candidates have been engaged in the project "The value chain from mineral deposit to beneficiated product with emphasis on

quartz". This is a Strategic University Program (SUP) and is being carried out in cooperation with e.g. NGU, Elkem ASA Silicon Division and several other industrial partners. At the Dept. of Materials Technology, researchers have been engaged in another SUP project: the project "From sand to solar cells".

Researchers at NGU have been working during many years on the exploration and investigation of possible quartz deposits in Norway. However, none of these projects has discussed the thermal properties of quartz for the ferrosilicon and silicon metal process.

3. CONCLUSION

The research activities carried out on the thermal properties of quartz and quartzite raw materials for the metallurgical production of ferrosilicon and silicon metal during the last five decades is numerous. Most of the literature that was found is from research carried out in Norway, both published and unpublished. A possible reason for this is that Norway has been the leading producer of ferrosilicon and silicon metal, combined with the confidentiality policy connected to the research carried out in the industry.

This review shows that much of the discussion about "good" and "bad" quartz has been related to the explosive disintegration of some quartz types at 850 to 1000 ºC. The different reasons discussed are the generation of tridymite and the alkali impurities that must be joining this phase transformation as well as the influence of mica on the thermal stability of the quartz.

The correlation between Al_2O_3 and/or K_2O content with observations in dilatometry indicates that mica is present in samples which show critical deflection in the interval between 850 and 1000 ºC.

Many of the papers discussed in this review are related to the properties of quartzites. However, pegmatitic and hydrothermal quartzes that show low thermal stability, but the mica is probably not the reason here.

Fluid inclusions in quartz are also a possible factor that influence the thermal properties of quartz and this should be studied in more detail. Although several researchers have investigated fluid inclusions, only Martinsen [15] has looked at the composition of these inclusions. Further investigations should continue this study and look at the fluid inclusions related to the formation and later alteration of the quartz.

It seems clear that no final conclusion has been made with regard to the parameters influencing the thermal properties. The investigations discussed in this paper consist of a vast collection of advanced techniques. They certainly form a basis for further investigations.

REFERENCES

[1] Schei, A., Tuset, J. K. and Tveit, H., "Production of High Silicon Alloys", Trondheim: Tapir Forlag, 1998.

[2] Geiss, H. P., "High temperature investigations with quartzite from the Gulodden quarry at Kragerø" (in Norwegian), Report to Fesil & Co., 1977.

[3] Birkeland, T. and Carstens, H., "Preliminary report on high temperature investigations of natural quartz", NGU Project B 2006 (in Norwegian), 1969.

[4] Lønvik, K., "Report on thermosonimetry investigations of 2 types of natural quartz" (in Norwegian), 1972.

[5] Lønvik, K., "A thermosonimetric investigation of 3 types of quartzite (concerning materials from Tinnfoss Jernverk, Bjølvfossen Ålvik og Salten Verk)" (in Norwegian), 1974.

[6] Lønvik, K., "Thermosonimetry", Thermochimica Acta, 110, 1987, pp. 253-264.

[7] Lønvik, K. and Smykatz-Kloss, W., "Comparative studies of structural transformations of carbonate and silica minerals by means of thermosonimetry and differential thermal analysis", Thermochimica Acta, 72(1-2), 1984, pp. 159-163.

[8] Birkeland, T., "Subject: Thermal stability of quartzite", Unpublished letter to D.L. Mathias, J. Molly and H. Berg, 1975.

[9] Seltveit, A., "Refractories" (in Norwegian), Trondheim: Tapir Forlag, 1992.

[10] Seki, K., Muroi, S.-I. and Morimoto, I., "Influence of raw materials on the production of 75 % ferrosilicon", in 3rd International Ferroalloys Congress, Tokyo (Japan), 1983.

[11] Kallfelz, P. L., "Quartz for production of silicon metal - criteria for the right choice. Study for Elkem Si-div", Internal report, With permission from Elkem, 2000.
[12] Malvik, T. and Vokes, F. M., "Final report to NTNF: Liberation properties of minerals" (in Norwegian), 1984.
[13] Malvik, T., "Evaluation of previous quartz investigations, methods and suggestions for follow-up", SINTEF internal report, Project title: Thermal properties of quartz, work note 2/23; Project no: 363023, (in Norwegian), Trondheim, 1986.
[14] Malvik, T., "Working paper: The importance of mica on the thermal shock properties of quartz materials", SINTEF internal report, Project title: Thermal properties of quartz, work note 3/23; Project no: 363023 (in Norwegian), Trondheim, 1986.
[15] Martinsen, M., "Report in the open SINTEF-project: Fluid inclusions in quartzites", SINTEF internal report, report no. 363030 (in Norwegian), 1987.
[16] Gemeinert, M., Willfahrt, M., Hager, I., Bortschuloun, D., Zeween, S. and Hadan, M., "On the Effect of Gas-Liquid Inclusions in Quartzes of Different Genesis on the Phase-Change and Melting Behavior of the Host Mineral" (in German). Zeitschrift Fur Geologische Wissenschaften, 18(1), 1990, p. 95-100.
[17] Malvik, T. "Relations between mineralogical texture and comminution characteristics for rocks and ore", in XVI International Mineral Processing Congress, Elsevier Science Publisher B. V., Amsterdam, 1988.
[18] Boasen, T. and Fjerdingstad. V., "A method for quantification of quartz cementation in clastic sediments by using scanning electron microscopy" (in Norwegian). in Norwegian Geological Society, Wintermeeting 1987, Trondheim, 1987.
[19] Malvik, T., "Method for characterizing grain boundaries/cementation in quartz materials", SINTEF internal report, Project title: Thermal properties of quartz, work note 4/23; Project no: 363023 (In Norwegian), Trondheim, 1986.
[20] Malvik, T. and Lund, B., "Problems involved with quartzite as a raw material for FeSi and Si metal production", Process Mineralogy IX, The Minerals, Metals & Materials Society, IX, 1990, p. 499-508.
[21] Birkeland, R., "Optimal quartz properties - method evaluation part 1", report no F10/03, Internal Report, With permission from Elkem (in Norwegian), 2004.

Paper II

Silicon for the Chemical Industry VIII
Trondheim, Norway, June 12-15, 2006
Eds.: H.A. Øye, H. Brekken, T. Foosnæs, L. Nygaard

Quartz for carbothermic production of silicon - effect of the process steps, handling and transport from mine to furnace

Kurt Aasly [1)], Terje Malvik [1)], and Edin Myrhaug [2)]
1) Dept. of Geology and Mineral Resources Engineering, NTNU, NO-7491 Trondheim, Norway.
2) Elkem ASA Silicon Division, Alfred Getz vei 2, NO-7465 Trondheim, Norway.

Abstract

Materials handling is important for keeping the required or optimal strength and fragment size of the materials. This paper presents a brief literature study on critical factors affecting the quality of quartz and quartzite as a raw material for the metallurgical production of ferrosilicon and silicon metal. Gravel- and rock quartz can be useful classification in qualitative terms, as the gravel quartz will be stronger than the rock quartz for two main reasons: Micro cracks are induced in the rocks by the blast, and natural selection has left only the mechanically strongest quartz boulders in the gravel deposit. Drilling and blasting combined with the processing of the raw materials are important for the generation of fines during further handling and finally inside the furnace. Further, it has been demonstrated that the total number of meters of fall that the quartz has been exposed to is crucial for the increase of fines during material handling. This is a problem on both the mineral production plant in the stages after the crushing and sieving and on the metallurgical plants from the unloading of the ship to the charging on the furnace. Other factors that might influence the final fines content are also mentioned.

Introduction

Materials handling is important for keeping the required or optimal strength and fragment size of the materials. Mineral processing plants depend on the size of the grinded ore for achieving the optimal recovery rate. Aggregate plants sell their products with specifications of the strength and size distribution of the materials, as do the producers of quartz and quartzite for the ferrosilicon and silicon metal ((Fe)Si) industry. To be able to get the right specification of the raw materials, the different parts of the production cycle need to compromise on the optimal production of the raw materials e.g. [1].

This paper presents a brief literature study on critical factors affecting the quality of quartz as a raw material for the metallurgical production of (Fe)Si. The emphasis has been on factors during production, transport and handling of the raw materials. The literature study has gone through work carried out on different parts of mineral production. The study is based on a small collection of published and unpublished (company internal) work with emphasis on answering the following questions:

- What affects the mechanical properties of the raw materials?
- How can unnecessary weakening of the quartz be avoided?
- How can unnecessary generation of fines be avoided?

The mechanical strength is important for avoiding size reduction of the quartz during handling and transport and will be critical for the generation of fine material. In this case, fines are defined as all material smaller than 20 mm. This is smaller than the size distribution that is set up as a requirement by the (Fe)Si producers e.g. [2].

The raw materials

The source for silicon (raw materials) for the metallurgical production of (Fe)Si, is quartz and quartzites consisting of minimum 98.5 % SiO_2, depending on the process requirements. Quartzite is the metamorphic equivalent of quartz rich sandstone, while quartz in this context is used for vein quartz and pegmatites.

Metallurgists often refer to the raw materials as either "rock quartz" or "gravel quartz". The first describes raw materials that are mined through blasting operations in a quarry/mine, while the second describes raw materials taken out by non-blasting operations through surface excavation of unconsolidated material. Rock quartz are either hydrothermal- or pegmatite quartz or quartzite, while gravel quartz are any type of quartz, deposited as e.g. fluvial material. The classification used by metallurgists is also useful in qualitative terms, as the gravel quartz will naturally be stronger than the rock quartz for two main reasons:

- Blasting induce micro cracks in the rocks quartz
- The gravel quartz has gone through natural selection as only the strongest quartz boulders "survive" the size reduction during transportation in the river.

In this paper, "quartz" will be used for both quartz and quartzite as a joint designation.

The process

The metallurgical (carbothermic) production of (Fe)Si is described by e.g. [2]: Quartz and carbon materials (+ iron ore) react at high temperatures to form silicon metal (ferrosilicon). The temperature at the top of the charge burden of the furnace is 700 – 1300 ºC and the temperature in the hottest parts of the furnace is more than 2000 °C. The ideal reaction can then be written as:

$$SiO_2 + 2C = Si + 2CO \quad \textbf{(1)}$$

In a real furnace, the process is much more complicated and consists of several sub-processes, which may be affected by the quality of the raw materials.

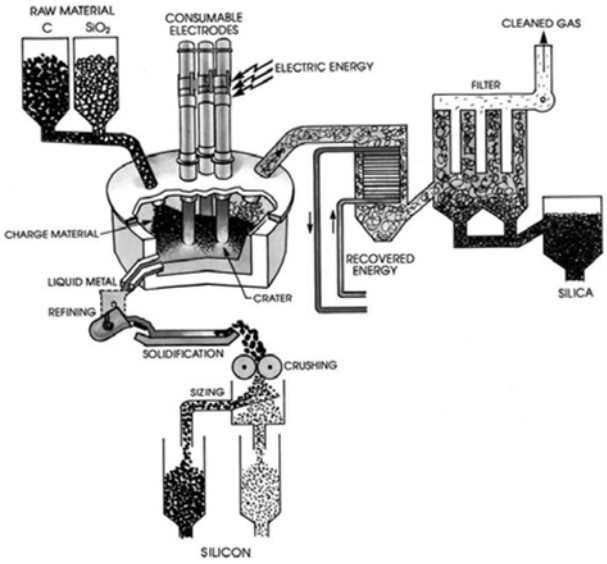

Figure 1: Sketch of a silicon furnace after [2]

The furnace sizes can be up to 40 MW with energy use up to 11-13 MWh/ton produced Si-metal for an optimal production process. However, small changes in the silicon recovery lead to dramatic changes in production costs pr. ton produced metal.
The industry has a set of requirements to the raw materials [2]:

- Chemistry (e.g. Al, Ti, B, P, Fe, Ca)
- Lump size (20 – 150 mm)
- Mechanical strength
- Thermal strength
- Softening properties

Chemistry and size are the most common specifications used by all (Fe)Si producers. Some (Fe)Si producers focus on/measure mechanical- and thermal strength although these are not included in the specifications to the supplier, and a few (Fe)Si producers focuses on softening properties or properties/measurements related to the softening properties. Further, additional requirements may be defined by the individual (Fe)Si producer, according to what is most optimal for the specific operation.

Raw material strength properties and fines

The raw material strength may be divided into mechanical strength and thermal strength, which in many cases probably are closely related. The mechanical strength is important to avoid too high size reduction of the raw materials and generation of fines that is brought in to the furnace. Whereas thermal strength is important to prevent the raw material from disintegrate and generate fines (decrepitate) as a result of the extreme heat inside the furnace during operation.
During operation, too much fines will affect the flow of SiO-gas in the furnace negatively. Any fines will fill the gas volume between large particles in the charge and

obstruct the gas-permeability in the furnace e.g. [2]. Further, SiO gas will be hindered from reacting with C to create SiC, which is an important partial reaction. This will lead to loss of SiO gas from the furnace and reduced productivity (the Si – recovery will be reduced).

The silicon metal industry uses requirements like chemistry, size distribution, mechanical- and thermal strength to select the suitable quartz raw materials for the process. Mechanical- and thermal strengths are tested by measuring the friability index (FI) and the thermal strength index (TSI) respectively. Testing is carried out by tumbling and sieving of unheated (FI) and heated (TSI) material (-25+20 mm size). The indexes are calculated from the grain size distribution after tumbling e.g. [3]. Birkeland [3] also discuss other indexes that can be calculated by using variations of these tests.

The resistance of different quartz types against size reduction/decrepitation is a function of rock properties. These properties can be tested by the methods mentioned above. However, the methods are not optimal and give only indicative results. For this reason, all new raw materials need to be tested in operational scale to decide if they are suited for the operation.

As mentioned above, the generation of fines and the mechanical strength of the quartz raw materials are also strongly affected by operational control during mining, processing and handling. Therefore, when the (Fe)Si industry try out new quartz raw materials for their process or experience problems with existing raw materials, they should control the raw material producers with regards to these factors to exclude operational problems as a cause of bad quality. Understanding and controlling the production and material handling may result in less generation of fines and better mechanical strength.

The Mine Site

The production of the raw material includes several steps (Figure 2) that includes the identification of customer and market requirements, geological understanding of the deposit via the actual process of mining and processing to the delivery to the customer. The steps from blasting to delivery also include critical points of loading and transport of the raw materials.

Between each step and after the processing, material handling plays a critical role. Especially after processing, it is important that the material handling is carried out such that the generation of fines is kept to a minimum. This chapter will discuss the consequence of the different steps on the rock strength properties and how they can be optimized.

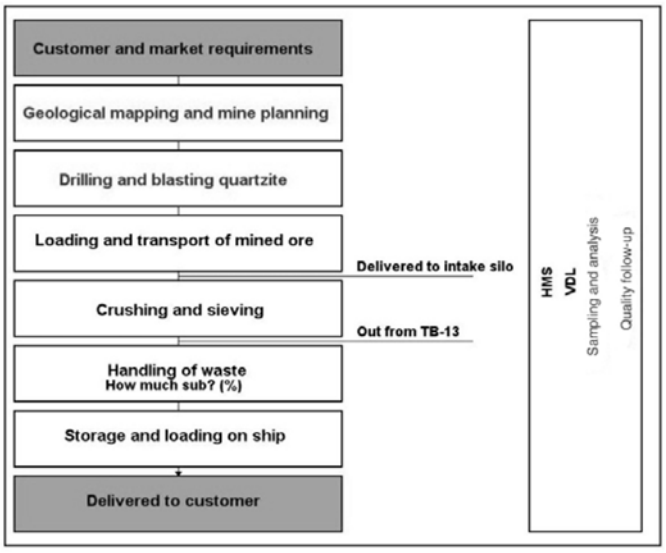

Figure 2: Flow chart of quartzite mine (from Trond Brenden-Veisal).

Identification of customer and market requirements/geological mapping and mine planning

Identification of customer and market requirements are important for a prospective producer of quartz raw material before further exploration can be carried out. This information gives the producer the chance to limit the exploration results by removing identified targets that fail to fulfill requirements that are easily checked in early stages. This is especially important for tonnage and bulk chemistry requirements. Geological mapping and mine planning can rapidly answer such questions on an early stage for deposits that are far outside the accepted values. Further, geological mapping and mine planning is an important tool during day-to-day operation to make decisions for where to produce from and in order to keep a stable product specification.

Drilling/blasting

Drilling and blasting is a critical point in the production of ore and industrial minerals. Research has been carried out, looking at the result of combined drilling/blasting and crushing on the quality and strength of the final product as well as on the final cost of the comminution process through the different distribution of energy in these processes e.g. [4-6]. Especially, the aggregate industry has spent a lot of effort on research on this topic. The findings for the aggregate industry can be used also for the ferrosilicon/silicon metal industry to achieve the best possible strength of a particular quartz source.

Nielsen [5] showed that the drill-hole pattern and the amount and type of explosives are important for the energy use during further crushing and grinding of the raw materials. This shows that the energy use during these processes reflect the internal strength in the material. The damage on the material can be explained by shockwaves from the

detonation that propagate through the rock mass and induce micro cracks in the surrounding rocks. These micro cracks reduce the resistance of the material against crushing.
According to Nielsen and Malvik [1], two factors are important for the crushing and grinding resistance of the ore: The powder factor (the amount of explosives) and velocity of detonation (VOD) of the explosives. An increase in one or both of these factors will reduce the crushing and grinding resistance of the ore. Another important factor for the formation of micro cracks in the rock is the drill-hole deviation [6]. Drill-hole deviation can cause excess power in some areas and damage the rock through uneven distribution of power, making a more unpredictable distribution of damage.
A natural consequence of the facts discussed above is that the blasting of rocks creates a halo around the drill hole, where the mechanical strength of the rock has been weakened due to the formation of micro cracks. The mechanical strength is thought to influence also on the thermal strength of the rock or to put it another way: the generation of blast induced micro cracks in the rock is likely to affect the thermal strength of the rock, as it probably is closely related to the mechanical strength.
However, the charge in the blast is not always important for how much damage is inflicted on the rock. As seen in [4], examples from two different aggregate quarries show that for a quarry where blasting happens with higher charge than in the second quarry, much less damage were induced on the aggregate from the first quarry than on the aggregate from the quarry where less charge were used. This is caused by a difference in the rock type (in the case of [4] Permian dolerite vs. tonalitic gneiss) and microstructure of the rocks which gives totally different susceptibility to blast induced damage [4]. This indicates, according to Jern [4], that the blast induced damaged is not only dependent on the charge but also on the initial rock strength, which is defined by the geological conditions (mineralogy, texture, etc). Here, the cohesion between the grains probably plays an important role.

Processing (crushing and sieving)

The first step in mineral dressing is, in most cases, fragmenting in one or several steps [7]. The first step of the fragmenting is coarse crushing (primary crushing) and is carried out by using e.g. a jaw crusher. The rocks are, with enormous force, defragmented to an expected (maximum) grain size. For primary crushing, characteristic grain size (d_{80}) for the feed is usually 300 – 1000 mm while the product d_{80} is 50 – 300 mm [7]. However, if the rock has been exposed to disproportionate power during blasting, the final grain size after crushing may, according to e.g. [5], be finer than expected.
Gravel quartz will naturally need more energy for the comminution process than the blasted rock quartz e.g. [5], as the gravel quartz has no blast induced micro cracks and have been naturally selected to contain only the mechanically strongest boulders. This makes the comminution process more energy demanding and also the generation of fines will be lower than for rock quartz.
Nielsen and Malvik [1] states that the three first stages of crushing have the best effect on opening the micro cracks generated by the blast. Therefore, quartz that has gone through several stages of crushing will have less chance of disintegrating during further handling.

Handling of waste

The fine materials that are generated through the production cycle are often a problem to sell. The only solution is often to dispose the rejected undersize material on a tailings disposal site. In some cases, the undersize material can be further screened to create fractions that can be sold cheap or even given away, e.g. to the local community as filling material etc.

Material handling incl. loading and transport

After blasting in the mine, the fragments are transported to the mineral processing plant. The plant is optimized for the size distribution of the different products delivered to different customers. An example of such a plant is sketched in Figure 3.

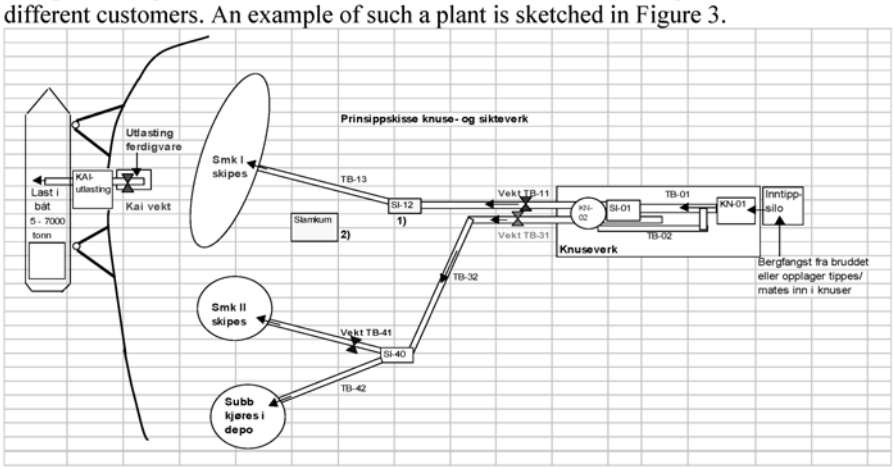

Figure 3: Flow chart crushing and sieving plant (from Trond Brenden-Veisal).

During the transport and processing in the plant, the quartz is passing by several reloading points during the handling. This involves in many cases that the material is exposed to several meters of free fall. Some producers use special arrangements to prevent high drops from the conveyor belt onto the storage pile as shown in Figure 4.

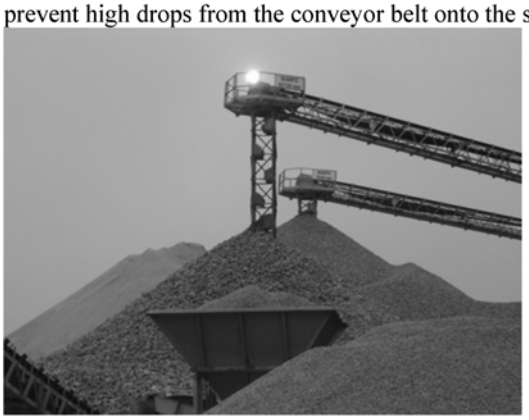

Figure 4: Example of tool for reducing height of fall for quartz raw materials.

Rock quartz that has been mined by blasting will be more weakened than gravel quartz that has not been exposed to blast induced damage. The natural selection that happens during transport of the gravel in a stream channel makes the gravel quartz even more resistant to size reduction by mechanical processes since only the strongest boulders remains intact in the deposit. This makes the rock quartz the most exposed to size reduction during handling and transport. As a result of this, most company internal reports consider only the rock quartz for the investigations of the effect of free fall heights on the generation of fines e.g. [8].
Legally the handling and transport can be divided into two parts – 1) hauling in the mineral production plant and 2) shipping and materials handling in the metallurgical plant. The responsibility of the material belongs, according international regulations, to the producers until the material passes the rail of the vessel. After this point, the responsibility of the material belongs to the customer, in this case the metallurgical plant.
Hauling is probably not among the most critical parts of the raw material line, however, even in this part the fragmented rocks are experiencing drops that contribute in fragmenting the rocks and creating smaller fragments. The part of the hauling that is prior to the crushing and screening is probably just contributing to reducing the costs of crushing (even if the results will hardly bee seen in the balance sheet). The hauling from the crushing and screening plant to the ship loading facilities, will contribute to the size reduction of the raw materials that are being or might be recognized at the smelter plant [8, 9].

Storage and loading on ship

The raw materials are usually transported from the mine to the smelter by bulk carrier ships. Loading is by conveyor belts and this gives a high drop to the bottom of the ship loading area. This drop is higher earlier in the loading process and will decrease according to the filling of the ship.
Also, the unloading of the ship is critical and might be optimized by selecting the proper unloading means and equipment.

Delivered to customer- handling at the smelter plant

The system for handling raw materials at the plant, include transport, storage, weighing and mixing. As the ship arrives at the smelter plant, the quartz is transferred from the ship to a conveyor belt by a feeding jaw. This is where the size reduction at the plant starts. The drop from the feeding jaw down on the conveyor belt can be several meters. Further, the quartz is transported on the conveyor belt to the raw material silo where the rock is spread out according to raw material type and specifications. Here, the highest drop of the cycle is experienced and according to grade of filling, up to 20 meters have been reported [10]. The number of drops in the raw material transport system of a silicon smelting plant can be above 20. The accumulated falling distance for a single raw material in the transport system over several drop points is known to be as much as 70 meters in worst case (pers. com. Tveit, H. 2004).
In an internal report, Tveit and Valderhaug [10] states that according to investigations (experiences) at one metallurgical plant, there is a significant increase in fines after increased cumulative fall for the raw material on its way through the plant (Table 1).

Table 1: Amount of fines (-1mm size) after increasing cumulative drop. After [10]. * before test.

Fall (m)	% fines
0*	0.2
2	0.65
16	1.4

Later tests show similar results e.g. [8, 9] and pers. com. H. Tveit (2004). In [8], the results of falling on the generation of fines are reported. The test was carried out by taking a sample of 1000 kg of rock quartz, which were repeatedly dropped 3 m into a steel container measuring 3 x 3 m. After each drop, the sample was sieved on pre-selected screens. The report demonstrates that:

- "the fines are mainly generated by falling occurred when handling
- the increase of fines content is directly proportional to the total height of the subsequent fallings
- the increase of fines pr meter of falling (Table 2)."

Table 2: The table shows the increase of fines pr meter of falling. After [8].

Fraction (mm)	Increase (%)
<10	*0.29*
10 - 20	*0.14*
20 - 30	*0.15*

Other factors

Outside storage

Storage of raw material outside combined with exposure to humid conditions in periods of freezing and thawing, might lead to frost erosion. This is a possible scenario if the quartz has fractures in the material where the water can enter and expand during freezing. This erosion might lead to the generation of fines if the material is exposed during longer periods. However, no literature seems to cover this subject.

Segregation

Segregation is a known problem in many processes. During handling of a material with a certain size distribution, coarse and fine particles of the material will segregate and accumulate at different places in a product pile or a silo. Loading of material from a product pile/silo will lead to an uneven size distribution when emptying the pile/silo. This prevents an even distribution of the fine material in the charge material. The segregation is of course not only related to the handling at the smelter plant but needs to be taken into account through the entire process from the mine to the furnace. Simple factors such as how to take out a load from storage and moving it are important. The choice of means of moving, where to start taking material in the pile and the cycle of taking out materials are also important.

Conclusion

This literature study has shown that control of the handling of raw materials can give much better quality of the raw materials for the metallurgical production of ferrosilicon and silicon metal.

What are described in this review article are factors that can be controlled during production and transport. The combined mining and processing of the raw materials should be optimized to prevent unnecessary generation of fines and at the same time the lowest product cost. The critical part of the cycle is probably the reloading of the raw materials where the total amount of fall meters should be kept on a minimum to lower the generation of fines in the material. This is a problem on both the mineral production plant in the stages after the crushing and sieving and on the metallurgical plants from the unloading of the ship to the charging on the furnace.

Further work will emphasize the understanding of the influence of the rock properties on the mechanical and thermal strength.

References

1. Nielsen, K. and T. Malvik, *Grindability enhancement by blast-induced microcracks,* Powder Technology. **105**(1-3), 1999, p. 52-56.
2. Schei, A., J.K. Tuset, and H. Tveit, *Production of High Silicon Alloys*. 1998, Trondheim: Tapir Forlag.
3. Birkeland, R., *Optimale kvartsegenskaper - metode evaluering del 1*. 2004, Kristiansand: Elkem Research. 25.
4. Jern, M., *The Geological Conditions for Aggregate production, with special focus on blasting and fines production*. 2004, Göteborg, Sweden: Chalmers Unicersity of Technology.
5. Nielsen, K.O., *Economic effects of blasting on the crushing and grinding of ores,* South African Institute of Mining and Metallurgy, 1999, p 251-255.
6. Nielsen, K.O., *The Economic Consequences of Drill Hole Deviation in Crushed Aggregate Production,* Explo '99, 1999,p 9-13.
7. Sandvik, K., M. Digre, and T. Malvik, *Oppredning av primære og sekundære råstoffer*. 1999, Trondheim: Tapir Forlag. 497.
8. Forjàn, C., *Fines Created by falling*. 1999, Internal report. p. 18.
9. Wiig, L., et al., *Fines in Quartz*. 2003, Internal report. p. 30.
10. Tveit, H. and A. Valderhaug, *FeSi 8000 Final Report*. 1993: Elkem Internal Report.

Paper III

ADVANCED METHODS TO CHARACTERIZE THERMAL PROPERTIES OF QUARTZ

K. Aasly, T. Malvik and E.H. Myrhaug[1]

Department of Geology and Mineral Resources Engineering, Trondheim, Norway
[1]Elkem ASA, Silicon Division, Alfred Getz vei 2b, Trondheim, Norway
E-mail: kurt.aasly@ntnu.no and terje.malvik@ntnu.no, edin.myrhaug@elkem.no

ABSTRACT

Six different types of quartz and quartzites used as raw materials by ferroalloy plants have been investigated with respect to their thermo mechanical properties. In order to investigate the effect of the thermal shock caused by the rapid heating of quartz when it enters the furnace, the following techniques have been used for both in situ investigations and investigations of pre-heated quartz:

- *Heating stage microscopy for in situ observation of heating effects.*
- *Shock heating of quartz in an induction furnace*

An optical microscope-mounted heating stage was used for in situ observations of the microscopic effects of heating up to 1300 ºC. The effects of heating were observed at different temperature intervals in different samples. The main temperature intervals were below 573 ºC and above 1000 ºC. The cause of the observed effects is interpreted as fluid inclusion decrepitation for T<573 ºC and structural implications (micro cracks, grain boundaries and remaining fluid inclusions) at T>1200 ºC.

Shock heating of the samples was carried out in an induction furnace to 1300 ºC for ten minutes. The effects of the heating were studied with different techniques such as direct observation during and directly after heating, optical microscopy and XRD. Combined transmitted and fluorescence light microscopy shows that the heated quartz show an opening of the grain boundaries and evenly distributed micro cracks that were not present in the unheated reference samples. In some of the heated samples, weak generation of cristobalite was detected by XRD.

1. INTRODUCTION

The mineral quartz (SiO_2) is the raw material for Si in the silicon and ferrosilicon ((Fe)Si) production. Quartz is built up of one Si bound to four O atoms such that in a SiO_4 tetrahedron where all the O-atoms are shared between neighboring tetrahedrons. α-quartz is the SiO_2 polymorph that is most stable at room temperature. The phase diagram for the silica system is shown in Figure 1. The phase transformation from α- to β-quartz has been described as a spontaneous and reversible reaction. The transformation from β-quartz to tridymite usually needs a catalyst, like alkali elements, to occur. Therefore, β-quartz probably transforms directly to cristobalite, a reaction that may start as low as 1100 °C [1]. This phase transformation is more time demanding than the β-quartz formation. Therefore, combined with the temperature span of the direct transformation from β-quartz to β-cristobalite, this results in only partial β-cristobalite formation in the quartz material during the experiments described in this paper and also most probably in the real (Fe)Si process. The amount of β-cristobalite in the real furnace is probably also depending on the retention time of the quartz, especially the time at high temperatures (>1470 °C).

Pure quartz suitable for the (Fe)Si process, occurs in nature as hydrothermal quartz, pegmatite quartz and quartzite. In metallurgical terms, quartz is often classified as rock quartz or gravel quartz. Gravel means

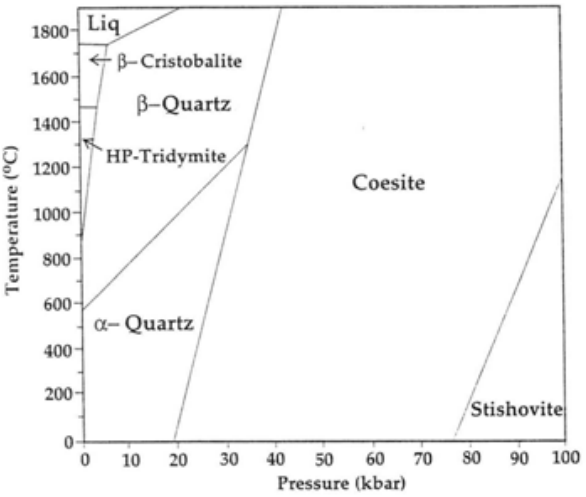

Figure 1: Phase diagram for the silica system [2]

quartz mined from fluvial deposits by excavations of unconsolidated material and rock quartz means quartz mined from bedrock by blasting operations.

This paper presents the results from two experiments where the thermal properties of quartz were investigated, both microscopically in-situ and by using secondary analytical techniques on heated material. By using a Linkam heating stage (Linkam TS 1500), the heating sequence was simulated and the mineralogical response to the heat could be observed. The main response to the heating was observed in two temperature intervals, between 180 and 573 °C and above 1200 °C.

To investigate the effects of the thermal shock, quartz samples were introduced to an induction furnace at 1300 ºC and heated for 10 minutes. After cooling in room temperature optical microscopy and XRD investigations were carried out on the heated samples and the unheated reference samples.

1.1 The Process

The metallurgical (carbothermic) production of (Fe)Si is described by e.g. Schei et al. [3]: Quartz and carbon materials react at high temperatures to form silicon metal. In ferrosilicon production, also iron ore is added. The temperature at the top of the charge burden of the furnace is 700 – 1300 ºC and the temperature in the hottest parts of the furnace is more than 2000 °C. The ideal reaction can then be written as:

$$SiO_2 + 2C = Si + 2CO \tag{1}$$

In a real furnace, the process is much more complicated and consists of several sub-processes, which may be affected by the quality of the raw materials.

The ferroalloy industry has a set of requirements to the quartz used as a raw material [3]:

- Chemistry (e.g. Al, Ti, B, P, Fe, Ca)
- Lump size (typical 10 – 150 mm)
- Mechanical strength
- Thermal strength
- Softening properties

Chemistry and size are the most common specifications used by all (Fe)Si producers. Some (Fe)Si producers focus on or measure mechanical- and thermal strength although these are not included in the specifications to the supplier, and a few (Fe)Si producers focuses on the softening properties or properties and measurements related to the softening properties. Further, additional requirements may be defined by the individual (Fe)Si producer, according to what is most optimal for the specific operation.

The raw materials are experiencing an extreme thermal shock as it enters the furnace and "bad" quartz respond quite different to the extreme thermal gradient compared to the "good" quartz. The raw materials are continuously fed by gravity on top of the furnace, such that all the raw materials are directly exposed to the hot charge material, and experience the highest thermal gradient. Otherwise, the raw materials are charged in cycles, such that the material lands on top of the charge burden in piles. Then the material in the center of the pile will be "isolated" from direct contact with the hot material and experience a slightly more gradient heating. The temperature on top of the charge burden might be as high as 700 – 1300 ºC. This means that the temperature interval is between room temperature and 1300 ºC, within seconds or minutes. The retention period for quartz in the furnace has been calculated by SiMod for a 25 MW Si furnace [4], and is on average 5.70 hrs but may be as low as 1 hour.

1.2 Previous Work

Birkeland and Carstens [5] reported results from a high temperature microscopy investigation where 1 mm thick and 6 mm circular samples of quartzite and single-crystal quartz were heated in a microscope heating stage (Leitz 1350 heating stage mounted on a Leitz Ortholux transmitted light microscope) to 1300 °C during 5 to 10 minutes and visual observations were recorded. Birkeland and Carstens [5] demonstrated that cracking occurred in most samples at around 300 – 400 °C and increasing with raising temperature up to the α-to β-quartz transition at 573 °C. Between 600 and 900 °C Birkeland and Carstens [5] see no activity related to the heating. Regenerated activity is seen between 900 and 1000 °C in several samples. This activity was reported as explosions that destroys the samples.

Birkeland and Carstens [5] also reported results from an experiment where samples from each of different quartzites were heated in a furnace to 1000 ºC with different heating rate. Two samples for heating were prepared as pieces measuring 1x5x5 cm: One sample was introduced to the furnace at room temperature and heated to 1000 ºC during 20 min, while the other sample was introduced directly to the furnace at 1000 ºC. Both samples were slowly cooled (2-3 hours), however, there are no specifications of how long the samples were kept at 1000 ºC. A third sample was used as an unheated reference. Some interesting observations were made by optical microscopy: The authors are surprised that the fluid inclusions planes did not seem to be important for the fracturing of the sample. Deformation structures like undulate extinction, sub-grain segmentation, deformation lamellae and deformation bands, and most of the inclusion planes, seem unaffected by the heating.

Geiss [6] reported an XRD investigation of heated quartz. The temperature that the heating was carried out to was not reported. The results from this experiment showed that only high-quartz was detected. Geiss [6] relates the lack of phase transformations other than β-quartz is related to the crushing of the samples and the effect this has on the lattice properties.

2. MATERIALS AND METHODS

2.1 Sample Material

The samples consist of six different types of quartz used as raw materials for the metallurgical production of (Fe)Si in Norway. The samples are both gravel- and rock quartz. Table 1 shows the different samples, listed with both metallurgical and geological type as described by Moen and Malvik [7].

Table 1: List of sample material and sample type. Metallurgical type = the differentiation that are used by metallurgists

Name	*Metallurgical Type*	*Quartz Type*
Sample A	Gravel	Hydrothermal/pegmatite
Sample B	Gravel	Hydrothermal/pegmatite
Sample C	Rock	Hydrothermal
Sample D	Rock	Pegmatite
Sample E	Rock	Meta-sandstone (quartzite)
Sample F	Gravel	Hydrothermal

A study performed by Elkem Research [8] describes the thermo-mechanical and mechanical properties of the samples used in these experiments. The thermo mechanical and mechanical properties varies between fairly good to good for all the samples.

2.2 High-Temperature Micro Thermometry

2.2.1 Equipment

The equipment used for the high-temperature micro thermometry is the Linkam TS1500 system. The stage is controlled by the temperature programmer via computer (PC) software (Linksys 32 DV (digital video)). The size of the sample cup is 7 mm in diameter and 3 mm deep. The heating stage is mounted on a Nikon Eclipse ME600 polarized and transmitted light microscope. A PixeLink firewire camera (1280x1024 pixel resolution) is mounted on the microscope and connected to the PC and is also controlled by the Linksys 32 DV software.

The temperature is controlled by the TMS94/1500 programmer via the S-type Pt/Rh thermocouple. After the end of a sample run, the images that were collected are stored together with temperature and light intensity

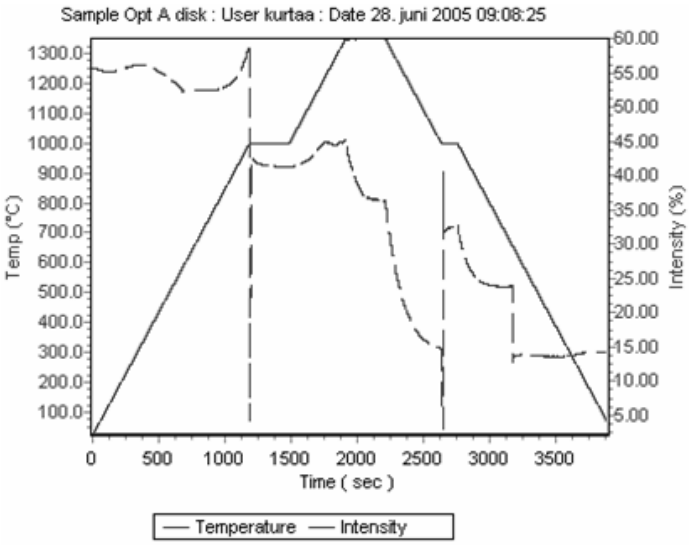

Figure 2: Example of temperature profile from the high-temperature micro thermometry investigation of Sample A.

(to the camera CCD) data in a project database. The images can later be saved and compressed into different image formats (jpeg, TIFF, etc) or into movie files (avi). The heating sequence is presented as a graph showing the temperature progress together with the intensity of the light (Figure 2). The experiments were carried out in a dark room to prevent unnecessary, unwanted light reaching the camera.

The temperature profile used for the experiments was 50 °C/min to 1350 °C with a five minutes hold at the current temperature at 1000 °C and at 1350 °C. Pictures was taken automatically every five seconds. The investigated part of the heating experiments was between the start of the temperature profile until the end of the five min. hold at 1350 °C. The cooling part of the experiments was not studied, because, in the real silicon process, the temperature never returns to room temperature.

2.2.2 Sample Preparation

The samples for the heating stage investigations were prepared as polished thick sections. The thickness of the samples was between 200 and 250 μm. The polished thick sections had to be broken to smaller pieces in order to fit the samples inside the sample cup.

2.3 Shock Heating of Quartz in Induction Furnace

2.3.1 Equipment

The furnace used for the shock heating experiments of quartz was an ASEA induction furnace from ca. 1950 working at 3830 Hz and with a capacity of 50 kg of steel. To monitor the temperature, a thermo element type S was used. A graphite crucible was used to hold the samples in the furnace.

Prior to placing each sample in the crucible, the furnace was heated to 1300 ºC. To avoid unnecessary breaking of the quartz, the samples were handled by using an appropriate pair of large tweezers. After the insertion the temperature was brought back to 1300 ºC (a small decrease in temperature was observed when the top cover was removed and the extra mass of the sample was introduced in the crucible). The sample was kept in the furnace for ten minutes to ensure homogeneous temperature distribution (1300 ºC). After ten minutes, the sample was removed by lifting the crucible and "pouring" the sample into a graphite bowl where it was left to cool at room temperature for a few minutes before they were transferred to tin cups for further cooling. The samples had cooled after approximately one hour, except Sample F, which was much less defragmented, and brought back to room temperature after more than two hours.

2.3.2 Sample Preparation

The samples were cut by diamond saw to cubes approximately 40 mm x 40 mm x 40 mm as seen in Figure 3. Due to the relatively small size of the sample material, Sample D was cut to a cube of 30 mm x 30 mm x 30 mm.

Polished Thin Sections

One polished thin section (PTS) from each of the heated samples and the corresponding unheated reference samples were prepared for polarized light optical microscopic investigations. The PTS were also impregnated with fluorescent epoxy for investigations in fluorescent light microscopy.

The optical microscopic investigations were carried out on a Nikon Eclipse E600 polarization microscope (transmitted light) equipped with a 2 megapixels digital camera (*Spot Insight Color* from Diagnostics Instruments). The fluorescence equipment (Nikon Super High Pressure Mercury Lamp) is connected to the same microscope.

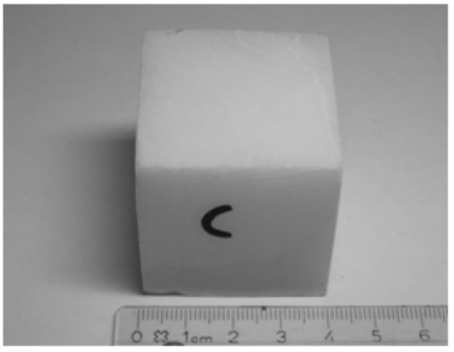

Figure 3: Example of sample preparation of quartz for shock heating in the induction furnace

XRD Analyses

Preparation of samples for XRD investigations were carried out in a laboratory disc mill. The samples were milled to approximately 40 μm grain-size. The milling time for each sample was 60 – 70 seconds at 710 rpm. The analyses were carried out on a Philips PW 1830 XRD.

3. RESULTS

3.1 High-Temperature Micro Thermometry

The typical observation for the samples was an activity related to decrepitation of fluid inclusions that started weakly around 180 °C and increasing with temperature up to the temperature for α-/β-quartz transition at 573 °C. This activity seems to be related mostly to the decrepitation of fluid inclusions but the opening of inter granular micro cracks are also observed. It is not possible to see if these micro cracks are related to fluid inclusions that lay beyond the focus depth. Further, from 600 to 1000 degrees, nothing happens within most of the samples. The exception is Sample F where all the experiments shows a moderate to high activity in the temperature interval from just below 900 °C to 1000°C. Also, one experiment of Sample D shows moderate activity around 900 – 1000 °C. In the temperature interval from 1200 – 1350 °C, most of the samples show a moderate to high activity. This is probably related to grain boundaries and existing cracks in the sample. In addition, possible remaining fluid inclusions will decrepitate in this interval. No minerals other than quartz were observed in the samples that were investigated by high-temperature micro thermometry.

The observations during the experiments are based on the observations of emerging cracks seen as dark lines in the image. Fluid inclusion decrepitation was seen as dark foggy areas probably related to the escaping fluids. In some samples, the sample was suddenly moving out of place during heating, as if it was defragmented explosively. Some samples were seen moving in one or the other direction in small steps, this were probably related to thermal drifting.

The results were after the initial in-situ observations, further checked by using the video and image options to confirm the observations. Also, the resulting temperature and intensity graphs could be used to verify the observations. Typically the intensity are steeply declining in the temperature interval of high activity of reactions while it is increasing or more stable for temperature intervals of low or no activity as seen in Figure 4 a) and b) and Figure 5 a) and b). Table 2 shows the results from the high-temperature experiments within the main intervals. Each sample is placed in a category according to the intensity of response to the heating within each interval. Here Category 0 means little or no activity observed, and Category 3 means high activity observed. The results are based on the visual observations and study of the data material after the experiments.

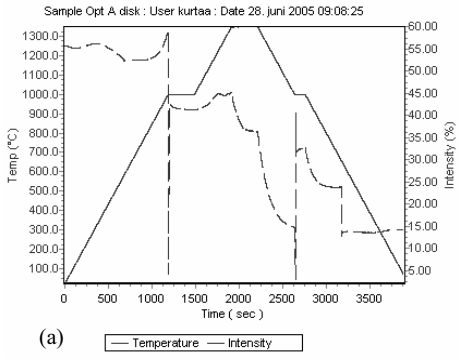

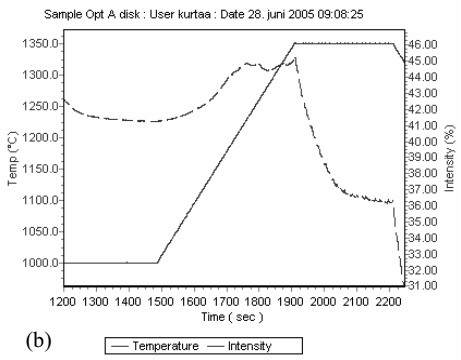

Figure 4: Temperature (line) and intensity (dashed) graphs of Sample A-2. a) Shows the entire experiment; b) shows the temperature interval 1000 °C to 1350 °C+ 5 min

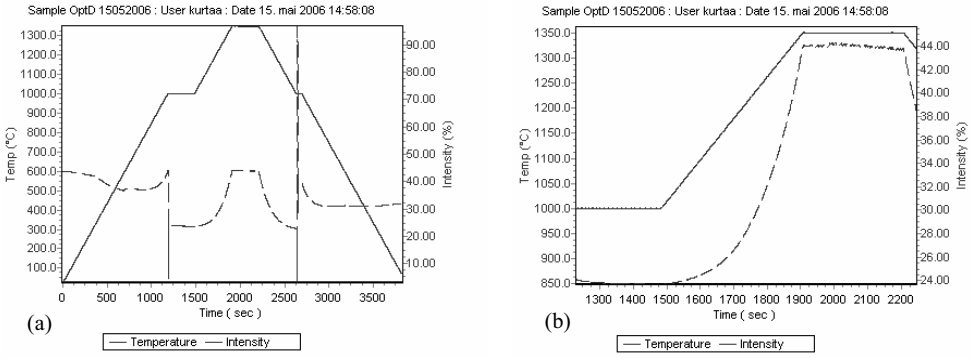

Figure 5: Temperature (line) and intensity (dashed) graphs of Sample D-3. a) Shows the entire experiment; b) shows the temperature interval 1000 °C to 1350 °C+ 5 min

Table 2: Results from investigations in the Linkam heating stage. Category 0 = little activity; Category 1 = some activity; Category 2 = moderate activity; Category 3 = high activity.

Sample		<573 °C	573-1000 °C	1000-1200 °C	1200-1350 °C	
A	1	0	0	0	3	
	2	3	0	0	3	
	3	2	0	0	3	
	Average	**1.7**	**0.0**	**0.0**	**3.0**	
B	1	3	0	0	3	
	2	2	0	0	3	
	3	2	1	1	3	
	Average	**2.3**	**0.3**	**0.3**	**3.0**	
C	1	2	0	0	2	
	2	2	0	0	2	
	3	1	0	0	2	
	Average	**1.7**	**0.0**	**0.0**	**2.0**	
D	1	1	0	0	2	
	2	2	2	0	2	
	3	2	0	0	0	
	Average	**1.7**	**0.7**	**0.0**	**1.3**	
E	1	2	1	0	2	
	2	1	0	0	2	
	3	1	0	0	2	
	Average	**1.3**	**0.3**	**0.0**	**2.0**	
F	1	1	2	0	3	
	2	1	1	0	1	
	3	1	2	0	2	
	Average	**1.0**	**1.7**	**0.0**	**2.0**	

3.1.1 General

The phase transformation from α- to β-quartz always occurs at 573 °C. This is also easily seen in the samples at this temperature. The effects vary from extreme to slight, but the rule of thumb is that it will always be seen during heating beyond this temperature. The intensity of the light in the samples will also usually show this effect as a sudden drop in intensity close to 573 °C and an increase in the intensity just after 573 °C (Figure 6).

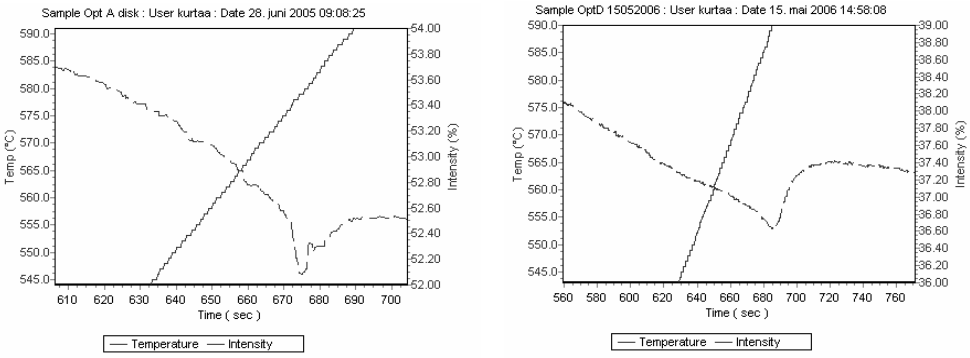

Figure 6: Examples of the intensity response to the phase transformation from - to -quartz in Samples a) A-2 and b) D-3.

3.2 SHOCK HEATING OF QUARTZ IN INDUCTION FURNACE

Prior to heating, each of the cubes was weighed and the weights are presented in Table 3, together with the weights of the +1.651 mm and -1.651 mm fractions obtained from the sample after heating.

Table 3: Weights of the prepared cubes for heating. The heated samples where weighed before and after heating

Sample	*Weight (g) Total sample*	*Weight (g) heated -1.651 mm*	*Weight (g) heated +1.651 mm*
Sample A	166.9	2.35	139.64
Sample B	167.0	1.67	163.76
Sample C	165.0	1.74	161.83
Sample D	82.0	0.58	78.69
Sample E	161.2	1.77	153.44
Sample F	160.0	1.83	121.60

3.2.1 Visual (and audible) observations during and after heating

Some of the samples had quick and "violent" response to the heat in the crucible. One could hear the crackling from some of the Samples (A, C and minor in D and E). Sample C responded so violent that one could hear the pieces of rock flying within the crucible. Table 4 lists the visual and audible observations during and after the heating of the quartz and Figure 7 shows microphotographs of Samples Warm C and Warm F after heating.

Table 4: List of visible and audible effects from heating

Sample No	*Visible effects*	*Audible effects*
Sample A	Many medium and small pieces.	Some crackling just after started heating
Sample B	Few but large pieces. Some small.	No
Sample C	Many medium and small pieces. Not as fine as expected.	Intense crackling immediately after started heating.
Sample D	Few but large pieces. Some small.	Minor
Sample E	Color changed from reddish to grey. Few but large pieces. Some small.	Minor
Sample F	One large piece and only few small.	Minor

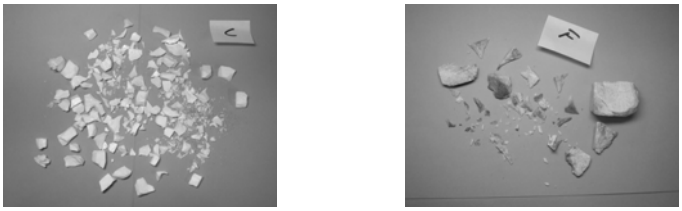

(a) (b)

Figure 7: Example of the resulting material after heating and removal of the -1.651 mm fraction. The fragmentation is due to the thermal shock. a) Warm C; b) Warm F.

3.2.2 Fines Generation

Sieves were used to find the amount of fine material (fines) in the sample material after heating (see Table 3). The samples were sieved on 1.651 mm screens and the + and - fractions were weighed. As the original sample material was of uniform size (except Sample D), the fines content of the heated sample is expected to say something about the thermal strength of the material. Table 5 shows the percentage fines in the sample after heating (fines index). This index is not the same as the heat index (HI) as described by i.e. Birkeland [8], since the heat index is based on other definition of sample material size used for the heating and are a measure of sample material +20 mm.

Table 5: Fines index of sample materials after shock heating to 1300 °C for ten minutes. Index is % fines (-1.651 mm) material of total sample before heating

Sample	*Fines Index*
A	1.41
B	1.00
C	1.05
D	0.71
E	1.10
F	1.14

3.2.3 Optical Microscopic investigations and fluorescent light microscopy

Polarized light microscopy

The fresh, unheated reference samples (e.g. Cold A), and the heated samples (e.g. Warm A), were investigated by optical microscopy to search for changes in the material as a result of the heating. As described above (see Table 1), the quartz raw materials are from different geological origin. The rock quartz is relatively easy to describe and relate to the genesis of the rocks, both macro- and microscopically: Samples C to E is typically well-defined quartzes of hydrothermal, pegmatitic and quartzite types, respectively. The gravel quartzes are macroscopically more difficult to classify because of the weathered surface of the boulders. Microscopically, Sample F can also be classified as typical hydrothermal quartz based on the irregular grain shape and –size. The gravel quartz in Samples A and B are microscopically very similar to Sample C and must therefore be classified as hydrothermal quartz, as well.

Trace amounts of other minerals than quartz are seen in Samples B, E and F, while Samples D shows one mica grain and Sample C has some very small unidentified mineral inclusions, probably mica. Fluid inclusions are present in vast amounts and in a wide size interval in Samples A to D. The fluid inclusions are of

several generations seen by the cross cutting fluid inclusion planes. Samples E and F show only minor amounts of fluid inclusions. Table 6 summarize the samples with type, relative grain size, content of other minerals (type) and position of these minerals.

Table 6: List of sample types, relative grain size, content and position of other minerals

Sample	Type	Rel. grain size	Other minerals	Pos. of trace minerals
A	Hydrothermal	V. coarse	None	-
B	Hydrothermal	V. coarse	Chlorite/mica	Grain boundaries
C	Hydrothermal	V. coarse	(mica)	Scattered
D	Pegmatite	Fine-coarse	(mica)	Scattered
E	Quartzite	Medium	Zircon; monazite; mica; tourmaline?	Scattered
F	Hydrothermal	Medium-coarse	Mica (or tourmaline)	Grain boundaries

Mineralogical properties such as undulate extinction and sub-grains are not affected by the shock heating. The fluid inclusion planes are still visible and seem unaffected in low magnification, however, in higher magnifications, it is obvious that most of the inclusions have decrepitated and thin micro cracks are often visible along these planes. The fluid inclusions in Samples Warm A to Warm D show an absence of bubbles. This is probably an indication of decrepitation of the fluid inclusions. However, the smallest inclusions in all samples and several inclusions in Sample D still contain bubbles, and thus seem to have survived the heating.

The heated samples usually show a more diffuse appearance of the quartz grains, which is probably related to micro cracks that have been induced in the rock as a result of the extreme heat. There are no evidence of the cause of these random micro cracks. Opening of the grain boundaries were also seen in some of the samples, especially Samples Warm D to Warm F. Figure 8 c) and d) show microphotographs (x-nichols) of Sample Cold F and Warm F respectively. It is easy to see that the grain boundaries have become more pronounced as a result of the high temperatures.

Fluorescent light microscopy

The Samples Cold A to Cold C show dense grain boundaries and low content of micro cracks that were filled with fluorescent epoxy.

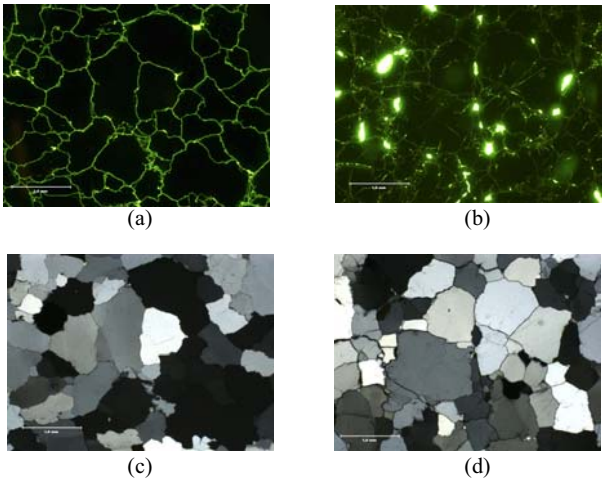

Figure 8: Examples of fluorescence image of Sample a) Cold F and b) Warm F. The respective polarized light microphotographs (x-nichols) are shown in c) Cold F and d) Warm F. The scale bar is 1 mm

Regular optical microscopy showed some significant differences between the fresh and the heated samples. When studying the samples with fluorescent light, all the samples showed a significant increase in the intensity of the light reflected by epoxy in the grain boundaries. The intensity of the micro cracks has also increased in most samples. For some samples i.e. Warm F, the intensity of pores and micro cracks suppressed the high intensity from the grain boundaries that were already present in the unheated Sample Cold F (Figure 8).

3.2.4 XRD investigations

XRD investigations were carried out on the unheated reference samples and on the heated samples. The results shows that for some of the quartz types, the heating to 1300 °C for ten minutes results in a beginning phase transition into β-cristobalite (Table 7). This is seen as emerging small peaks at the 2θ values related to β-cristobalite accompanied by a lowering of the intensity of some of the 2θ peaks for quartz. No HP-tridymite was seen in the XRD investigations.

Table 7: List of cristobalite formation in the different types of quartz. The "peak change" reflects the change in the quartz peaks

Result\Sample	*A*	*B*	*C*	*D*	*E*	*F*
Cristobalite formation	No	Minor	Minor	No	Major	Minor
Peak change	Major	No	Major	Minor	No	Minor

4. DISCUSSION

The high-temperature micro thermometry shows that there are two main temperature intervals that are important during heating of quartz samples. These are the interval between ca. 180 °C up to 573 ° C and the interval from ca 1200 °C to the end of the experiment at 1350 °C. There were also observed some activity in some samples around 900-1000 °C. Since almost all samples display high activity in response to the heating at the high temperatures, this is probably not a crucial type of activity. There should be more concern about the activity that happens at slightly lower temperatures around 900 to 1000 °C. Malvik and Lund [9] related this temperature interval to mica impurities. However, no mica minerals were seen in the investigated samples that were used for the experiments. The low temperature interval below 573 °C can also be significant for the thermal properties. If the decrepitation of the fluid inclusions takes place over a short temperature interval for several planes, this could contribute to a severe fracturing of the quartz.

Shock heating of the quartz shows by observation of the heating experiments that there are vast differences in the behavior of the different quartz types. The most extreme behavior was displayed by Sample C, where the crackling was very intense as judged by the sounds from inside the heating furnace and the fragmenting of the sample was also intense. Sample F had only minor fracturing. Further investigations by microscopic methods showed that the heating of the samples introduced an opening of the grain boundaries in most samples accompanied by the development of micro cracks, either as short disconnected cracks in a dense pattern or as a network of connected micro cracks. The fluid inclusion planes also show networks of micro cracks that are probably a result of the decrepitation of the fluid inclusions. This is in contrast to the observations made by [5], which concluded that the fluid inclusion planes were not important for the fracturing of the samples.

The mica seen along grain boundaries in Samples Cold B and Cold F, which were not seen at all in the heated Samples Warm B and Warm F, indicates that mica is responsible for the fracturing of the samples. This is also supported by the high-temperature micro thermometry investigations, especially for Sample F, where moderate activity was seen at the temperature interval around 900 - 1000 °C, which is also the conclusion by Malvik and Lund [9].

The HP-tridymite formation seems to be ruled out as a cause of the effect seen around 900 – 1000 °C as no HP-tridymite were seen from the XRD investigation. The lack of HP-tridymite formation is probably related

to the purity of the quartz samples, as well as the short retention time at 1300 °C. This is also supported by the investigations by Geiss [6] who reported only β-quartz from similar investigations.

5. CONCLUSION

The high-temperature micro thermometry investigations shows that the thermal effects in quartz are related to fluid inclusions and intra grain micro cracking at low temperatures (<573 °C). The high temperature effects are related to existing cracks and grain boundaries as well as the decrepitation of remaining fluid inclusions, while the effects seen at moderate temperature between 900 – 1000 °C is probably related to mica minerals in grain boundaries, although no mica was observed in the investigated areas of the samples. The importance of mica for the effects in the interval 900 – 1000 °C were supported by the effects of the shock heating in Samples D and F where mica were observed along grain boundaries in the unheated samples and a resulting wide opening of these grain boundaries in the heated samples.

REFERENCES

[1] Harders, F. and Kienow, S., “Feuerfestkunde: Herstellung, Eigenschaften und verwendung feuerfester Baustoffe”, Berlin: Springer, 1960.
[2] Klein, C. and Hurlbut, C. J., “Manual of Mineralogy”, 21st edn., New York: John Wiley, 1993.
[3] Schei, A., Tuset, J. K. and Tveit, H., “Production of High Silicon Alloys”, Trondheim: Tapir Forlag, 1998.
[4] Foss, B., Halfdanarson, J. and Wasbø, S., "Dynamisk Si-modell - Simon v. 1.50", Technical Report, SINTEF-report no STF72 F00307, 2000.
[5] Birkeland, T. and Carstens, H., “Preliminary report on high temperature investigations of natural quartz”, NGU Project B 2006 (in Norwegian), 1969.
[6] Geiss, H. P., “High temperature investigations with quartzite from the Gulodden quarry at Kragerø” (in Norwegian), Report to Fesil & Co., 1977.
[7] Moen, K. and Malvik, T., “A brief investigation of optimal quartz for Elkem Silicon”, Internal report, With permission from Elkem, 2002.
[8] Birkeland, R., “Optimal quartz properties - method evaluation part 1”, Report no F10/03, Internal Report, With permission from Elkem (in Norwegian), 2004.
[9] Malvik, T. and Lund, B., “Problems involved with quartzite as a raw material for FeSi and Si metal production”, Process Mineralogy IX, The Minerals, Metals & Materials Society, IX**,** 1990 p. 499-508.

Paper IV

Application of Cathodoluminescence to Evaluate the Physical Properties of Metallurgical Quartz

K. Aasly[a*], J. Götze[b], T. Malvik[a] and E. H. Myrhaug[c]

Submitted to Materials Characterization, December 2007

[a] *Norwegian University of Science and Technology, Department of Geology and Minerals Resources Engineering, Sem Sælandsv. 1, NO-7491 Trondheim, Norway*

[b] *TU Bergakademie Freiberg, Institute of Mineralogy, Brennhausgasse 14, D-09596 Freiberg, Germany*

[c] *Elkem ASA, Alfred Getz vei 2, NO-7465 Trondheim, Norway*

[*] *Corresponding Author: kurt.aasly@ntnu.no, Tel: (+47) 735 94 914, Fax: (+47) 735 94 814, Mob: (+47) 934 43 511*

Abstract: Cathodoluminescence microscopy and spectroscopy were applied for the micro-characterization of six different quartz raw materials for production of ferrosilicon and silicon metal. Samples were shock heated to 1300 °C and cathodoluminescence was used to investigate effects of shock heating compared to unheated reference samples. In two samples results of the shock heating were seen as spotted red cathodoluminescence that may be related to cristobalite formation or associated structural processes. This is probably caused by bond breaking of Si-O bonds in the crystal lattice during these processes. Grain boundary fracturing was revealed by cathodoluminescence in most of the samples as a result of the shock heating, most pronounced in two of the most fine-grained samples. This paper shows that cathodoluminescence is able to distinguish different types of quartz materials and that the samples show different reactions to shock heating, resulting in different luminescence effects in the different materials.

Keywords: *Cathodoluminescence, quartz, silicon production, shock heating*

Introduction

During the last few decades cathodoluminescence (CL) has proved to be a powerful technique for the investigations of textural features of minerals [e.g. 1, 2, 3]. Several investigations have proved that quartz of different types and origin shows distinctive luminescence characteristics during electron bombardment [e.g. 4, 5, 6]. This characteristic luminescence is caused by lattice defects derived from chemical substitution or growth related features such as point defects or non-stochiometry. Point defects can be subdivided into 1) extrinsic (trace elements) and 2) intrinsic defects (lattice defects) as illustrated in Figure 1.

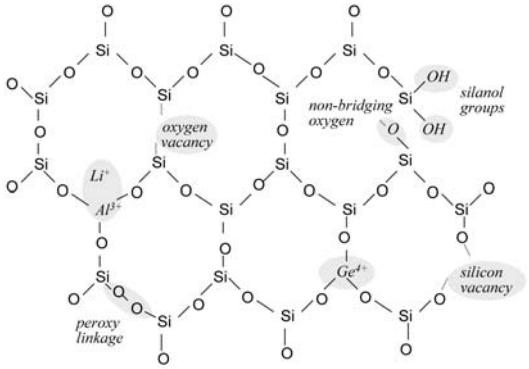

Figure 1 Schematic quartz structure showing the most common intrinsic and extrinsic lattice defects [modified after 7].

The luminescence is observed as internal zoning or color differences within minerals. The technique is widely used to detect information not available by other analytical methods (e.g. optical microscopy). This includes growth zoning and distinguishing different generations of crystallization. For quartz arenites and quartzites different sources for detrital grains and quartz overgrowth can be revealed with CL.

Quartz from igneous and regional metamorphic rocks mostly show characteristic, stable luminescence with two emission bands centered around 450 and 650 nm. Quartz from igneous rocks show a predominance in the 450 nm band causing different shades of blue CL colors [e.g. 7, 8, 9]. The luminescence at 450 nm has been associated with a twofold coordinated Si on an O vacancy [e.g. 10, 11]. Quartz from regional metamorphic rocks is dominated by the 650 nm emission band causing a reddish to reddish-brown CL color [e.g. 12, 13] and this luminescence is related to a non-bridging oxygen hole center, NBOHC [14].

Hydrothermal quartz typically shows short-lived blue or bottle-green CL colors [e.g. 5]. Götze et al. [7] relate the transient blue CL, which changes to brown CL during electron beam irradiation, to the decrease in the luminescence intensity in the emission bands just below 400 nm and/or at 500 nm. Götze et al. [15] detected another yellow CL emission in hydrothermal vein quartz and agate of acidic volcanics. The luminescence emission band is centered at ca. 580 nm. The yellow emission at 560-580 nm was first seen by Rink et al. [16] in TL spectra of natural hydrothermal quartz and interpreted as related to oxygen vacancies.

Götze et al. [17] found that the luminescence of quartz from granitic pegmatite is characterized by a transient bluish-green luminescence emission with bands at around 400 nm and 505 nm.

Quartz raw materials for the metallurgical production of ferrosilicon and silicon metal (Fe)Si are met by requirements to their mechanical and thermo-mechanical properties. The mineralogical properties that influence these qualities are not fully understood and hence the test methods are not perfect. Thus, all new raw materials need to be tested on an operational scale to see whether they are suited for the operation.

In this study, CL was regarded as a possible method to swiftly distinguish between high quality and low quality metallurgical quartz. Thus, optical CL microscopy and spectroscopy were evaluated as potential test methods. The objectives for these investigations were to see what kind of information CL on heated quartz and unheated reference samples may provide and whether this information implies the metallurgical quality of the quartz.

Materials and Methods

Quartz samples

The samples comprise different quartz qualities that are used for the metallurgical production of FeSi and Si-metal. Metallurgists classify the different types of quartz as gravel quartz and rock quartz. Rock quartz may be hydrothermal vein quartz, pegmatite quartz and meta-sandstone (quartzite) mined from bedrock. The gravel quartz is quartz mined by non-blasting operations by excavation of unconsolidated material (e.g. fluvial deposits). The source material for the detrital quartz grains in the gravel quartz is mainly the same as that classified as rock quartz.

Sample	Metallurgical type	Quartz type	Bulk impurity (%)
A	Gravel	Hydrothermal or pegmatite	0.08531
B	Gravel	Hydrothermal or pegmatite	0.13471
C	Rock	Hydrothermal	0.04341
D	Rock	Pegmatite	0.22562
E	Rock	Meta-sandstone (quartzite)	0.40381
F	Gravel	Hydrothermal	1.01001

Table 1 List of sample material and type (Metallurgical type = as used by metallurgists). Chemical analyses are taken from Birkeland [18] and given as total impurities (a total of 16 elements analyzed including: Al, Ca, Fe, Ti, K, Li, Mg and Na).

The samples are named Sample A to Sample F in Table 1 and are sorted according to both metallurgical and geological types. The samples were gathered from raw material shipments [18], and the size of the specimens varied from 10 to 150 mm.

A study performed by Elkem Research [18] using established industrial methods to investigate the thermo-mechanical properties of these samples shows that the thermal strength index is fairly good for all samples. In contrast, the heat index is good for most samples except for Sample B that shows bad resistance against heating. Mechanically, Sample C is of poor quality whereas the rest of the samples have fairly-good to good quality. The dust index shows fairly-good quality for all samples. For a full description of the methodology for the mechanical and thermo-mechanical tests see e.g. Birkeland [18].

The six samples were shaped with a diamond saw to cubes with dimensions 40x40x40 mm[1]. Unfortunately, Sample D was too small and was therefore made as 30x30x30 mm cube. Further, the samples were heated in an induction furnace (one sample at a time) at 1300 °C, and kept at this temperature for ten minutes. After the heating and quenching, one polished thin section (PTS) was made from each of the heated samples (Warm A to Warm F) and from each of the unheated material (reference samples Cold A to Cold F). More details about the heating experiments and results from other investigations of the products from the heating experiments such as polarized- and fluorescent light microscopy and X-ray diffraction (XRD) analysis can be found in Aasly et al. [19]. It was especially interesting to see that phase transformation from quartz to cristobalite was detected in some of the samples by XRD [19]. Samples B, C and F showed “minor” cristobalite formation and Sample E showed “major” cristobalite formation.

Sample pairs comprising polished thin sections from the fresh reference samples and the heated samples (e.g. Cold A and Warm A) were carbon coated before the CL investigations. To avoid false spectra developed by the electron bombardment, the samples were not exposed to an electron beam before the CL measurements.

[1] This specific size of the samples was chosen for the reason that this seemed to be the largest size that was possible to make from the available material. This size is also within most of the size fractions used in the process.

Sample	Acquisition (s)	Color-1	λ-1	λ-1-1	Color-2	λ-2	λ-2-1	Comment
Cold A	5	stable deep blue-violet CL color	460	635				+FI trail
Cold B	5	stable "bottle green"	570	460				
Cold C	20	stable violet	650	480				
Cold D	20-40	transient blue	440	650	dark blue	440	650	decrease in 440 stable 650 (weak decrease); In ColdD-1, 440/540 where 540 decrease with time.
Cold E-Blue1	10	stable bright blue quartz	450	650				650=630-650
Cold E-Blue2	10	stable medium blue quartz	450	650				450 and 650 equal intensity
Cold E-Blue3	10	stable dark blue quartz	650	450				
Cold E-Volcanic	10	stable red	630	450				marked low in the spectrum between the two peaks
Cold E-Hydrothermal	10	stable "bottle green"	580					
Cold F	10	transient blue	480		dark brownish	480	650	480 and 650 equal intensity - decrease of 480 and near stable 650
Warm A	5	stable purple	650	460				+FI trail
Warm B	5	stable weak red/purple	570	460				B-3: 635/460
Warm C	20	stable reddish-purple	635	460				weak at 515 - greenish tint
Warm D	20-60	varying, changing from reddish to violet	670	450				Additional peak at 550; The varying colors are defined by differences in the relative value of the blue 464 nm peak compared to the dominating red emission
Warm E-Blue1	10	stable bright blue quartz	450	650				
Warm E-Blue2	10	stable medium blue quartz	450	650				450 and 650 equal intensity
Warm E-Blue3	10	stable dark blue quartz	650	450				
Warm E-Spotted red	10	stable spotted red within grains	N.A.					spotted red CL in connection with internal cracks/fractures and possibly along some grain boundaries are observed in the heated sample; weak zonation from core and outwards.
Warm F	10	greenish-blue	505	635	dark blue, almost brownish	505	635	+ weaker initial 413; 505 decrease with time 635/413 near constant. Also spotted red CL

Table 2 Results from CL microscopy and spectroscopy investigations. Color-1, λ-1 and λ-1-1 refer to the colors observed, the main and the minor luminescence peaks, respectively. For transient luminescence the data are indicated by Color-2, λ-2 and λ-2-1. Acquisition time for the CL spectra in the different samples is given in seconds.

Instrumentation

CL data were acquired with a hot cathode CL microscope, HC1-LM as described by Neuser et al. [20]. The system was operated at 14 kV accelerating voltage and a current density of about 10 µA/mm^2. Luminescence images were captured "on-line" during CL operations using a peltier cooled digital video camera (KAPPA 961-1138 CF 20 DXC). CL spectra in the wavelength range 380 to 850 nm were recorded with an Acton Research SP-2356 digital triple-grating spectrograph with a Princeton Spec-10 CCD detector that was attached to the CL microscope by a silica-glass fiber guide. The wavelength of the CL spectrometer was calibrated against a Hg lamp. Each spectrum was obtained with a certain acquisition time (Table 2), depending on the intensity of the CL emission.

Results and discussion

The main results from CL microscopy and spectroscopy investigations are listed in Table 2. The Table shows the major and minor emission bands for each specimen. Deviations and other remarks are noted in the comment field. The initial CL is given as Color-1 and Wavelength-1, while in the case of transient CL emission, the CL color after prolonged electron beam irradiation is given as Color-2 and Wavelength-2.

In the description of each quartz type, only selected images and spectra are presented. The final results are based on a minimum of four investigated areas of one thin section for each of the quartz types.

Sample A (gravel quartz)

Sample A is a coarse-grained quartz rock with aggregates of fine-grained recrystallized quartz. Oriented sub-grain formation and undulate extinction in elongate bands are signs of stress. The sample is loaded with several generations of fluid inclusions, scattered and in thick bands. Accessory minerals comprising a few grains of muscovite are only observed in one thin section. Polarized light micrographs of Cold A and Warm A are shown in Figure 2a and e.

Sample Cold A is characterized by a stable deep blue-violet CL color (Figure 2b) and the spectrum is dominated by a broad emission band in the blue region around 460 nm and a lower peak in the red region around 635 nm (Figure 2c). The CL emission is stable over time during electron beam irradiation. This CL signature is typical for quartz from igneous rocks [e.g. 7, 8, 9] and the main emission is associated with a twofold coordinated Si on an O vacancy [e.g. 10, 11]. The characteristic CL color seen in sample Cold A changes to purple in sample Warm A (Figure 2f) and is dominated by red CL emissions around the 650 nm band

(Figure 2g). There is also a relatively weak blue emission around the 460 nm band, which is seen as a shoulder on the emission peak. This feature is best seen in the low intensity spectrum in sample Warm A-4 where the relative difference between the two peaks is lower than for Warm A-2. The CL signature from Warm A is similar to the signature of regional metamorphic rocks [12, 13], which also is related to NBOHC [14].

Some of the large fluid inclusion trails in the sample show an initial bright blue CL color (Figure 2b) caused by a dominating blue emission around the 430-460 nm band (Figure 2c). This emission is transient and changes towards pink-violet colors (Figure 2d) caused by the predominance of the red region around the 635 nm emission band. This is a result of a decline in the intensity of the blue emission accompanied by an increase in the red emission. This transient, bright blue color is typical for hydrothermal quartz [e.g. 5] and, therefore, may be a result of hydrothermal overprint. The luminescence center is interpreted as Al substitution for Si with cations charge balancing the Al [5]. This is supported by microprobe analysis showing higher Al content over the fluid inclusion trail, as discussed later (Figure 3 and Table 3). The increase in the 635 nm band may represent the creation of additional non-bridging oxygen hole centers (NBOHC) during electron bombardment. For sample Warm A, the large fluid inclusion trails show a stable, pale reddish CL color similar to the color seen in the FI trail in Cold A after prolonged e-beam irradiation (no spectrum obtained of this feature in Warm A). This indicates that the luminescence centers were removed by the heating.

The intensity of the emission for the unheated samples is relatively low, only up to 600 counts over 5 seconds for the highest peak (120 counts/second). For the heated samples, the intensity is low, not exceeding 300 counts for the highest peak. Acquisition time for the spectra was 5 seconds (<60 counts/second for the main peak).

The shift towards a decrease in the blue emission and an increase in the red emission in Sample Warm A, with the result that the two bands are level in intensity, is similar to the change in emission spectra with time, during electron beam irradiation of the fluid inclusion trails as seen in Sample Cold A. Accordingly, it is suggested that sample heating has the same effects on the lattice defects as the irradiation with electron beam over time and generates NBOHC.

Sample A was interpreted as hydrothermal vein quartz or pegmatite quartz by optical microscopic investigations. The CL spectra indicate that the quartz is from igneous rocks and is overprinted by hydrothermal activity. However, the large grain size and the absence of other minerals than quartz favor the hydrothermal- or pegmatite quartz interpretation.

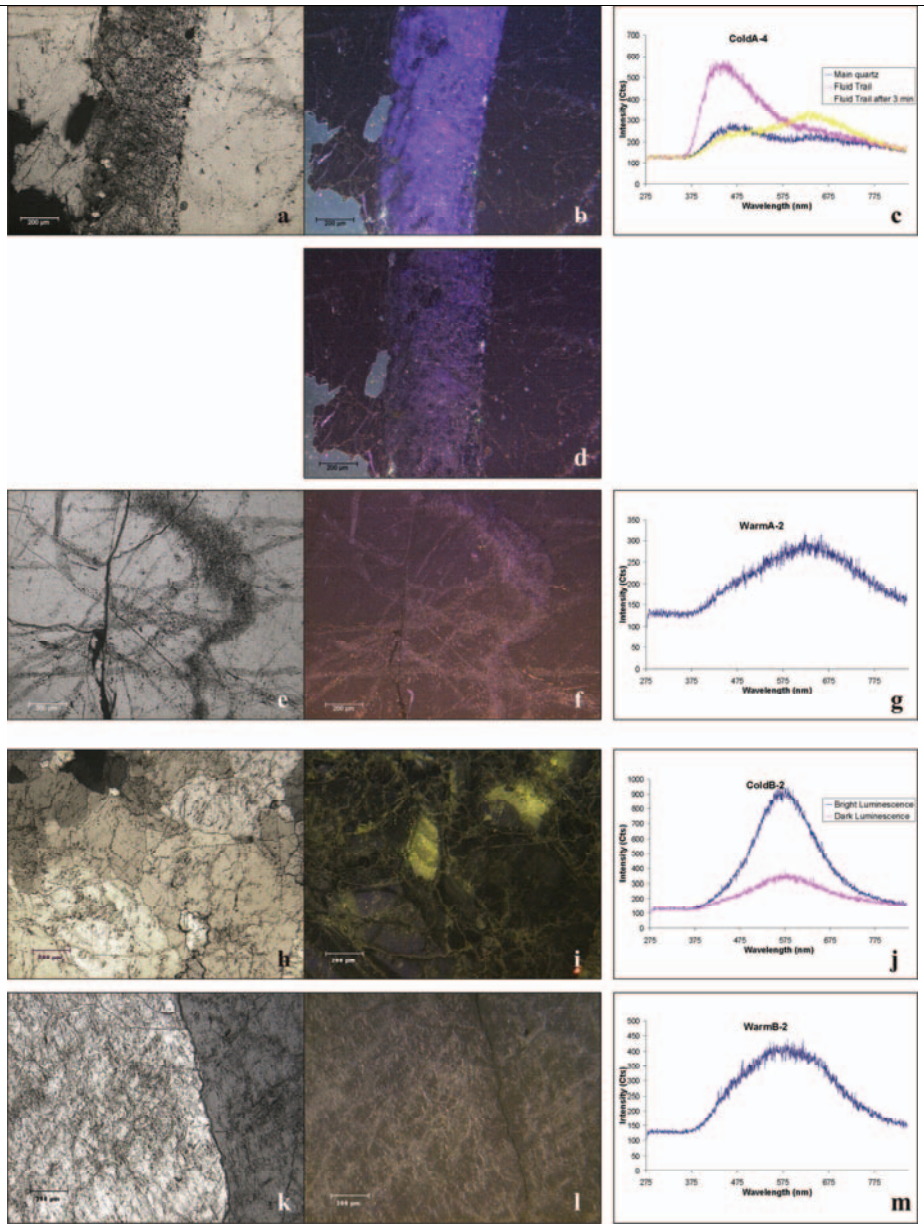

Figure 2 a to g show sample Cold A and Warm A. a, b and d show optical and CL micrographs of sample Cold A. b and d show the initial and transient luminescence from a large fluid inclusion trail in the quartz. c shows the CL spectra from Cold A (main quartz, initial and transient luminescence from the fluid inclusion trail). e and f show the optical and CL micrograph from Warm A. g shows the CL spectrum for Warm A. h to m show sample Cold B and Warm B. h and i show the optical and CL micrograph of Cold B. J shows the CL spectrum from Cold B. k and l show the optical micrograph and CL micrograph of Warm B. m shows the CL spectrum from Warm B.

Heating of quartz similar to Sample A may result in micro- or nano-fracturing generating NBOHC and therefore the luminescence characteristics of Sample Warm A.

Microprobe analysis

Two of the areas in sample Cold A that were investigated by CL were later analyzed with electron probe microanalysis (EPMA). A line-scan was performed over the two CL areas (Figure 3), one showing a thick band of late fluid inclusions with the luminescence characteristics described above. The second area consisted of homogeneous original CL colors. The Al content increased over the fluid inclusion trails, with a peak at 0.09% (900 ppm). Three extreme Al-values may be a result of the analysis point intersecting a micro inclusion of an Al-rich mineral (such as clay- or mica minerals). There is also a strong positive correlation of Al and Fe in the fluid inclusion trail (r_{Fe}=0.97485758). K and Na did not show the same correlation with Al (r_K=0.35949515 and r_{Na}= -0.01316907). This is in contrast to the analyses outside the fluid inclusion trail where the correlation looked quite different (Table 3).

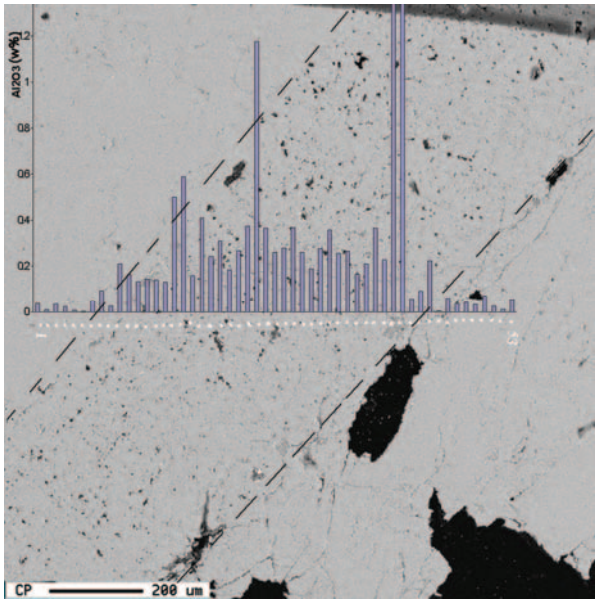

Figure 3 Shows backscatter electron image from EPMA with Al content by WDS over the fluid inclusion trace in Sample Cold A (seen as bright blue luminescent in Figure 2). Al content as Al_2O_3 in W%. The fluid inclusion trace seems more dusty than the more ordinary quartz areas and has been defined by thin dotted lines. Note how the Al content rises within the fluid inclusion trace. Two spike values are seen and may represent mineral inclusions in the quartz.

Elements	r-overall	r-Inside $_{FI\text{-}trail}$	r-Outside $_{FI\text{-}trail}$
Al-K	0,39134955	0,359495154	0,573013288
Al-Na	0,02604626	-0,013169065	0,445694168
Al-Ca	0,51184911	0,522941564	0,42495944
Al-Fe	0,97488839	0,974857577	0,491412137

Table 3 Correlation coefficients for the results from EPMA analysis in sample ColdA-4. The correlation coefficients are calculated for all samples, samples inside the fluid inclusion trail and outside the fluid inclusion trail. The analyses were carried out as oxides (e.g. Al_2O_3).

Sample B (gravel quartz)

Sample B is similar to Sample A, a coarse-grained quartz with aggregates of fine-grained recrystallized quartz. Oriented sub-grain formation and undulate extinction in elongated bands are signs of stress. The sample is loaded with several generations of primary and secondary fluid inclusions. Rare grains of muscovite are located in grain boundaries or fractures. Polarized light micrographs of Cold B and Warm B are shown in Figure 2h and k.

The yellowish-green luminescence seen in sample Cold B (Figure 2i) is dominated by the yellow emission around 570 nm (Figure 2j), with a weak shoulder created by blue emission around 460 nm. This CL emission is stable during electron bombardment. Dark and bright luminescence areas both show dominant yellow emission around the 570 nm band, although with intensity differences (Figure 2j) leading to the contrasted images. Sample Warm B shows a weak red/purple CL emission (Figure 2l) like the one seen in sample Warm A (Figure 2f). However, the emission is broader and characterized by the dominating yellow-green emission around 570 nm and the weaker blue emission around 460 nm. In another area in Sample Warm B, the CL emission is characterized by the dominating red emission around 635 nm and a minor blue emission around 460 nm seen as a shoulder on the main peak. The 570 nm emission is not dominant in this area. This is probably caused by the decrease of the luminescence in the yellow band at 570 nm, thus leading to a more pronounced emission in the red and blue bands (650 and 460 nm) because of the broad appearance of the main peak. This is supported by the differences in the luminescence spectra in one area of the heated sample where the yellow 570 nm CL is intact and dominates the emission while it is not dominant in other areas. This might be an effect of the intensity differences of the 570 nm within the reference samples as seen in the high- and low intensity areas.

In the Cold B CL micrograph (Figure 2i), weak violet CL is seen. However, this emission is transient and deteriorates quickly under electron beam irradiation and, therefore, no good spectra were obtained.

The Cold B CL intensity is relatively strong with up to 1100 counts over five seconds acquisition time (220 counts/second for the main peak). This intensity decreases after heating such that the CL emission in Warm B is low, with approximately 400 counts over 5 seconds (80 counts/second for the main peak).

Stable bottle-green luminescence is typical for hydrothermal quartz [15]. Rink et al. [16]related the CL at 570 nm to oxygen vacancies, whereas Itoh et al. [21] and Stevens Kalceff and Phillips [22] associated CL emission bands between 570 and 590 nm in irradiated amorphous SiO_2 and α-quartz to the self-trapped exiton (STE).

Sample B was interpreted as a hydrothermal vein quartz or pegmatite quartz by optical microscopic investigations. The hydrothermal vein quartz interpretation is supported by the CL investigations.

Sample C (rock quartz)

Sample C is very coarse-grained hydrothermal milky quartz with elongated parallel oriented sub-grains and undulate extinction. There are few well-defined grain boundaries in the thin sections. Fractures and cracks are filled with recrystallized quartz and the density of fluid inclusions is very high. Polarized light micrographs of Cold C and Warm C are shown in Figure 4a and d.

The unheated reference sample Cold C shows a low-intensity luminescence in the red and blue bands causing violet CL colors (Figure 4b). The CL spectra (Figure 4c) show a dominating, stable emission with red 650 nm and blue 480 nm bands. The red (650 nm) emission is of slightly higher intensity than the blue emission. The heated sample Warm C shows a reddish-purple CL color (Figure 4e) with a more or less dominating red emission around 635 nm and an accompanying emission band in the blue at 460 nm (Figure 4f). Variations in the visible CL color (dark violet to reddish-purple) and intensity within the sample can be explained by varying intensity ratios of these two CL emissions.

There is also a weak emission in the green CL at approximately 515 nm, which probably causes the greenish tint seen in the CL images.

The maximum intensity of the highest peak is very low with up to 600 counts at 20 seconds acquisition time (30 counts/second). In contrast to the previous quartz types, Sample C shows an increase in the CL emission after heating, to a maximum of 40 counts/second. The shape of the spectra remains the same i.e., only the intensity of the CL emission increases. The differences in the CL intensity are not significant and might as well be coincident, for example tied to slight differences in the thickness of the carbon coating.

This type of luminescence where the emission around the 650 nm band is dominant, followed by a lower emission around the 450 nm band, is typical for quartz from regional metamorphic rocks [12, 13]. The high intensity of NBOHC [14] can be explained by the mechanical stress during metamorphic processes.

The content of impurity elements in Sample C is lower than in the other samples investigated (Table 1), this may explain the relatively low CL intensity in the unheated quartz. The insignificant changes in the luminescence spectra but a possible weak increase in luminescence intensity may indicate increasing content of lattice defects in the heated quartz.

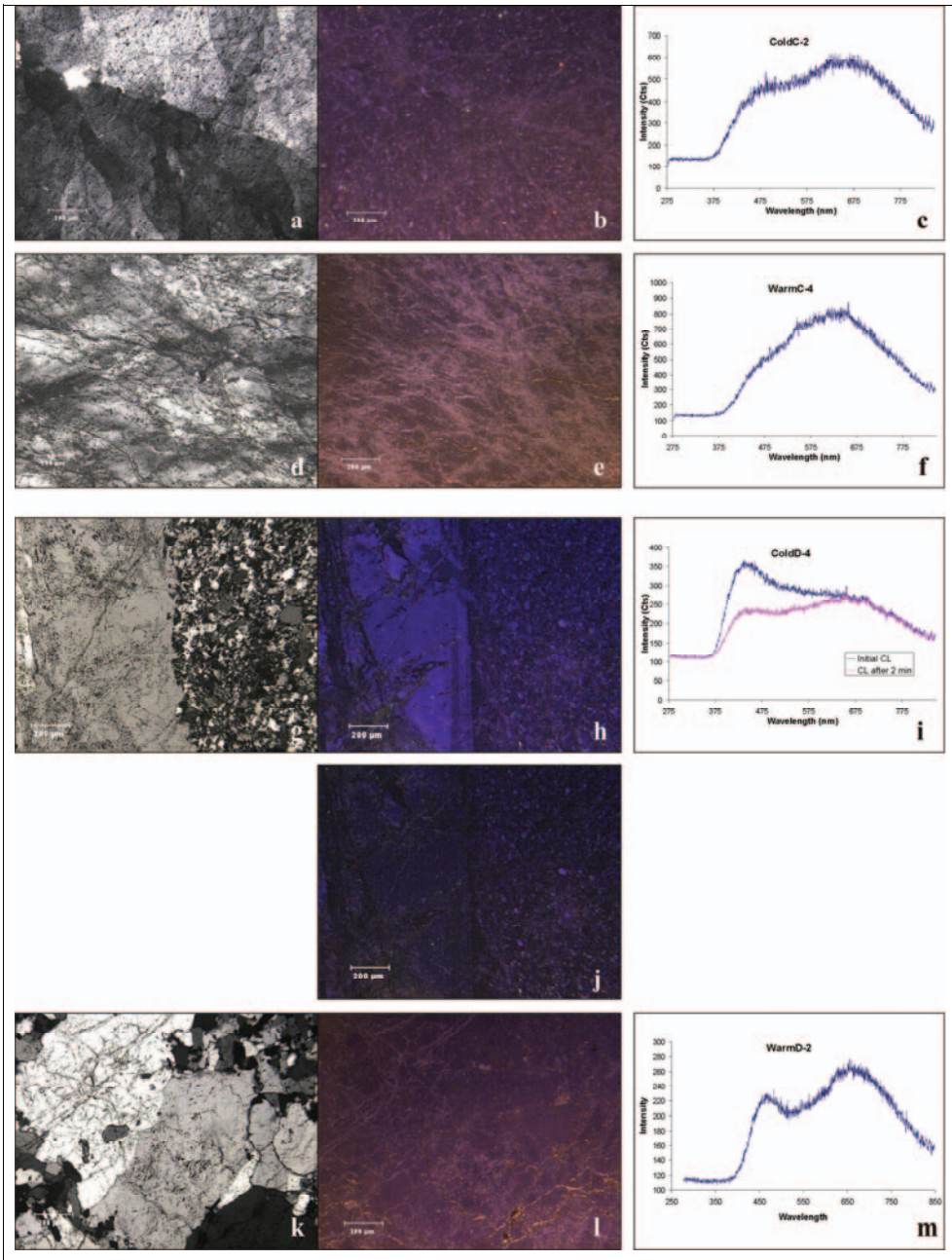

Figure 4 a to f show sample Cold C and Warm C. a and b show optical and CL micrograph of Cold C. c shows Cl spectrum for Cold C. d and e show optical and CL micrographs of Warm C. f shows CL spectrum for Warm C. g to m show sample Cold D and Warm D. g, h and j show optical and CL micrographs of Cold D. h and j show initial and transient CL respectively. i shows initial and transient CL spectra for sample Cold D. k and l show optical and CL micrographs of sample Warm D. m shows CL spectrum for sample Warm D.

Sample D

Sample D resembles pegmatite quartz. The grains are inequigranular, recrystallized and strain free amongst the remains of strained primary quartz featuring undulatory extinction. Polarized light micrographs of Cold D and Warm D are shown in Figure 4g and k.

In Cold D-4, (Figure 4h and j), the CL emission is characteristically transient blue, changing to dark blue during electron beam irradiation. This effect resulted from a decrease in the blue 440 nm band and a slight decrease in the red 650 nm emission band (Figure 4i). The coarse-grained and fine-grained quartz grains show similar CL colors indicating that they belong to the same generation of quartz. Another type of blue CL observed in sample Cold D-1 is caused by the blue 440 nm and the green 540 nm emission bands. In spectra Cold D-1a and ColdD-1b of the coarse-grained part of the area, the blue 540 nm emission decreases relatively to the 440 nm with time (10 seconds) during e-beam irradiation. Sample Warm D shows varying CL emissions changing from reddish to violet colors (Figure 4l). These are dominated by the red 670 nm and the blue 450 nm emission bands. In addition, a low peak is observed around the green 550 nm emission band. The varying colors are defined by differences in the relative value of the blue 464 nm peak compared to the dominating red emission at 670 nm (Figure 4m).

The maximum intensity of the highest peak is very low with up to 360 counts at 20 seconds acquisition time (19 counts/second). This decreases in the sample Warm D to maximum intensity up to 190 counts at 20 seconds acquisition time (9 counts/second).

Heating the samples changes the CL spectra of Sample D. The transient blue emission that changes to a darker blue-violet color during e-beam irradiation, responds to heating with a more reddish or violet color. The spectra are dominated by the same peaks in Warm D as in Cold D after e-beam irradiation. However, the dominant emission peaks at 450 and 650 nm are more pronounced in Warm D compared to Cold D after irradiation by the e-beam. Accordingly, the red part of the spectra becomes more pronounced. The other quartz types that were investigated obtain the same luminescence colors as those resulting from e-beam irradiation, after they were heated.

Although the spectral positions do not fit perfectly with those described by [17], the initial CL colors and the decrease of stable emission intensity of the red emission band are similar to those described as typical for pegmatite quartz [17] as opposed to hydrothermal quartz.

Sample E (rock quartz)

Sample E is a typical meta-sandstone comprising well-rounded detrital grains with relatively open grain boundaries. There are dust rims inside the single grains suggesting optically continuous autigenic quartz overgrowths. Aggregates of mica minerals occur sporadically, and rare accessory minerals, zircon and monazite may also be observed in the thin section. Polarized light micrographs of Cold E and Warm E are shown in Figure 5a and d.

Given that this is a detrital sample with possible composite origins of the grains, it is not surprising to find several different CL colors. Three main types of quartz were observed in sample Cold E (Figure 5b): One type showing bright blue CL color, one medium blue and one dark blue. In addition, a few quartz grains with pinkish CL color and a few quartz grains with greenish CL color were observed. Grains of zircon and monazite featured distinctive CL emissions and alteration halos in the enclosing quartz. The CL intensity of these minerals is much higher than the CL intensity in the quartz and the shape of the CL spectra shows characteristically narrow peaks.

The CL images show only weak quartz overgrowth on the quartz grains. This supports the optical microscopic interpretation that this is a meta-sandstone.

Blue Quartz: The different blue quartzes have main emission in the blue 450 nm band and the red 650 nm band. However, the difference between the varieties of blue quartz lies in the distribution of the emission amongst these two bands (Table 4 and Figure 5b and c):

Quartz type	**Major band (nm)**	**Minor band (nm)**
Bright blue	450	630-650
Medium blue	450 and 630-650	-
Dark blue	630-650	450

Table 4 Emission bands in nm for the different types of blue quartz in Sample Cold E and Warm E. The band 630-650 nm contains varieties of main peak emission supposed to be from the same luminescence centers only with minor deviation between samples.

The sample Warm E shows the three main types of quartz (bright blue-, medium blue- and dark blue luminescent quartz), although not as distinctively different in CL images as in sample Cold E (Figure 5b). As for the reference sample, the different blue quartzes show main emission in the blue 450 nm band and the red 650 nm band. Similarly, the difference between the different types of blue quartz lies in the distribution of the emission between these two bands (Table 4 and Figure 5e and f).

The emission pattern with predominance in the blue 450 nm emission band is recognized [e.g. 7, 8, 9] as typical igneous quartz. The predominance of the red emission around the 650 nm band, however, is more common for regional metamorphic quartz [e.g. 12, 13].

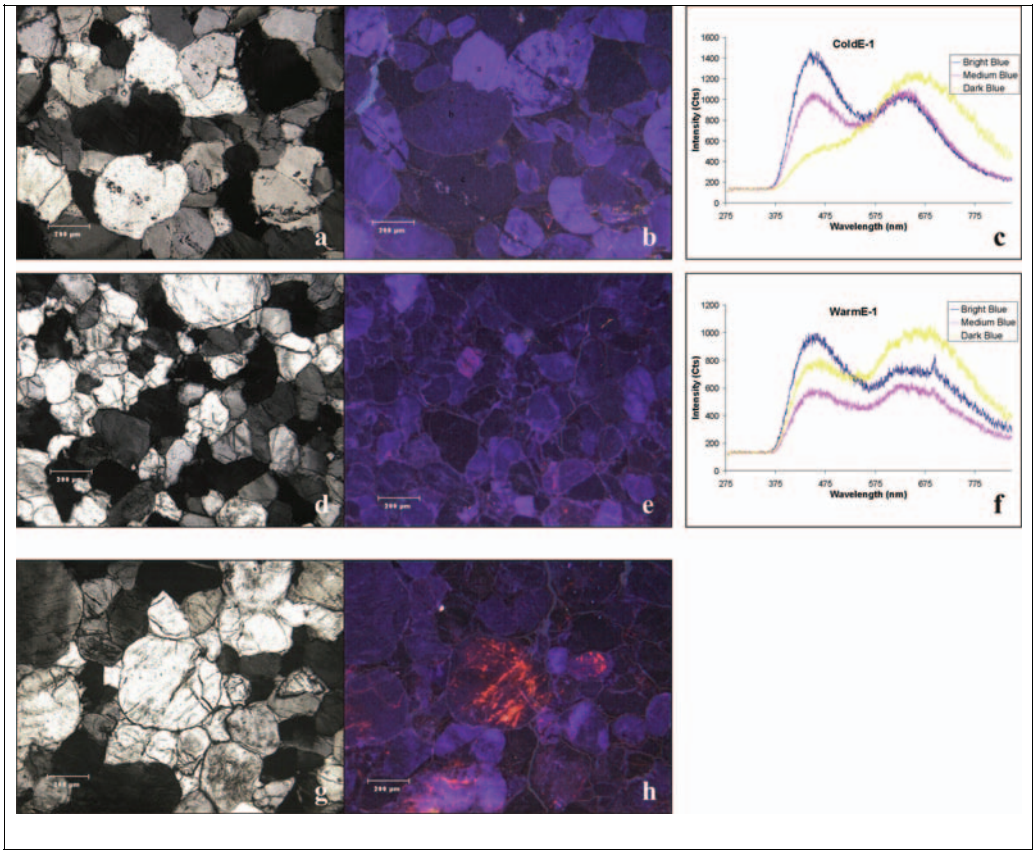

Figure 5 shows sample Cold E and Warm E. a and b show optical and CL micrographs of Cold E. Note the luminescence differences between the different shades of blue. These define three types of blue quartz (marked a, b and c and are bright-, medium- and dark blue quartz respectively). c shows CL spectra for the three types of blue quartz in Cold E. d and e show optical and CL micrographs of Warm E. The three types of blue quartz may still be recognized but the differences in luminescence properties are not that large. f shows the CL spectra for the three types of blue quartz in Warm E. g and h show optical and CL micrographs of the "spotted red CL" in Warm E. Note how the red CL are located around fractures and grain boundaries in the originally blue quartz.

The intensities of the main peak(s) are almost similar for the three different types of quartz but generally, the medium quartz shows slightly lower intensities than the bright quartz and with the dark quartz slightly lower than the medium quartz. Max intensities are 210 counts/second, 130 counts/second and 120 counts/second respectively. However, the intensities vary amongst the grains in the sample. For the heated samples, the maximum

intensities for the main peaks are approximately 100 counts/second for all types of blue quartzes.

The pinkish red quartz in Cold E is dominated by emission in the red band at around 630 nm, with a much lower emission in the blue band at 450 nm. There is also a marked low in the spectrum between the two peaks. The distinct pinkish red luminescence is typical for volcanic quartz [7].

The yellowish-green quartz in Cold E is dominated by a stable emission at around 580 nm [15] and is the same as seen in Sample Cold B. Yellowish-green quartz (570 nm emission is typical for hydrothermal quartz.

Other minerals: A few grains of zircon and monazite were seen in the sample. These showed luminescence intensities much higher than for the quartz. The spectrum is also typical for these kinds of minerals with typical narrow peaks for certain elements such as the REE.

A striking feature in some of the quartz grains in the heated sample Warm E is the spotted red CL located at, or adjacent to, micro cracks and grain boundaries in the single grains (Figure 5g and h). This feature is not observed in the unheated reference sample Cold E and is probably a result of heating. The emission from the spotted red CL might be related to non-bridging oxygen hole centers (NBOHC). However, Aasly et al. [19] reported significant cristobalite formation in Sample E. Thus, spotted red CL emission might represent cristobalite formation or a precursor to this transformation. However, cristobalite has previously been reported showing blue luminescence [e.g. 23].

Another effect that is clearly a result of heating is the opening of the grain boundaries in the heated sample as compared to the unheated reference sample Cold E. This can be seen as more pronounced grain boundaries in sample Warm E (Figure 5).

The mix of different CL characteristics ranging from igneous- and regional metamorphic rock as the main source for the quartz grains to volcanic and hydrothermal vein quartz as additional sources confirms the geological interpretation of this quartz rock as a low-grade metamorphic quartzite or meta-sandstone. A more high-grade metamorphic quartzite would show more constantly similar and low luminescence quartz grain with non-luminescence overgrowth.

Sample F (gravel quartz)

Sample F is inequigranular crystalloblastic quartz with 120°-triple junctions. The quartz seems strain free and shows a weak layering comprising alternating bands with coarse-grained and fine-grained quartz. Polarized light micrographs of Cold F and Warm F are shown in Figure 6a and e.

Sample Cold F is a typical hydrothermal quartz, showing transient blue luminescence (Figure 6b and d) dominated by emission in the blue band at 480 nm as seen in Figure 6c. The dominating blue emission decreases with time, and after approximately two minutes, the CL color has changed to dark brownish and the spectrum shows equal intensity for the blue emission around 480 nm and the red emission around 650 nm. This is caused by a decrease in the blue emission and near constant emission in the red band (Figure 6c). A weak zonation may be seen in the Cold F samples (Figure 6b and d) as dark blue cores with slightly brighter blue rims. This effect remains after several minutes with continuous e-beam irradiation, although the luminescence characteristics (colors) have changed. Sample Warm F shows a widespread separation of the individual grains as a result of grain boundary opening caused by the heating. Some green CL intensity may be related to green luminescent epoxy occupying open grain boundaries. The transient greenish-blue CL (Figure 6f and h) is dominated by the green 505 nm, the red 635 nm and the weaker blue 413 nm emission bands (Figure 6g). The green emission decreases with time, whereas the red and blue emissions remain constant such that, after minutes of electron beam irradiation, the CL color has changed to dark blue, almost brownish.

Small spots with red CL similar to the spotted red CL in Warm E are observed. The spotted red CL is situated at internal micro-cracks/fractures and grain boundaries and may probably be related to NBOHC.

The maximum intensities for the main peaks are approximately 50 cts/sec. However, the intensities of the transient luminescence decrease noticeably after minutes of electron beam irradiation to 30-40 counts/second. For sample Warm F, the maximum intensities for the main peaks are up to 140 cts/sec. However, the intensity decreases significantly after minutes of electron beam irradiation to 30-40 counts/second. Because of the transient effect of the luminescence, it is difficult to compare the maximum intensities of samples Cold F and Warm F. However, it indicates that the maximum intensities increase after heating as seen in Sample C.

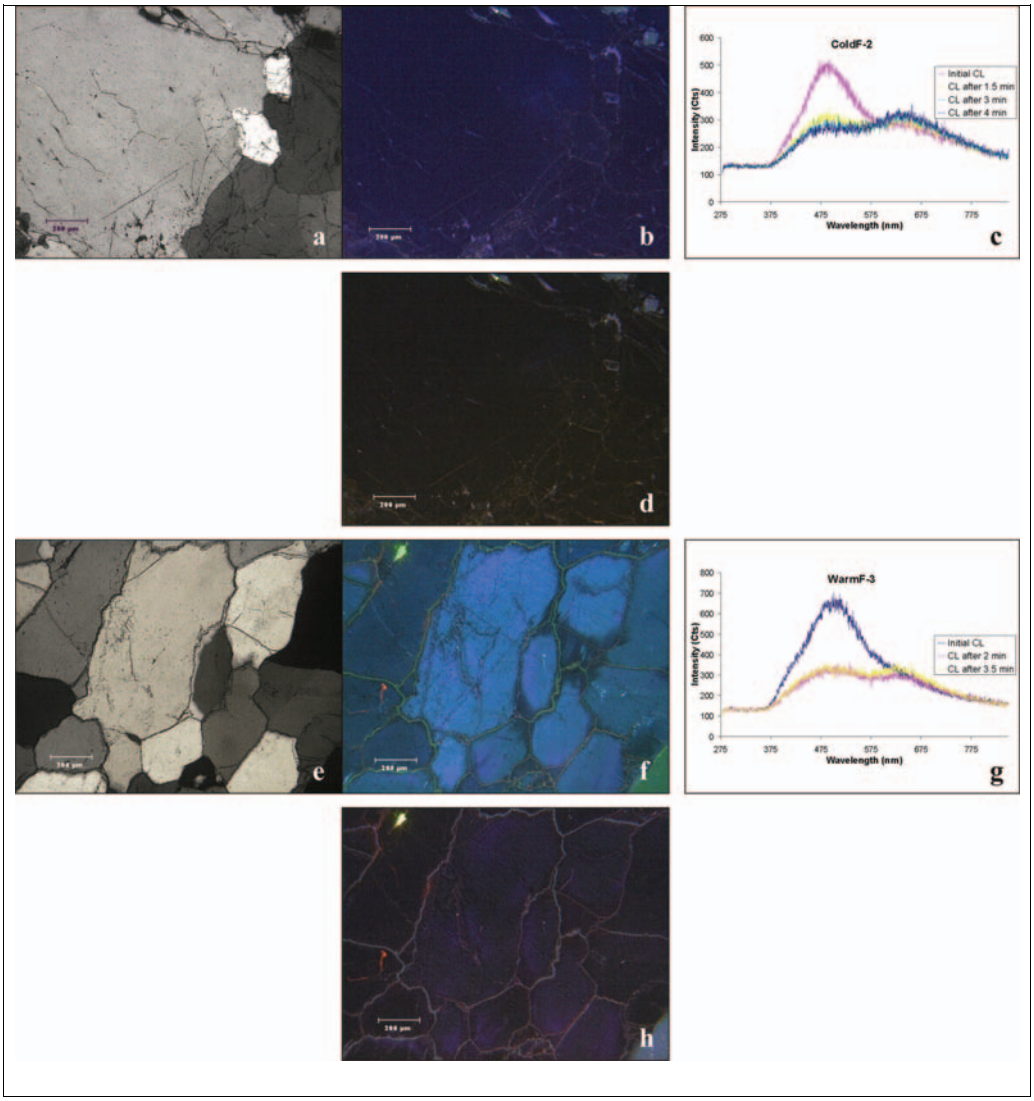

Figure 6 shows sample Cold F and Warm F. a, b and d show optical and CL micrographs of Cold F. b and d show initial and transient CL respectively. c shows CL spectra for initial and transient CL in Cold F. e, f and h show optical and CL micrographs of Warm F. f and h show initial and transient CL respectively. g shows initial and transient CL spectra for Warm F.

The effect of transient CL emission with time during electron beam irradiation is seen in both the unheated sample Cold F and the heated sample Warm F. However, the initial CL colors and CL spectra are different for the two samples. The main emission is the blue CL color around 480 nm in sample Cold F and green CL around 505 nm in sample Warm F. However, the green luminescence of the epoxy filling in the open grain boundaries might contribute to the shifted peak position of the CL spectra. The intensity of the CL emission in sample Warm

F is 1.5 – 2 times higher than the intensity in sample Cold F. This cannot be explained by low content of impurities (Table 1), as is the case for sample C, since sample F is the quartz with the highest content of impurities.

Implications for choice of quartz raw materials

As it was expected, the different types of quartz demonstrated characteristically different luminescence as already implied by earlier publications and summarized by Götze et al. [7]. Furthermore, distinctive differences in luminescence characteristics were expected between the unheated reference samples and heated samples.

The different quartz types show varying effects of the heating, which results in either an increase or a decrease in the luminescence intensity of the heated samples compared to the reference samples. For some samples or for specific areas within a specific sample, there are changes in the luminescence characteristics: The dominating emission band changes in the heated samples compared to the reference samples as an effect of intensity changes. In samples with originally transient CL emission, the transient effect disappears as a result of the heating, and the spectra are similar to those after irradiation by an electron beam. In other samples, entirely new emission bands that were not seen in the unheated reference sample appear. These bands occur as the dominating emission, as an effect of the heating.

A remarkable feature was observed in the heated samples of the specimens E and F. A characteristic spotted red CL was located within grain boundaries or fractures/cracks. This can probably be interpreted as a result of the generation of NBOHC (650 nm emission). These NBOHC may have been generated as a result of thermal fracturing of the rocks. This thermal fracturing may generate micro- or even nano-cracks in the rock, which again may lead to the generation of NBOHC. However, Aasly et al. [19] reported cristobalite formation in the same heated quartz samples. Cristobalite has been reported showing blue luminescence [e.g. 23], however, the red luminescence might represent the cristobalite formation or a precursor to this. Although it is not clear whether the CL directly originates from the cristobalite phase, NBOHC may possibly be related to the initial formation of cristobalite through the amorphous transition phase that is expected to occur in advance of any cristobalite nucleation [e.g. 24, 25]. The transition phase as well as cristobalite has a considerably higher volume than quartz and therefore severe fracturing is expected during heating. This volume expansion is likely to cause NBOHC, and therefore, the heat generated CL in Samples E and F. The lack of these effects in the other samples may be caused by the relative short heating time leading to no or only neglectable amounts of cristobalite (and transition phase) during heating.

Another feature observed in the CL investigations is that the grain boundaries were opened as an effect of heating in samples E and F. It was most pronounced in Sample F where epoxy occupies the grain boundaries and, apparently, causes a transient greenish CL emission. For rocks such as Sample E and F comprising numerous small grains with a relatively open grain boundary texture these open grain boundaries may be seen as an advantage during the heating. It may be assumed that for these fine-grained samples, the fracturing of the quartz fragments is not so significant, since each single quartz grain has space around it to accommodate the volume expansion, taking place during heating. The result may be less fracturing of the fragments during heating. In contrast, samples with large grains and more dense grain boundaries result in a fragmentation of the complete quartz fragment during heating. This in accordance with what is known, that fine-grained rocks are usually mechanically stronger than coarse-grained rocks. However, it is also commonly agreed, that fine grained quartz and open grain boundaries results in mechanically weak quartz, whereas coarse grained quartz with dense grain boundaries results in a mechanically stronger quartz.

Although several distinguishing features are seen in the CL spectra of the heated samples, the cause of these features is not yet completely understood. Future studies should focus on this challenge. Still, different types of quartz show distinguishing properties that can be used to characterize the origin of the different types of quartz.

Conclusions

The present cathodoluminescence study has proved that shock heating of different types of quartz causes different effects with respect to the CL emission. These effects are revealed by CL microscopy as well as in the related CL spectra. It seems that the luminescence centers of initially transient quartz are removed in the same way as they disappear during electron beam irradiation. It is also shown that luminescence centers of other types of quartz seem to be less affected by shock heating, although new luminescence centers occur in limited areas within grains that otherwise seem unaffected.

The experiments have also shown that CL may be a good technique for detecting initial phase transformations in quartz beyond the α-β transformation. In this paper, the cristobalite or a precursor to cristoblalite in the quartz–cristobalite transformation has been indicated in samples Warm E and Warm F. This is indicated by the formation of “spotted red CL” features that were not seen in any of the other samples. This spotted red CL is probably related to generation of NBOHC that may have been caused by cristobalite or the amorphous transition phase that is asumed to be related to the quartz-cristobalite transformation.

Acknowledgement: The authors thank Steinar Prytz for help with the induction furnace heating, Kjetil Eriksen and Arild Monsøy for great help with preparing samples for the heating experiments as well as the polished thin sections for CL investigations. Thanks to Elkem ASA for funding this research.

References

1. Marfunin, AS. Spectroscopy, Luminescence and Radiation Centers in Minerals: Springer-Verlag Berlin Heidelberg New York 1979.

2. Pagel M, Barbin V, Blanc P, Ohnenstetter D. Cathodoluminescence in Geoscience: An Introduction. In: Pagel M, Barbin V, Blanc P, Ohnenstetter D, editors. Cathodoluminescence in Geoscience. Berlin Springer Verlag; 2000, p. 1-21.

3. Remond GG. Cathodoluminescence applied to the microcharacterization of mineral materials: a present status in experimentation and interpretation. Scanning microscopy 1992;6(1):23-68.

4. Ramseyer K, Baumann J, Matter A, Mullis J. Cathodoluminescence Colors of Alpha-Quartz. Mineralogical Magazine 1988;52(368):669-677.

5. Ramseyer K, Mullis J. Factors Influencing Short-Lived Blue Cathodoluminescence of Alpha-Quartz. American Mineralogist 1990;75(7-8):791-800.

6. Watt GR, Wright P, Galloway S, McLean C. Cathodoluminescence and trace element zoning in quartz phenocrysts and xenocrysts. Geochimica Et Cosmochimica Acta 1997;61(20):4337-4348.

7. Götze J, Plötze M, Habermann D. Origin, spectral characteristics and practical applications of the cathodoluminescence (CL) of quartz - a review. Mineralogy and Petrology 2001;71:225-250.

8. Müller A, Lennox P, Trzebski R. Cathodoluminescence and micro-structural evidence for crystallisation and deformation processes of granites in the Eastern Lachlan Fold Belt (SE Australia). Contributions to Mineralogy and Petrology 2002;143(4):510-524.

9. Müller A, Seltmann R, Behr HJ. Application of cathodoluminescence to magmatic quartz in a tin granite - case study from the Schellerhau Granite Complex, Eastern Erzgebirge, Germany. Mineralium Deposita 2000;35(2-3):169-189.

10. Fitting HJ, Barfels T, Trukhin AN, Schmidt B. Cathodoluminescence of crystalline and amorphous SiO2 and GeO2. Journal of Non-Crystalline Solids 2001;279(1):51-59.

11. Skuja L. Optically active oxygen-deficiency-related centers in amorphous silicon dioxide. Journal of Non-Crystalline Solids 1998;239(1-3):16-48.

12. Neuser RD, Richter DK, Vollbrecht A. Natural quartz with brown/violet cathodoluminescence - Genetic aspects evidence from spectral analysis. Zentralblatt für Geologie und Paläontologie Teil 1 1989;7/8:919-930.

13. Zinkernagel U. Cathodoluminescence of quartz and its application to sandstone petrology. Contributions to Sedimentology 8 1978;1-69.

14. Sigel JGH, Marrone MJ. Photoluminescence in as-drawn and irradiated silica optical fibers: an assessment of the role of non-bridging oxygen defect centers. Journal of Non-Crystalline Solids 1981;45(2):235-247.

15. Götze J, Plötze M, Fuchs H, Habermann D. Defect structure and luminescence behaviour of agate - results of electron paramagnetic resonance (EPR) and cathodoluminescence (CL) studies. Mineralogical Magazine 1999;63(2):149-163.

16. Rink WJ, Rendell H, Marseglia EA, Luff BJ, Townsend PD. Thermoluminescence Spectra of Igneous Quartz and Hydrothermal Vein Quartz. Physics and Chemistry of Minerals 1993;20(5):353-361.

17. Götze J, Plötze M, Trautmann T. Structure and luminescence characteristics of quartz from pegmatites. American Mineralogist 2005;90(1):13-21.

18. Birkeland R. Optimal quartz properties - method evaluation part 1 Internal Report (in Norwegian). Kristiansand: Elkem Research 2004.

19. Aasly K, Malvik T, Myrhaug E. Advanced methods to characterize thermal properties of quartz. Proc INFACON XI. New Dehli, India, February 18-21; 2007.

20. Neuser RD, Bruhn F, Götze J, Habermann D, Richter DK. Cathodoluminescence: method and application (in German). Zentralblatt für Geologie und Paläontologie 1995;1/2:287-306.

21. Itoh C, Tanimura K, Itoh N. Optical studies of self-trapped excitons in SiO2. Journal of Physics C: Solid State Physics 1988(21):4693-4702.

22. Stevens Kalceff MA, Phillips MR. Cathodoluminescence Microcharacterization of the Defect Structure of Quartz. Physical Review B 1995;52(5):3122-3134.

23. Marshall DJ. Cathodoluminescence of geological materials. Boston: Unwin Hyman 1988.

24. Chaklader ACD. X-Ray Study of Quartz-Cristobalite Transformation. J. Amer. Ceram. Soc. 1963;46(2):66-71.

25. Chaklader ACD, Roberts AL. Transformation of Quartz to Cristobalite. J. Amer. Ceram. Soc. 1961;44(1):35-41.

Paper V

Is not included due to copyright

Paper VI

Quartz in the Silicon Furnace

Kurt Aasly[1], Terje Malvik[1] and Edin Myrhaug[2]

Prepared for submission

[1] *Norwegian University of Science and Technology, Department of Geology and Mienral Resources Engineering, Sem Sælands v. 1, NO-7491 Trondheim, Norway*

[2] *Elkem ASA, Alfred Getz v. 2, NO-7465 Trondheim, Norway*

Abstract

Samples from one FeSi furnace and one Si furnace have been investigated with respect to the thermal and thermo-mechanical properties of quartz and especially the phase transformations in quartz during the progress of the smelting process. The samples were drilled from the furnaces after the process was stopped, and gives an opportunity to investigate the interior of the furnace and the effects of the process on the raw materials.

Optical microscopy and X-ray diffraction were used to investigate the thermal and thermo-mechanical behavior of the quartz and especially the silica phase transformations.

It has been shown that quartz transforms to cristobalite rather quickly but that the speed of the transformation is depending on the position in the furnace. Tridymite is surprisingly found in the FeSi furnace, however in the more inactive part of the charge. The formation of tridymite in the FeSi furnace is explained by the somewhat higher amount of impurities in the FeSi.

The results presented here have provided more knowledge about the silica phase transformations in the silicon furnace and also how the quartz material reacts to the temperatures in the process.

Introduction

During operation, the high temperatures in the carbothermic furnace for production of ferrosilicon and silicon-metal ((Fe)Si) makes measurements and investigations of reactions and temperatures difficult. However, this work is a result of gained access to samples from two furnaces, one FeSi and one Si-furnace, which can be viewed as snap shots of the interior of the furnaces at the point where the process was stopped. The objective of this research is therefore to look at what types of stress has been put on the quartz raw materials during its way through the furnace and how this has resulted in deformation and crystallographic changes in the quartz as a result of the high temperatures in the furnace. Thus, the quartz samples taken from the two furnaces have been investigated with focus on thermal and thermo-mechanical behavior generally and SiO_2 (silica) phase transformations especially.

The carbothermic process

Carbothermic production of ferrosilicon and silicon metal is thoroughly described by Schei *et al.* (1998). Figure 1 shows an illustration of a typical silicon metal production site. In general, quartz and carbon materials react at high temperatures to form silicon metal. In the ferrosilicon furnace, iron ore (pellets) are added as source for Fe.

The ideal reaction for silicon production can then be written as:

$$SiO_2 + 2C = Si + 2CO \quad \textbf{(1)}$$

In a real furnace, the process is much more complicated and consists of several sub-processes, which may be affected by the properties and quality of the raw materials.

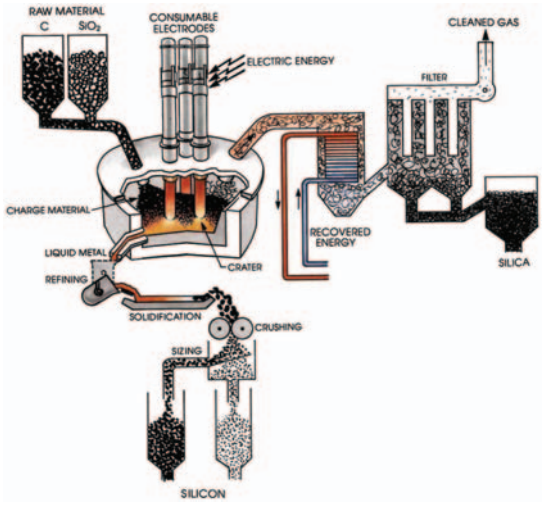

Figure 1 Sketch of a silicon furnace (Schei *et al.*, 1998)

Quartz in the furnace

The source of Si in the carbothermic furnace is quartz (SiO_2). The industry has a set of requirements to the raw materials (e.g Schei *et al.*, 1998):

- Chemistry (e.g. Al, Ti, B, P, Fe, Ca)
- Lump size (typically 10 – 150 mm)
- Mechanical strength
- Thermo-mechanical strength
- Softening properties

Industrial experiences have shown that softening properties of the quartz together with mechanical and thermo-mechanical strength may affect the performance of the (Fe)Si furnaces.

Chemistry is the most important parameter for the quartz since some of the impurities will highly influence the quality of the product. Because of the requirements to the lump size, the quartz that is used as raw material for (Fe)Si production need to be of acceptable chemical qualities with no refinement needed. Some improvement of the chemical quality may be achieved by hand picking and/or optical sorting during further processing.

The raw materials mix is charged on the top of the furnace, which may hold temperatures in the range 700 to 1300 °C (Grådahl *et al.*, 2000). After charging, the raw materials will move trough the furnace at a rate equivalent to retention time ranging from one to two hours and upwards. Average retention time for quartz in the furnace is calculated by SiMod (Foss *et al.*, 2000) to be 5.7 hours for a 25 MW furnace. Figure 2 and Table 1 shows the temperature profile and the data for calculating the profile. The retention time is defined as from charging

to the raw material enters the crater wall (Foss *et al.*, 2000). The time span is related to the position of the raw materials inside the furnace. Raw materials close to the electrodes tend to move faster through the charge than the raw materials in the peripheral parts of the furnace. This is probably related to the temperature gradient in the furnace, which is higher closer to the electrodes and the electric arc. Areas in the peripheral parts of the furnace and probably a small area in the center of the furnace between the electrodes seem to show the lowest temperatures and thus, the mass flow (activity of the charge) in these parts are slower than close to the electrodes. The temperature in the hottest parts of the furnace is more than 2000 °C

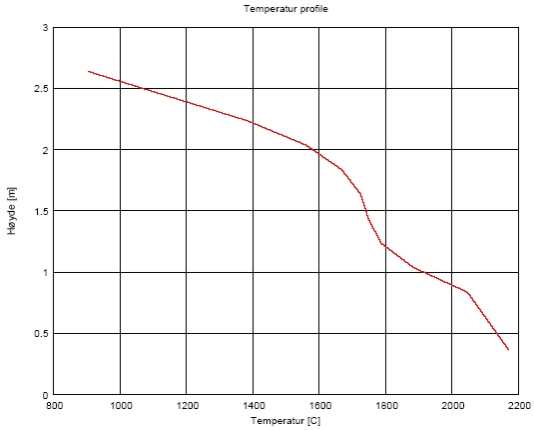

Figure 2 Temperature profile from Si-Mod (Foss *et al.*, 2000).

Table 1 Data for calculation of temperature profile in Figure 2.

Data for 25 MW furnace (Captured from standard model in SiMod)			
Cross- section area	20	m	
Furnace height (internal)	2.737	m	
Quartz-feeding	5473	kg/h	
Density of quartz	2600	kg/m^3	
Amount of quartz in charge	73	%	
Packing	60	%	i.e. 40% gas
Portion “active” cross sectional area	50	%	

Myrhaug (2003) subdivides the inner structures of the Si-furnace into characteristic zones. The following of these zones are investigated in this paper and shown in Figure 3a.

3) Arc crater wall of SiC with some Si
4) Mixture of SiC, SiO_2 and Si
5) Partly converted reduction materials
6) Top of charge with SiO-condensate

Schei *et al.* (1998) illustrates the inner structure of a furnace in Figure 3b based on experiments with pilot scale furnaces. The figure shows a silicon- or high silicon ferrosilicon

furnace shortly before stoking. The main feature of the furnace is the cavity surrounding the electrode. The cavity walls consist of sintered SiC crystals in the lower parts partly mixed with molten silicon. The upper parts of the cavity walls consist of carbon lumps, molten silica and condensate, where the carbon lumps are partly converted to SiC. Outside the cavity wall, charge material closest to the cavity are reactive but further outside, the temperature is not high enough to keep the charge reactive. As the roof of the cavity is saturated and no reactions take place in the upper charge, the cavity is stoked down and new charge is filled on top.

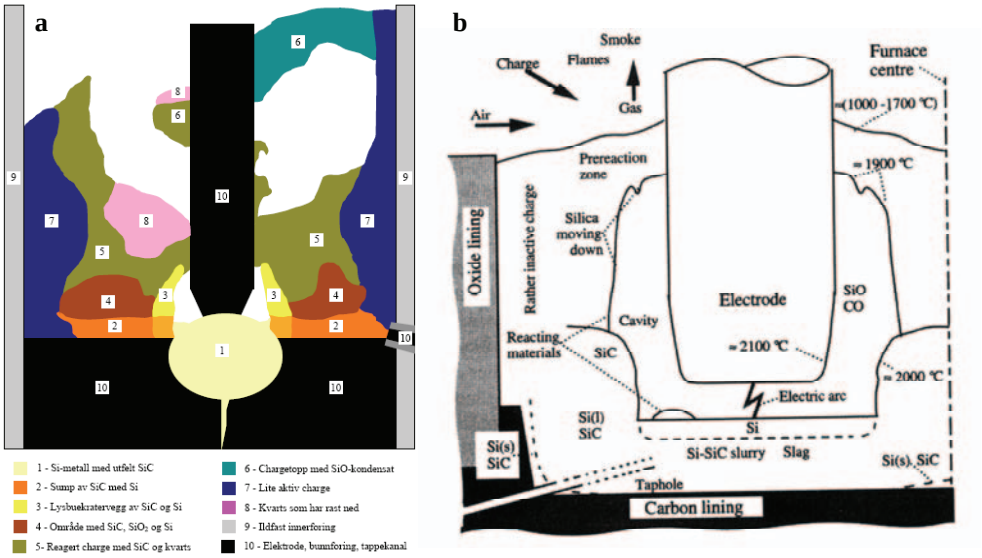

Figure 3 a): Schematic illustration of cross section with indicated zones (Myrhaug, 2003); **b):** Illustration of a silicon or high silicon ferrosilicon inner structure (Schei *et al.*, 1998).

Silica Polymorphism

The silica system has been studied by several researchers and is one of the most studied mineral systems. However, it also appears to be one of the most complex and least understood. The α- to β- quartz transition has been determined to occur at 573 °C (Figure 4) and is a spontaneous and reversible reaction. However, the transformations from β-quartz to HP-tridymite and from β-quartz/HP-tridymite to β-cristobalite are less understood. The nature of these transformations has been discussed by several authors (e.g. Fenner, 1913; Floerke, 1957; Holmquist, 1961; Deer *et al.*, 1992; Stevens *et al.*, 1997). It seems to be an established knowledge that the β-quartz to HP-tridymite formation is depending on a minimum content of impurities (alkalis, especially Na and Ca; and Al) to act as catalysts (e.g. Floerke, 1957; Holmquist, 1961; Stevens *et al.*, 1997). In the absence of such catalyst, β-quartz will transform directly to β-cristobalite, probably with an intermediate non-crystalline phase (e.g. Chaklader and Roberts, 1961; Chaklader, 1963). The transformations from β-quartz to HP-tridymite and from HP-tridymite to β-cristobalite take place at 870 °C and 1470 °C, respectively (Figure 4). Both phase transformations are reconstructive and slow. However, the transformation temperature from β-quartz to β-cristobalite seem to vary and is reported to be far below 1470 °C. Temperatures down to 1100 °C have been reported (Harders and Kienow, 1960).

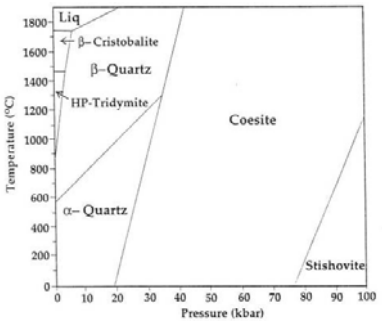

Figure 4 Phase diagram for the silica system (Klein and Hurlbut, 1993).

Previous investigations of the thermal properties of quartz as a raw material for production of (Fe)Si has shown that β-cristobalite formations starts at temperatures as low as 1250°C (Aasly *et al.*, 2007, In prep. 2008). However, no HP-tridymite formation was detected in these previous investigations.

Materials and methods

Pilot scale Si furnace

Operation and raw materials

The pilot furnace operation is thoroughly described by (Myrhaug, 2003). The furnace was a one-phase, 100-150 kW silicon furnace charged with only one type of quartz and a mix of 90% charcoal and 10% wood chips. The furnace was operated in cycles with stoking, charging and tapping.

The quartz used in the pilot Si-furnace was a Si-quality hydrothermal quartz containing relatively low amounts of trace elements.

Sampling

After the pilot furnace were shut down and cooled, the furnace was filled with epoxy and a 5 cm thick slice was made by wire saw along the vertical plane in the middle of the furnace. 18 samples were drilled from the slice and were first described by Myrhaug (2003). The positions of these samples are shown in Figure 5.

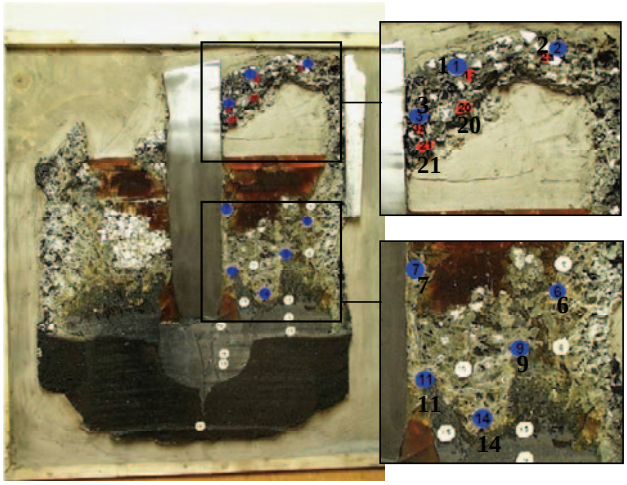

Figure 5 Shows the sample positions in the pilot furnace plate (After Myrhaug, 2003). The blue and white points are the samples investigated by Myrhaug (2003). Blue points show the position of the polished thin sections investigated in this paper. The red dots marks the sample positions for XRD samples that were not taken from the polished section slabs. The charge top on the left side of the furnace has fallen down after the operation was stopped and thus, the sampling was only carried out on the right side where the correct position of the material is intact.

Samples for XRD analysis were carefully selected among these samples, and only those determined to contain quartz by Myrhaug (2003) were chosen. However, due to hardness or lack of accessible quartz, some of these samples were not possible to sample for quartz. Thus, the sample for XRD was taken from a piece of quartz or SiO_2 that were located immediately next to the drill hole on the plate. Additionally, two samples were taken from the furnace plate (charge top), not related to the 18 existing samples (Samples 20 and 21).

Myrhaug (2003) carried out microprobe (EPMA) investigations of the samples and described the material relations including quartz in some of the polished samples (Table 2).

Table 2 Shows the material relations in the samples from the pilot scale furnace (after Myrhaug and Monsen, 2002; Myrhaug, 2003).

Sample no.	Area in furnace	Description
1	Top of charge with SiO-condensate	Quartz, SiO-condensate and charcoal from top of the charge
2	Top of charge with SiO-condensate	Quartz, SiO-condensate and charcoal from top of the charge
3	Top of charge with SiO-condensate	Quartz and charcoal with some SiC from top of the charge
6	Rather inactive charge	Area with SiO_2 and Si from condensed SiO, quartz and charcoal from the middle parts of the charge outwards near the lining
7	Reacted charge with SiC and quartz	Area with smelted quartz, charcoal and green SiC on charcoal form in the middle of the charge near the electrode
9	Reacted charge with SiC and quartz	Area with smelted quartz, SiC and Si a distance above the furnace bottom between the electrode and lining
11	Reacted charge with SiC and quartz	Area with smelted quartz, SiC and Si in upper wall to arc crater
14	Reacted charge with SiC and quartz	Area with SiC, condensate from SiO, smelted quartz and Si and Si just above SiC/Si swamp at the furnace bottom, between electrode and lining

Industrial scale FeSi furnace

Operation and raw materials

The industrial furnace was a three-phase FeSi furnace running at 42 MW. The inner diameter of the furnace was 11 300 mm. The furnace produced FeSi75, running on a charge mixture of a FeSi quality quartzite and a mixture of coal and coke + iron pellets.

Sampling

Drill cores were retrieved from the furnace after shutdown for relining. After the furnace had cooled for a few days, epoxy was poured into selected areas of the furnace and left to cure. The investigated drill cores include seven holes: three were drilled from each of two different openings (p-4 and p5-6) in the smoke hood. The dip of the drill holes were between 40-50° and 15-32° respectively. The seventh drill core was drilled horizontally at 2325 mm above the furnace bottom.

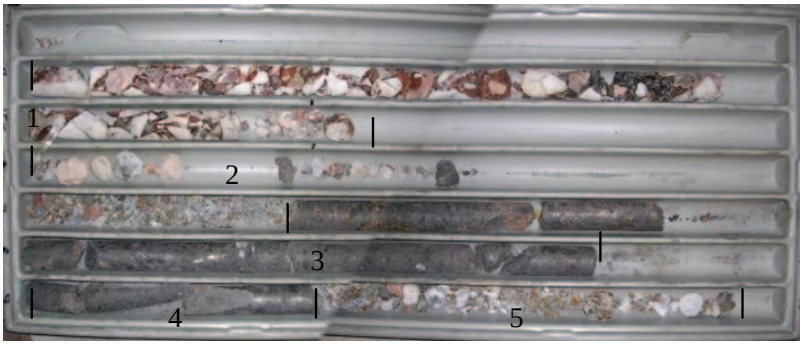

Figure 6 Overview of BH3p5-6. The core was logged to contain: **1)** unreacted charge with quartz, coal/coke and iron pellets (4.15 – 5.45 m); **2)** loose pieces of green condensate and SiC (7 – 7.5 m); **3)** electrode (7.5 – 9.1 m); **4)** carbide (9.1 – 9.4 m); **5)** condensate and charge including quartz (9.4 – 10 m). Note the large pieces of quartz in the charge top. The image is "bent" on the mid part because of merging of two separate pictures of slightly different angle to the core box.

An overview image of drill core BH3p5-6 is shown in Figure 6. The top (1) of the core contains unreacted charge with large quartz grains and coal/coke as well as iron pellets. Further, (2) a small zone of more reacted material containing SiC and some condensate are found. A part of an electrode is also seen (3) before the core enters into a zone of mostly black SiC (4). At the end of the core is a zone of condensate (green) and charge material with some more or less altered quartz (5). Table 3 shows a description of the material sampled for PTS and XRD in drill cores BH1 and BH2 p5-6.

Table 3 Detailed description of the sampled intervals for XRD and PTS in drill cores BH1 and BH2 p5-6

Sample No.	From (m)	To (m)	Description of sample material
BH1p5-6no1	2,2	2,3	Porous material containing some green material, quartz (corroded) and some metallic plus C-material
BH1p5-6no2	5,35	5,40	More massive, still different grains are visible. SiO2 cementation (melted quartz)?
BH1p5-6no3	5,80	5,85	Evidently partial (-fully?) altered quartz. Fine-grained, obviously affected by heat.
BH2p5-6no1	1,60	1,75	Charge? Large quartz fragments with various material (see core log). Quartz is evidently fragmented after heating.
BH2p5-6no2	4,0	4,1	More heat affected (corroded) quartz. Something like BH1p5-6 no 3.
BH2p5-6no3	7,1	7,25	A lot of melted quartz matrix around green- (SiC?), metallic- and C- material.

Analytical method

XRD

XRD analyses were carried out at the Department of Geology and Mineral Resources Engineering, NTNU, on a Philips PW 1830 XRD with CuK_{α} radiation.

Polarized light microscopy

Some of the samples were investigated by polarized light microscopy. Pieces of the samples were prepared as polished thin sections (PTS) for later investigations by transmitted- and polarized light microscopy. These samples were from the pilot furnace (as listed in Table 2) and three samples from each of drill cores BH1 and BH2 p5-6 from the industrial furnace (Table 3).

The size of the PTS is 28 mm x 48 mm and thus, only covers a small part of the drill-core.

Sampling method and cause of choice

Both the plate from the pilot scale furnace and the drill cores from the industrial furnace were examined and sampled with focus only on pieces of quartz. To make sure that no SiO_2 peaks were diluted by the content of other materials during XRD analysis, the samples were prepared as a thin layer of materials scraped off the samples onto a glass plate. Additionally, samples from the pilot scale furnace and selected samples from the FeSi furnace were investigated by optical microscopy.

Pilot scale furnace samples were originally prepared as polished sections for the work by Myrhaug (2003) and re-prepared for the microscopic (transmitted- and reflected light) investigations for this paper. The polished sections were cut close to the polished surface and prepared as polished thin sections.

Samples from BH1 and BH2 p5-6 from the Industrial scale furnace were also prepared as polished thin sections for microscopic investigations.

Results

Although several other phases than silica have been detected by XRD, these will generally not be commented up on as these are not considered relevant for this work.

Pilot scale Si furnace

Microscopically, obvious remains of the charged quartz are only found in PTS Pilot 1 and Pilot 2 (Figure 7a,b and c). These quartz fragments, although easily recognized as quartz, are totally different from the original quartz raw material as this appears microscopically (Figure 7d). These remains shows that the quartz has been subject to stress related to the high temperature and encountered micro- and grain boundary fracturing. Indications of emerged phase transformations were also observed under crossed polars as very small-scaled (microscopic) extinction domains, indicating cristobalite. However, small remains of quartz like extinction are seen within the possible cristobalite phase, especially in sample Pilot 1 (Figure 7c).

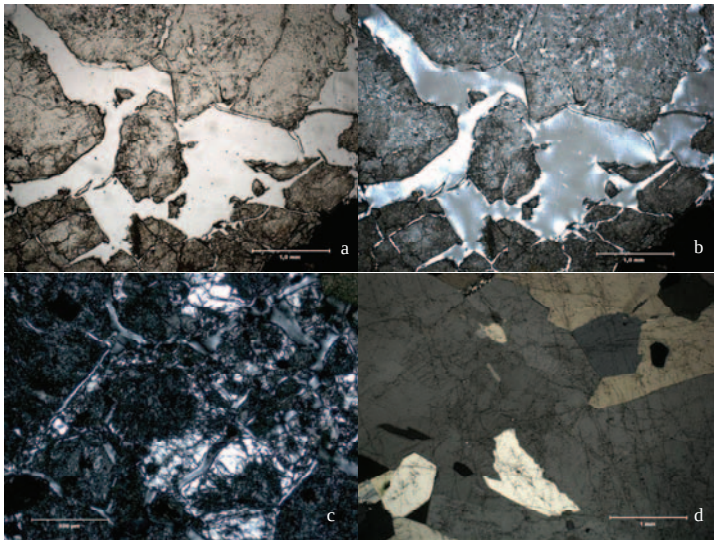

Figure 7 a): Sample Pilot 2 showing quartz with extensive fracturing because of the heat (polarized light); **b):** Same as a but crossed polars. Now the extinction pattern does not resemble quartz but are more fine-grained and probably shows that this quartz has transformed to cristobalite. **c):** Sample Pilot 1 in crossed polarized light. The quartz is similar to a and b but also shows more evident remains of quartz within the cristobalite. **d):** Reference sample of the unheated quartz used in the pilot furnace.

Table 4 Shows XRD results from scrape-off samples from Pilot scale Si-furnace. Sample 7a shows an extreme background count – up to 20%. (Crist = cristobalite; Qtz = quartz; Bckgr = back ground level). The "a" denotation in Sample no.'s indicates that the XRD sample is not taken from the drill core sample but from areas on the plate close to the drilled sample. Sample 20 and 21 is not related to any drill core sample.

Sample no.	XRD res
1a	Crist
2a	Crist
3a	Crist, Qtz, Bckgr
6	Crist, Bckgr
7a	Crist, Bckgr
9	Crist, Bckgr
11a	Crist, Bckgr
14	Crist, Bckgr
20	Crist
21	Crist, Qtz

Five samples were taken from the top of charge (Zone 6 in Figure 3a). The two samples closest to the electrode (Samples 3a and 21) returned both cristobalite and quartz as the present silica phases (Table 4). Additionally, Sample 3 indicates the presence of an amorphous phase by an observed elevated background level in the XRD results. The three other samples (Samples 1a, 2a and 20) returned only cristobalite as the present silica phase. None of these samples returned elevated background level. Further down, within Zone 5, five samples (Samples 6, 7, 9, 11a and 14) shows that cristobalite is the only SiO_2 phase present in this zone. Additionally, all the samples show an elevated background content.

Sample 11a was taken from near the top of Zone 3 (the arc crater wall) and Sample 9 near the top of Zone 4 (Mixture of SiC, SiO_2 and Si). No different phase composition was seen in these two samples.

Industrial scale FeSi furnace

Initial optical microscopic investigations of PTS from drill cores 1 and 2 (BH1 and BH2) from port 5-6 showed that the quartz fragments changed in appearance between the different samples. In some of the thin sections from the upper parts of the drill cores, the quartz appeared practically unaltered (Figure 8a and b). However, the samples show a more fractured texture similar to what was seen by microscopic investigations of the shock-heated samples as reported by Aasly *et al.* (2007). Also, a fracture containing more fine grained material shows textures under crossed polars that may be caused by cristobalite. In the same PTS, a zone containing mixture of fragments of reduction material, quartz and condensate was seen (Figure 8g and h). Here, smaller disintegrated quartz fragments occur. These are also showing typical quartz extinction.

Further down, into the depth of the furnace (and closer to the electrode) the quartz is more altered. At higher temperature parts of the furnace, phases resembling cristobalite are seen microscopically (Figure 8d and f). In microscopic investigations of BH1 PTS no. 3 by plane-polarized light, the relicts of the original detrital grains of the meta-sandstone is seen, but the heat has made the grain boundaries open and some of the grains appear to have started to soften (Figure 8c). Using crossed polars, the typical quartz extinction is not seen. However, each grain shows microscopic domains of extinction, which indicates cristobalite (Figure 8d). This has later been confirmed by XRD.

Microscopic investigations of BH2 PTS no. 2 show similar textures as BH1 PTS no.3. However, textures resembling tridymite as described by (e.g. MacKenzie and Guilford, 1980) with typical wedge shaped twinned crystals are seen using crossed polars (Figure 8e and f). XRD analysis confirms that this sample contain significant tridymite.

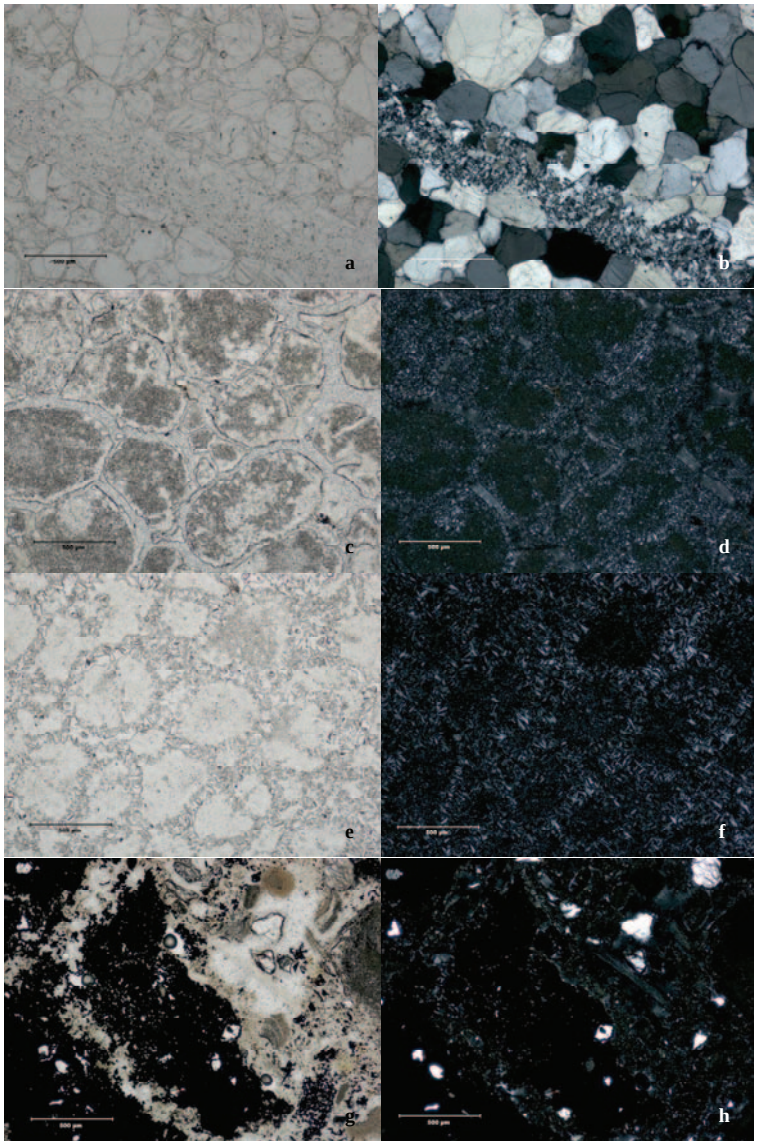

Figure 8 a): typical detrital quartz vein as seen in the original quartz. The detrital grains are cross cut by a small fracture containing more fine-grained material. **b):** same as a but crossed polars. **c):** the shape of the detrital grains are still recognizable but the grain boundaries are significantly opened. **d):** same as c but crossed polars. The typical extinction pattern of the original quartz is not recognized, however, the microscopic appearance resembles fine-grained cristobalite. **e):** As for c, the shape of the detrital grains is recognized and the grain boundaries are opened contains wedge shaped fragments. **f):** Same as e but crossed polars. The wedge shaped material seen especially between the grains is typical tridymite. **g):** mix of reduction material, condensate (SiO_2) and quartz. Small quartz fragments scattered around. These are remains of disintegrated quartz. **h):** Same as g but crossed polars. The quartz fragments show typical quartz extinction.

Table 5 Shows XRD results from small scrape-off samples from drill cores from FeSi furnace. (Crist = cristobalite; Trid = tridymite; Qtz = quartz; bckgr = elevated background level). XRD and XRD(2) refers to the first analysis and re-analysis of the samples respectively. Re-analyses were carried out on new material. None SiO_2 phases are not included in the table.

Drill core	Sample no	XRD scrape off	XRD(2) scrape off
BH1 p5-6	1	Crist,	Crist
BH1 p5-6	2	Crist, Qtz, bckgr	Crist, bckgr
BH1 p5-6	3	Crist, bckgr	Crist
BH2 p5-6	1	Qtz, Crist,	Crist
BH2 p5-6	2	Crist, Trid, bckgr	Crist, Trid, bckgr
BH2 p5-6	3	Crist, Qtz, bckgr	Crist, bckgr
BH3p5-6	1	Qtz	Qtz
BH3p5-6	2	Qtz	Qtz, bckgr
BH3p5-6	3	Qtz	Qtz, Crist
BH3p5-6	4	Qtz	Qtz
BH3p5-6	5	Qtz	Qtz
BH3p5-6	6	Crist, Qtz	Crist
BH3p5-6	7	Crist	Crist , bckgr
BH3p5-6	8	Qtz, Crist	Qtz
BH3p5-6	9	Qtz	Qtz
BH3p5-6	10	Crist	Crist, Qtz, bckgr
BH3p5-6	11	Crist, bckgr	Crist, bckgr
BH1p4	1	Crist	Crist
BH1p4	2	Crist	Crist
BH1p4	3	Crist, Trid, bckgr	Trid, Crist, bckgr
BH1p4	4	Crist, Trid, bckgr	Trid, Crist, bckgr
BH1p4	5	Quartz, Crist, Trid, bckgr	Trid, Qtz, Crist, bckgr
BH1p4	6	Crist, Trid	Crist, Trid
BH2p4	1	Crist	Crist
BH2p4	2	Crist	Crist
BH2p4	3	Crist	Crist
BH2p4	4	Crist	Crist
BH2p4	5	Crist, Bckgr	Crist, bckgr
BH2p4	6	Crist, Bckgr	Crist, bckgr
BH3p4	1	Crist,	Crist, Qtz
BH3p4	2	Crist, Trid	Crist, bckgr
BH3p4	3	Crist	Crist
BH 2325H	1	Crist	Crist

XRD investigations show that cristobalite is the dominant silica phase in this furnace (Table 5). However, quartz is strongly represented in some samples, especially in samples from the top of charge where the quartz looks rather unaltered in BH3p5-6. Tridymite is also seen in two of the drill core samples (BH2 p5-6 and BH1 p4). Tridymite was also detected by XRD in a third drill core sample (BH3 p4) but this was not confirmed by re-analysing.

Discussions

As shown in Table 5, tridymite is actually formed inside the furnace during operation, this in contrast to what was found by Aasly *et al.* (In prep. 2008), where no tridymite was found in any samples after heating for as long as 5.5 hrs at 1550 °C. The differences between the experimental results and the results from the actual furnace may be related to the impurity contents in the two: The experiments were run on pure FeSi- and Si-quality quartz and placed inside a pure graphite crucible during heating. No, or at least minimal amounts of reactions take place between the quartz sample and the graphite crucible. In the furnace, quartz is necessarily mixed with reduction materials where reactions take place between the reduction materials and the quartz. The impurity content in the operational furnace is higher than in the experimental and thus catalyst elements that enhance the tridymite formation may be present in the furnace.

Silica phases - relations

Si-furnace

The XRD results indicate that the quartz is rapidly transformed to cristobalite in the top of the charge (zone 6). It was expected that the quartz closest to the electrodes would have a more rapid phase transformation due to the highest temperatures in this part. However, the presence of quartz in the vicinity of the electrode and the absence of quartz in the more distal parts of the furnace indicates that the phase transformation is more rapid further away from the electrodes, or it may simply be an image of the mass flow in the furnace which is higher closer to the electrodes because of higher temperatures near the electrodes which results in lower retention time. Thus, the quartz closer to the electrode have been exposed to the furnace heat for a shorter period of time than the material distal from the electrode, where the temperatures are relatively low and the mass flow of the charge is lower giving longer retention time. The elevated background level in Sample 3a could indicate an amorphous transition phase, but may also be a result of SiO condensate, which is also amorphous.

Just below the top of the charge (in Zone 5), the presence of cristobalite and absence of quartz indicates that all quartz fragments have been transformed to cristobalite before it enters this zone from the top of the charge. The high background level is probably reflecting SiO condensate and possibly some intermediate transition phase.

FeSi-furnace

The XRD results from the FeSi furnace indicate mainly the same as those from the Si-furnace. Quartz is mainly seen in one of the drill cores (BH3p5-6) where quartz is the dominating silica phase. Cristobalite is only seen in the lower parts of this drill core. This drill core seem to have penetrated the upper levels of the charge where the charge materials are relatively unreacted (e.g. Figure 6) and the quartz fragments, coal/coke and iron pellets are relatively easily recognized. The cristobalite content is limited to only those samples that are more porous and obviously more altered by the furnace heat.

Tridymite vs. no tridymite in Si vs. FeSi

The XRD results indicate that tridymite is only present in the FeSi furnace. Tridymite was found in samples from drill-hole BH1p4 and Bh2p5-6 and appear to be limited to the parts of the furnace that are below the upper charge, and away from the cavity walls. This is the rather inactive charge (Schei *et al.*, 1998) and the temperature is relatively low compared to the area around the electrodes. Obviously, the quartz has enough time at suitable temperatures for tridymite to form.

K and Ca impurities are highest in the Si-furnace because of the impurity levels in the charcoal used in the pilot scale furnace. The impurity levels of these elements are approximately 100% higher than those of the raw materials for the FeSi furnace. Na, Al and Fe impurity levels are highest in the FeSi-furnace and related to high Na content in the coal used for this FeSi operation leading to the Na content of microsilica of the FeSi process being approximately 100% higher than in microsilica from the Si-process. Al contents are 50 to 100% higher in the raw materials for FeSi and are reflected by the same difference in Al impurity in the FeSi vs. Si product. The Fe content is naturally significantly higher in the FeSi process since Fe is a part of the process.

It is known that a catalyst is necessary for achieving transformation into tridymite (e.g. Floerke, 1957; Holmquist, 1961; Stevens *et al.*, 1997). The most common element mentioned, as such catalysts are Na, but also other alkalis such as Ca, K and Al are mentioned (e.g.

Floerke, 1957; Holmquist, 1961; Stevens *et al.*, 1997). However, the importance of Fe as a catalyst is has not been mentioned in the literature.

Impurity contents and tridymite

The quartz used in the FeSi process has a slightly higher content of impurities than the quartz used in the Si process. This is related to the chemical quality of the final product and may be seen as an explanation to why tridymite is seen in the FeSi furnace but not in the Si furnace. However, previous investigations of the phase transformations in (Fe)Si quartz (Aasly *et al.*, 2007, In prep. 2008) did not show any tridymite formation in both Si-quartz or FeSi-quartz. These investigations where carried out by heating only the quartz to different temperatures with no influence of the other types of raw materials used in the processes. Thus, the chemical quality of the quartz alone cannot be used as an explanation to why tridymite is formed in the FeSi furnace but not the Si furnace. However, the total content of impurities in the furnaces is also influenced by the impurity content in the other raw materials such as the carbon materials (coal/coke/wood-chips) and the iron pellets (FeSi furnace). Also, possible impurities in the electrode must be taken into consideration.

Silica phases vs. depth in furnace

It seems that the phase transformation from quartz to cristobalite is achieved at rather shallow depths in the furnace. However, there are indications that some quartz may "survive" in the quartz structure (preferably as β-quartz) all the way to the bottom of the furnace. This may be a result of core drilling, where some materials fall through the drill hole and occupies space at depths where quartz is not naturally found. However, cavities present during operation may cause quartz falling quickly down through the furnace during operation and thus the quartz appears to have made a short cut through the process (furnace).

General

One important difference between the two furnaces (except type of operation) is that the size of the furnaces is very different. This makes the cooling process different, where the pilot scale furnace cools down during one or two days whereas the FeSi furnace needs several days to cool down. This might be important, as all the samples investigated in this paper have been cooled before sampling. The cooling interval may have some significance to the phase transformations from high-temperature silica polymorphs to low-temperature silica polymorphs as described by (e.g. Stevens, 1997; Stevens *et al.*, 1997). They showed that the amount of cristobalite formed in pure Iota quartz was depending on the cooling rate. The possibility that the tridymite in the FeSi furnace is formed during cooling must be taken into consideration. This is because of the difference in cooling rate in the two furnaces.

Schei (1977) states that results from large furnaces and small pilot scale furnaces down to 50 kW show qualitative similarities, indicating that pilot scale furnaces are well suited for studying basic phenomena and mechanisms present in the industrial furnaces and gain new knowledge from this.

Conclusions

This investigation of the quartz and silica material from two different furnaces shows that the cristobalite transformation is achieved rather quickly inside the furnace, with cristobalite mainly formed in the top of the charge (zone 6). Cristobalite is present in most of the samples from both furnaces. However, quartz is also present to a certain degree in several samples from the top of the charge. This is especially seen in samples from the Pilot furnace in samples from positions close to the electrode, whereas only cristobalite is seen further away

from the electrodes. The cause of this has been interpreted as a result of the relatively high temperatures leading to increased mass flow and shorter retention time near the electrodes compared to further away from the electrodes.

Tridymite seem to form in the FeSi furnace but not in the Si furnace. The most obvious reason must be the content of certain impurity elements in the FeSi furnace compared to the Si furnace. However, the difference in the cooling rate of the furnaces may also be a possible cause, since the FeSi furnace stays at high temperatures for a longer period of time, which gives time to the formation of tridymite.

The results presented here have provided more knowledge about the silica phase transformations in the silicon furnace and provided knowledge of how the quartz material reacts to the temperatures in the process. These results should be used as foundation for further investigations. Such investigations should be carried out on the existing or new furnace materials in order to understand the implications of the silica phase transformations on the silicon process.

Acknowledgements The authors thank Torill Sørløkk and Kjell Kvam for help with XRD analyses, and Kjetil Eriksen and Arild Monsøy for great help with preparing drill core samples for the heating experiments. Thanks to Elkem AS for providing some of the materials and for funding the analytical part of this research.

References

Aasly, K., Malvik, T., and Myrhaug, E. (2007) Advanced methods to characterize thermal properties of quartz. *INFACON XI*, **1**, p. 381-392. MacMillan, New Dehli, India.

Aasly, K., Malvik, T., and Myrhaug, E. (In prep. 2008) Heating of quartz and formation of cristobalite.

Chaklader, A.C.D. (1963) X-ray study of quartz-cristobalite transformation. *J. Amer. Ceram. Soc.*, **46**, 66-71.

Chaklader, A.C.D., and Roberts, A.L. (1961) Transformation of quartz to cristobalite. *J. Amer. Ceram. Soc.*, **44**, 35-41.

Deer, W.A., Howie, R.A., and Zussman, J. (1992) *An introduction to the rock-forming minerals, 2nd ed.* Longman Scientific & Technical, Harlow, Essex.

Fenner, C.N. (1913) The stability relations of the silica minerals. *Am. Jour. Sci.*, **XXXVI**, 331-384.

Floerke, O.O.W. (1957) Structural anomalies in tridymite and cristobalite. *Amer. Ceram. Soc. Bull.*, **36**, 142-148.

Foss, B., Halfdanarson, J., and Wasbø, S. (2000) "Dynamisk si-modell - simon v. 1.50", technical report, sintef-report no stf72 f00307.

Grådahl, S., Johansen, S.T., Nubdal, G., Ravary, B., Laclau, J.C., Vassbotn, T., and Hellevik, L.R. (2000) Environment and furnace processes part iii (in norwegian). SINTEF Report no. STF24 F00600, Trondheim, Norway.

Harders, F., and Kienow, S. (1960) *Feuerfestkunde: Herstellung, eigenschaften und verwendung feuerfester baustoffe.* Springer, Berlin.

Holmquist, S.B. (1961) Conversion of quartz to tridymite. *J. Amer. Ceram. Soc*, **44**, 82-86.

Klein, C., and Hurlbut, C.J. (1993) *Manual of mineralogy, 21st edn.* John Wiley, New York.

MacKenzie, W.S., and Guilford, C. (1980) *Atlas of rock-forming minerals in thin section.* Longman, London.

Myrhaug, E. (2003) Non-fossil reduction materials in the silicon process: Properties and behaviour. *Dept. of Materials Technology*, **Dr. ing.** Norwegian University of Science and Technology, Trondheim.

Myrhaug, E., and Monsen, B. (2002) Silisiumsmelteforsøk i 150kw pilotovn høsten 2001. "Bruk av biokarbon i norsk ferrolegeringsindustri". SINTEF, Trondheim, Norway.
Schei, A. (1977) Ferrosilisiumprosessens metallurgi. Elkem Spigerverket a/s, R & D Center for A/S FESIL & CO.
Schei, A., Tuset, J.K., and Tveit, H. (1998) *Production of high silicon alloys*. Tapir Forlag, Trondheim.
Stevens, S.J. (1997) Temperature dependence of the cristobalite alpha-beta inversion. *J Therm Anal*, **49**, 1409-1415.
Stevens, S.J., Hand, R.J., and Sharp, J.H. (1997) Polymorphism of silica. *J Mater Sci*, **32**, 2929-2935.